DEGREE OF DOCTOR OF PHILOSOPHY IN
ELECTRONICS AND TELECOMMUNICATIONS

DOCTORATE SCHOOL IN
INFORMATION AND COMMUNICATION TECHNOLOGIES

XXIV Cycle

UNIVERSITY OF MODENA AND REGGIO EMILIA

INFORMATION ENGINEERING DEPARTMENT

Ph.D. DISSERTATION

Analytical and graphical design of linear compensators by using Inversion Formulae

Candidate:
Stefania CUOGHI
Advisor:
Prof. Roberto ZANASI
The Director of the School:
Prof. Giorgio VITETTA

DOTTORATO DI RICERCA IN
ELECTRONICS AND TELECOMMUNICATIONS

SCUOLA DI DOTTORATO IN
INFORMATION AND COMMUNICATION TECHNOLOGIES

XXIV Ciclo

UNIVERSITÀ DEGLI STUDI DI MODENA E REGGIO EMILIA

DIPARTIMENTO DI INGEGNERIA DELL'INFORMAZIONE

TESI PER IL CONSEGUIMENTO DEL TITOLO DI DOTTORE DI RICERCA

Analytical and graphical design of linear compensators by using Inversion Formulae

Tesi di:
Stefania CUOGHI
Relatore:
Prof. Roberto ZANASI
Il Direttore:
Prof. Giorgio VITETTA

This work is dedicated
to all those who believed in me.

Contents

Introduction

This Ph.D. thesis focuses on the results of a research activity on the design of new methods for the synthesis of classical regulators, useful in educational and industrial environments. In classical control design, the gain and the phase margins are important frequency-domain measures used to assess robustness and the performance of a control system. Moreover, specifications on the phase margin and the gain crossover frequency are common because these two parameters together often serve as a measure of the performance of a control system. In the continuous time, several methods have been developed in order to meet these specifications [1]. These can be divided into approximated and exact methods. The first ones are normally based on numerical or graphical trial-and-error solutions or fuzzy neural networks. They are widely used in industry because they provide a reasonably good tuning of the compensator parameters using automated algorithms. However they are usually not easy to use for teaching purposes or for solving the problem exactly. This makes the synthesis procedure rather clumsy, and less suitable for educational purposes. It is very difficult to construct a written exercise, or test, of exam, in which the control design problem consists in classic trial-and-error design method.

An alternative method that can be successfully employed both in an educational and in a practical context is based on the so-called Inversion Formulae. The method is based on a closed-form formula that expresses the frequency response of the compensator at a generic frequency in polar form. Since the gain and phase margins and crossover frequency specifications result in the assignment of the magnitude and argument of the frequency response of the compensator at the desired gain or phase crossover frequency, the Inversion Formulae enable the parameters of the compensators to be computed directly given the frequency domain specifications. The basic principle of the method was introduced for the first time in 1982 in [2]. It was employed for the numerical and graphical design of first order Lead and Lag controllers and appeared in the Italian control textbook [3]. This undergraduate textbook has been by far the most utilised one in University courses and technical secondary institution (*Istituti Tecnici*) courses throughout Italy over the past twenty years. Due to its popularity, the same technique has later appeared in other University textbooks in Italy, see e.g. [4]- [7] and nowadays it is taught in several Italian Universities. However, the success of this technique for educational purposes has so far remained confined within the Italian control literature.

The great educational value of the method is motivated by the following facts.

1. The numerical solution can be directly carried out by by pen, paper and a scientific calculator on the only knowledge of the transfer function of the plant. This makes the method very suitable to be employed in all forms of written questions and exercises;

2. The synthesis procedure forces the students to follows the classical order of taking into account the steady state specifications first, and then to design the remaining part of the compensator;

3. Even though the synthesis methodology can be carried out by pen and paper, this technique has also an important graphical counterpart. The Inversion Formulae enable the control system design problem to be solved analytically with pen and paper, or graphically on Nyquist, Bode or Nichols plots (without necessarily using trial-and-error or iterative procedures), thus retaining important links to other parts of a programme of a course of Control, [8];

4. Unlike the traditional design methodologies, the feasibility of the design procedure can be checked *a priori*. Furthermore, once the Bode gain of the compensator is computed from the steady-state requirements, very simple considerations can lead students to the selection of the most suitable type of compensator to be employed;

5. The mathematical tools that are needed to explain the method are basic notions of trigonometry and complex numbers. Hence, the use of Inversion Formulae reinforces the use of manipulations of complex numbers which is crucial in control systems education;

6. The situations in which some of the parameters of the compensator turn out to be positive can be fruitfully linked to important considerations on the shape of the Bode and Nyquist plot of the compensator;

7. The method based on the Inversion Formulae can be implemented as an extremely simple algorithm, for example using MATLAB®.

The many advantages of this method compared to other techniques proposed in classical textbook, and tested by several years of practical teaching experiences, led to start a deep research activity in order to extend the Inversion Formulae method to other type of compensators. For several years the research on the extension of this method to second order PID and Lead-Lag regulators to meet both gain and phase margins and given crossover specifications has been frozen, this is due to the complexity of the computations. This thesis describes how this result has been obtained without a significant increase in the design complexity, see [8]- [13]. This is an important advantage, because Lead-Lag and PID networks offer additional flexibility with respect to standard first order Lead and Lag networks, that results in the ability to satisfy further specifications or constraints. Both the numerical and the graphical solutions to

meet specifications on phase and gain margins have been also extended to the design of discrete Lead-Lag and PID regulators, see [14]- [16]. This extension is relevant for industrial purposes, because nowadays compensators are often implemented by microprocessors and calculations are performed in the discrete time domain.

The flexibility of the method has been used to design Lead-Lag controllers to meet other design requirements. Usually the synthesis of the three parameters of a second order compensator is done simultaneously, on the base of the design specifications. However the complexity of the design procedure can be reduced using Inversion Formulae method. That is two of the three parameters of the controller can be easily synthesized to exactly meet two requirements, such as the phase margin and the gain crossover frequency. These frequency specifications are known to be related to the peak overshoot, the rise time and the bandwidth of the closed-loop system. An open research problem is to find the best way to synthesize the third parameter on the base of the characteristics of the plant to be controlled. Some methods which can be employed to solve this problem are presented in this thesis, see [12]. They are address to synthesized the third parameter of the regulator to meet a good settling time or a good resonance peak of the closed-loop step response of the system.

This thesis is organized as follows. The first chapter deals with the formulation of the considered control problems and the description of their design requirements in terms of system robustness and performances. In the second chapter the Inversion Formulae method for the synthesis of Lead and Lag networks is recalled. This method is compared with the classical solution on Bode diagrams. The third and fourth chapters are about the extension of the Inversion Formulae method to continuous and discrete time Lead-Lag compensators. The fifth and sixth chapters deal with the synthesis of PID regulators by using Inversion Formulae method both in continuous and in discrete time domains. All the design procedures have been applied to solve many numerical examples. The correspondent graphical representations in the Bode and the Nyquist diagrams clearly show the effectiveness of the presented design methods. Conclusions and appendix end this thesis.

Chapter 1

Formulation of the control problem

1.1 The control system and the design specifications

Let us consider the closed loop system shown in Fig. 1.1, where $G(s)$ denotes the transfer function of the LTI (Linear Time Invariant) plant to be controlled, which is assumed to be stable and which may have a transport delay. The plant $G(s)$ may also include the integration terms and the gain K required to meet the steady-state accuracy specifications. Moreover, let $C(s)$ denote the regulator with unity static gain. The families of compensators that are considered in this thesis are the phase-correction networks (Lead, Lag and Lead-Lag) and the PID controllers. These are the two most studied and utilized types of compensators, and are those that are introduced in all undergraduate and postgraduate textbooks of control feedback design.

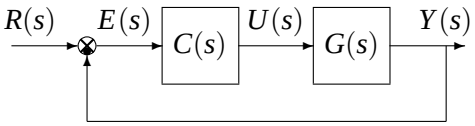

Figure 1.1: Unity feedback control structure.

In Figure 1.1, the symbols $R(s)$, $U(s)$ and $Y(s)$ respectively represent the Laplace transforms of the reference signal $r(t)$, of the control input $u(t)$ and of the controlled output $y(t)$. Let $E(s)$ represent the Laplace transform of the tracking error $e(t) \stackrel{\text{def}}{=} r(t) - y(t)$.

The common trend in both traditional and modern approaches to control education is to formulate the feedback control problem as one in which the design specifications are first expressed using time domain parameters of the response (speed of the response, overshoot, undershoot, steady-state accuracy, *etc*). These requirements are then transformed into frequency domain specifications (DC gain, bandwidth, resonant peak, phase and gain margins, crossover frequencies, *etc*). Alternatively – but less realistically from a practical perspective – the design specifications can be expressed from the very beginning in

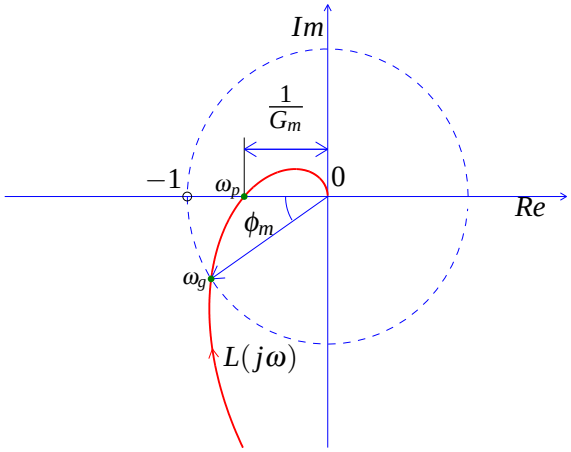

Figure 1.2: Design specifications: gain margin G_m, phase margin ϕ_m, gain crossover frequency ω_g and phase crossover frequency ω_p.

the frequency domain. In both situations, the design is effectively carried out using frequency domain considerations on Bode, Nyquist or – nowadays less frequently – Nichols plots, which constitute different types of graphical representations of the frequency responses involved in the control problem.

Specifications on the phase and gain margins and on crossover frequencies have always been extensively utilized in feedback control system design to ensure a desirable performance and to obtain a robust control system, see Fig. 1.2. To express these specifications mathematically, we define the loop gain transfer function as the product $L(s) \stackrel{\text{def}}{=} C(s)\,G(s)$. When $L(s)$ is strictly proper and the polar plot of $L(j\omega)$ for $\omega \geq 0$ has a single intersection with the unit circle and the negative real semiaxis (except for the trivial intersection at the origin as $\omega \to \infty$), the gain and phase margins are well defined, and ensure that the polar plot of $L(j\omega)$ does not encircle the critical point -1 in view of the simplified version of the Nyquist criterion, [17]. We denote by ω_g the gain crossover frequency, i.e., the frequency at which the polar plot of $L(j\omega)$ intersects the unit circle. Hence, ω_g is such that $|L(j\omega_g)| = 1$, and the phase margin is defined as the angle $\phi_m \stackrel{\text{def}}{=} \arg L(j\omega_g) + \pi$. Similarly, we denote by ω_p the phase crossover frequency, i.e., the frequency at which the polar plot of $L(j\omega)$ intersects the negative real half-axis. As such, ω_p is such that $\arg L(j\omega_p) = -\pi$, and the gain margin is defined as $G_m \stackrel{\text{def}}{=} 1/|L(j\omega_p)|$.

The phase and the gain margins are related to the distance of the loop gain frequency response $L(j\omega)$ from the critical point -1. Thus, on the base of the Nyquist criterion, these specifications are indicators of relative stability and robustness of the system. Moreover, specifications on the phase margin and the gain crossover frequency are often used together as a measure of the performance of a control system. Indeed, the phase margin is loosely related to characteristics of the response such as the peak overshoot and the resonant peak. The gain crossover frequency is known to affect the rise time and the bandwidth, thus it is related to the velocity of the system in tracking an input reference signal and the ability to reject

Design Problem	*Phase margin* ϕ_m	*Gain margin* G_m	*Gain crossover frequency* ω_g	*Phase crossover frequency* ω_p
A	$\times$		$\times$	
B		$\times$		$\times$
C	$\times$	$\times$	$\times$	
D	$\times$	$\times$		$\times$
E	$\times$	$\times$		

Table 1.1: Main Design Problems and design specifications addressed in the thesis.

noise and disturbances. [17].

A classical Design Problem proposed in nearly all classical textbooks of Automatic Control courses is the following.

Design Problem A: *Design a controller $C(s)$ to meet the specifications on the phase margin ϕ_m and on the gain crossover frequency ω_g, i.e., such that*

$$|L(j\omega_g)| = 1 \quad \text{and} \quad \arg L(j\omega_g) = \phi_m - \pi. \tag{1.1}$$

An alternative control problem can be formulated by specifying the gain margin and the phase crossover frequency:

Design Problem B: *Design a controller $C(s)$ to meet the specifications on gain margin G_m and on the phase crossover frequency ω_p, i.e., such that*

$$|L(j\omega_p)| = G_m^{-1} \quad \text{and} \quad \arg L(j\omega_p) = -\pi. \tag{1.2}$$

These problems can be solved by using a first order compensator. In some cases, the compensators with a richer dynamic structure will allow an additional degrees of freedom to be exploited to the end of satisfying a further specification. In particular, Lead-Lag and PID compensators are characterized by three degrees of freedom that can be used to satisfy three dynamical specifications as required by the following design problems.

Design Problem C: *Design a compensator $C(s)$ to satisfy requirements on the phase margin ϕ_m, the gain margin G_m and the gain crossover frequency ω_g.*

In other words, $C(s)$ must guarantee that a frequency $\omega_g > 0$ exists such that (1.1) and (1.2) hold. Other control problems can be formulated as follows.

Design Problem D: *Design a compensator $C(s)$ to satisfy requirements on the phase margin ϕ_m, the gain margin G_m and the phase crossover frequency ω_p.*

Design Problem E: *Design a compensator $C(s)$ to satisfy requirements on the phase margin ϕ_m and the gain margin G_m.*

The table 1.1 summarizes the main Design Problems considered in this thesis.

Chapter 2

Lead and Lag networks

Lead and Lag compensators are characterised by a first-order model and they are described by two parameters, which are the time constants of the real zero and the real pole. Due to the simplicity of their structure, and their easy implementation in electrical circuits, Lead and Lag controllers are the first networks described in almost all control textbooks.

2.1 Lead and Lag compensators

The classical form of Lead controller with unity static gain is the following

$$C_{Lead}(s) = \frac{1+\tau s}{1+\alpha\tau s}, \tag{2.1}$$

where $\tau > 0$ and $0 < \alpha < 1$. An equivalent form of the same compensator is given by

$$C_{Lead}(s) = \frac{1+\tau_1 s}{1+\tau_2 s}, \tag{2.2}$$

with the constraint $\tau_1 > \tau_2 > 0$. The zero z_c and the pole p_c of $C_{Lead}(s)$ are

$$z_c = -\frac{1}{\tau} = -\frac{1}{\tau_1}, \qquad p_c = -\frac{1}{\alpha\tau} = -\frac{1}{\tau_2}. \tag{2.3}$$

Let γ_0 and γ denote, respectively, the steady-state gain and the high frequency gain of $C_{Lead}(s)$, that is

$$\gamma_0 = \lim_{s\to 0} C_{Lead}(s) = 1, \tag{2.4}$$

$$\gamma = \lim_{s\to\infty} C_{Lead}(s) = \frac{1}{\alpha} = \frac{\tau_1}{\tau_2}. \tag{2.5}$$

The Bode and the Nyquist diagrams of $C_{Lead}(j\omega)$ for $\tau = 0.1$ and different values of γ are shown in Fig. 2.1 and 2.2. Notice that $\gamma = \frac{p_c}{z_c} > 1$ is the maximum gain of the controller. The Nyquist plot of $C_{Lead}(j\omega)$ is a semicircle with center C_0 and radius R_0 which depend only on α, that is

$$C_0 = \frac{1}{2}\left(1+\frac{1}{\alpha}\right), \qquad R_0 = \frac{1}{2}\left|1-\frac{1}{\alpha}\right|.$$

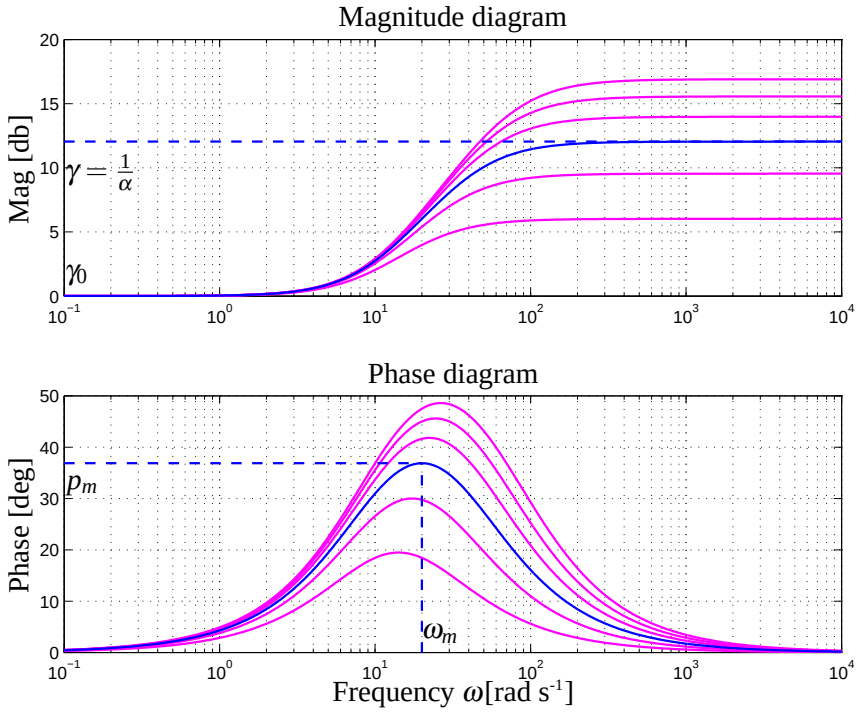

Figure 2.1: The Bode diagrams of $C_{Lead}(j\omega)$ for $\tau = 0.1$ and $\gamma = \frac{1}{\alpha} = [2:1:7]$. The blue line is for $\tau = 0.1$ and $\gamma = \frac{1}{\alpha} = 4$.

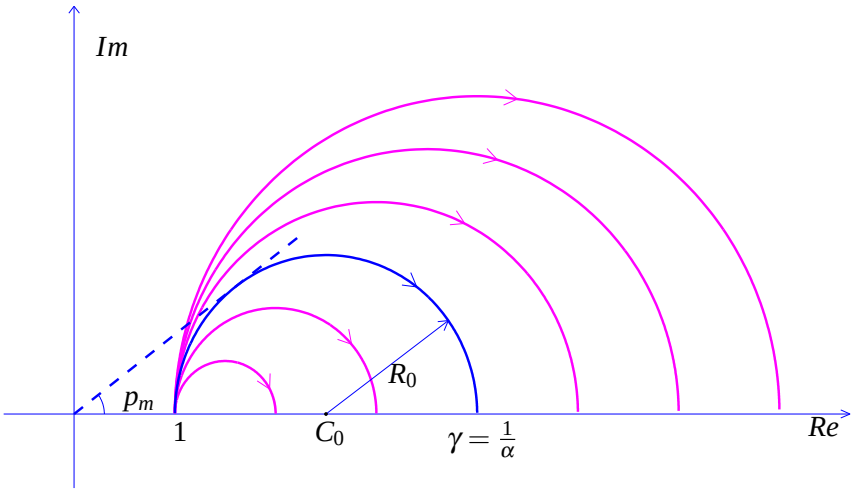

Figure 2.2: The Nyquist plot of $C_{Lead}(j\omega)$ for $\tau = 0.1$ and $\gamma = \frac{1}{\alpha} = [2:1:7]$. The blue line is for $\tau = 0.1$ and $\gamma = \frac{1}{\alpha} = 4$.

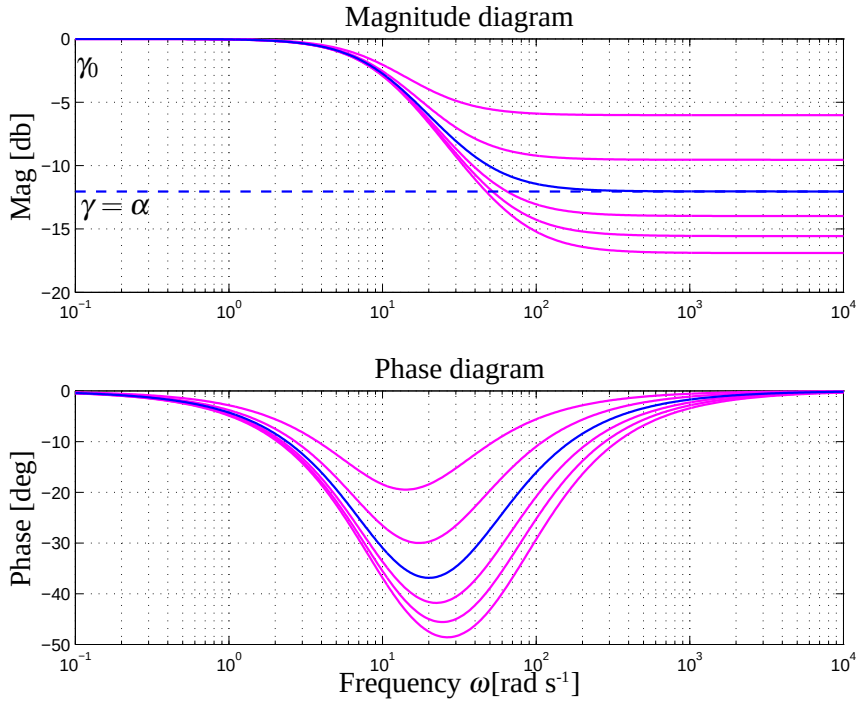

Figure 2.3: The Bode diagrams of $C_{Lag}(j\omega)$ for $\tau = 0.1$ and $\gamma = \alpha = 1./[2:1:7]$. The blue line is for $\tau = 0.1$ and $\gamma = \alpha = 1/4$.

The Lag controller with unity static gain can be expressed by the following two equivalent forms

$$C_{Lag}(s) = \frac{1+\alpha\tau s}{1+\tau s} = \frac{1+\tau_1 s}{1+\tau_2 s}, \tag{2.6}$$

where $\tau > 0$, $\alpha \in (0,1)$, or equivalently with $0 < \tau_1 < \tau_2$. The zero z_c and the pole p_c of $C_{Lag}(s)$ can be expressed as in (2.3). The steady-state and the high frequency gains of $C_{Lag}(j\omega)$ are respectively

$$\gamma_0 = \lim_{s\to 0} C_{Lag}(s) = 1,$$
$$\gamma = \lim_{s\to\infty} C_{Lag}(s) = \alpha = \frac{\tau_1}{\tau_2} < 1.$$

The Bode and the Nyquist diagrams of $C_{Lag}(j\omega)$ for different values of γ are shown in Fig. 2.3 and 2.4. Notice that γ is the minimum gain of the controller.

2.2 Classical solution of Design Problem on phase margin specification

A classical solution based on Bode diagrams of the Design Problem *A* using Lead and Lag controllers is briefly recalled. This is described in many Automatic Control books [18]-[20] and is still used in many university courses.

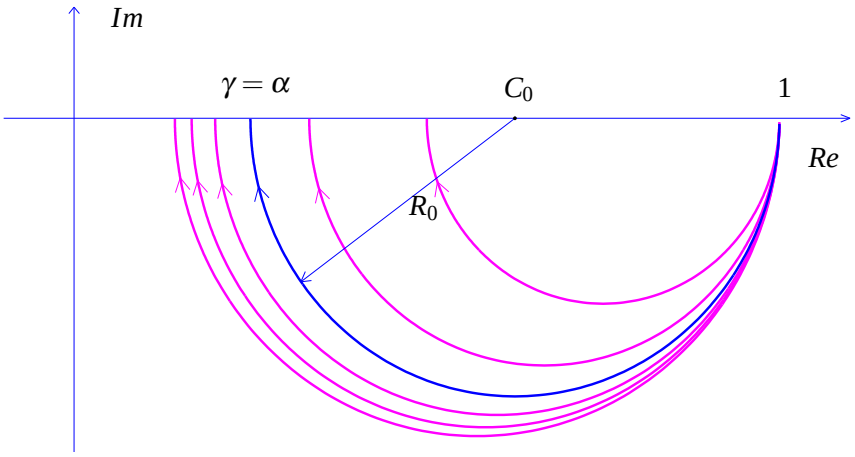

Figure 2.4: The Nyquist plot of $C_{Lag}(j\omega)$ for $\tau = 0.1$ and $\gamma = \alpha = 1./[2:1:7]$. The blue line is for $\tau = 0.1$ and $\gamma = \alpha = 1/4$.

2.2.1 Design of Lead controllers

The design of a Lead controller (2.1) is obtained by selecting the pole and zero of the compensator in such a way that that the maximum phase lead p_m of the compensator is placed at the gain crossover frequency of the uncompensated system. The undesired shift in the magnitude of the loop gain, which causes the phase margin of the controlled system to be different from p_m, is compensated using a trial-and-error procedure. The main steps of the design method are described below in more details.

Step 1. *Draw the Bode plot of $G(j\omega)$ and calculate the phase margin ϕ_G of the uncompensated system.* Let $\omega_{g'}$ be the gain crossover frequency of $G(j\omega)$.

Step 2. *Calculate the parameter α of the regulator*. As previously described, $\gamma = \frac{1}{\alpha}$ is the maximum gain of the regulators. As is well known, α is geometrically related to the maximum compensator phase shift p_m by the following well-known relation

$$\alpha = \frac{1 - \sin p_m}{1 + \sin p_m}. \tag{2.7}$$

The value of p_m is designed in such a way that at $\omega = \omega_{g'}$ the phase margin is ϕ_m, i.e.

$$p_m = \phi_m - \phi_G + F_s. \tag{2.8}$$

Since at frequency $\omega_{g'}$ the gain of the controller is not equal to 0db, as a rule of thumb a safety factor F_s of about 10° is introduced in (2.8). In most applications that value is sufficient. However, in some cases a higher value of F_s is needed to satisfy the required phase margin specification. This may require multiple iterations of the previous step of the design procedure.

Step 3. *Determine the value of the compensated gain crossover frequency.* It can be proved that the magnitude of the compensator at frequency ω_{max}, where the controller has the maximum phase shift p_m, is

$$|C(j\omega_{max})| = \frac{|j\frac{\omega_{max}}{z_c}+1|}{|j\frac{\omega_{max}}{p_c}+1|} = 10\log_{10}\left(\frac{1}{\alpha}\right), \tag{2.9}$$

and it depends on α. This magnitude shifts the gain crossover frequency $\omega_{g'}$ of the uncompensated system to a higher value ω_g in the compensated system. To satisfy the phase margin specification ϕ_m without changing p_m and α designed in Step 2, the gain crossover frequency ω_g of the compensated system has to be chosen such that the following relation holds

$$|G(j\omega_g)| = -10\log_{10}\left(\frac{1}{\alpha}\right) = 10\log_{10}(\alpha). \tag{2.10}$$

In this way, if the regulator is designed in such a way that $\omega_{max} = \omega_g$, the compensated system has a magnitude of 0db at $\omega = \omega_g$.

Step 4. *Determine z_c and z_p.* The pole and the zero of the regulator are selected so that $\omega_{max} = \omega_g$. The frequency ω_{max} is the geometric mean of z_c and p_c, that is, $\omega_{max} = \sqrt{z_c p_c}$. It follows that z_c and z_p can be designed using the following relations

$$z_c = \omega_p\sqrt{\alpha}, \qquad\qquad p_c = \frac{z_c}{\alpha}, \tag{2.11}$$

where $\alpha = \frac{z_c}{p_c}$ is given by (2.7). From (2.11) it follows that $\tau = -\frac{1}{z_c}$.

Numerical example

Example 1. Given the plant $G(s) = \frac{25}{s(s+1)(s+10)}$, design a Lead controller to satisfy a phase margin $\phi_m = 50^\circ$.

Solution: The Bode and the Nyquist plots of $G(s)$ are shown in green in Fig. 2.5 and 2.6. The uncompensated phase margin is 27°, for $F_s = 10^\circ$ $\alpha = 0.295$ and the designed compensator is

$$C_{Lag}(s) = \frac{0.9161s+1}{0.27s+1}. \tag{2.12}$$

The corresponding loop gain frequency response is shown in red in Fig. 2.5 and 2.6, the phase margin of the compensated system is 48.1° and the gain crossover frequency is $\omega_g = 2$ rad s^{-1}. The phase margin can be increased by choosing a higher value of F_s. The plots of the compensated loop gain frequency responses $L(j\omega, F_s) = G(j\omega)C(j\omega, F_s)$ for $F_s \in [13^\circ : 6^\circ : 25^\circ]$ are shown in purple in Fig. 2.5 and 2.6.

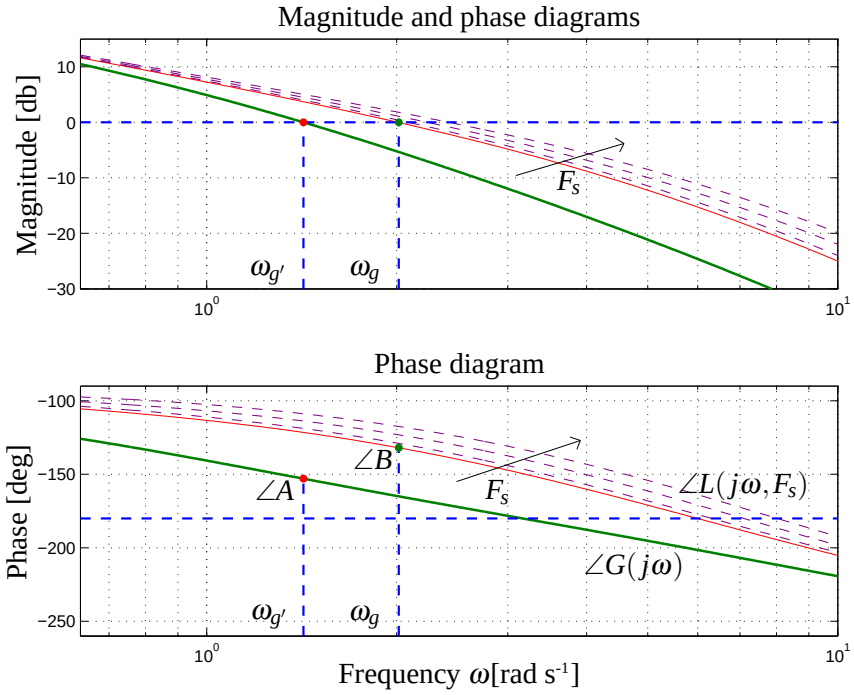

Figure 2.5: Example 1. The Bode plots of $G(j\omega)$ and $L(j\omega, F_s)$ obtained using a Lead compensator.

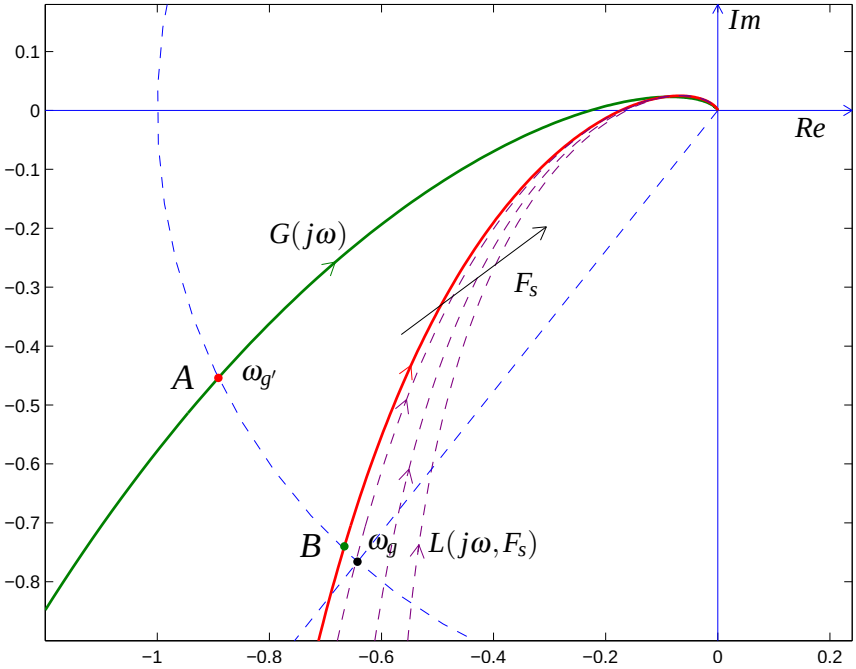

Figure 2.6: Example 1. The Nyquist plots of $G(j\omega)$ and $L(j\omega, F_s)$ obtained using a Lead compensator.

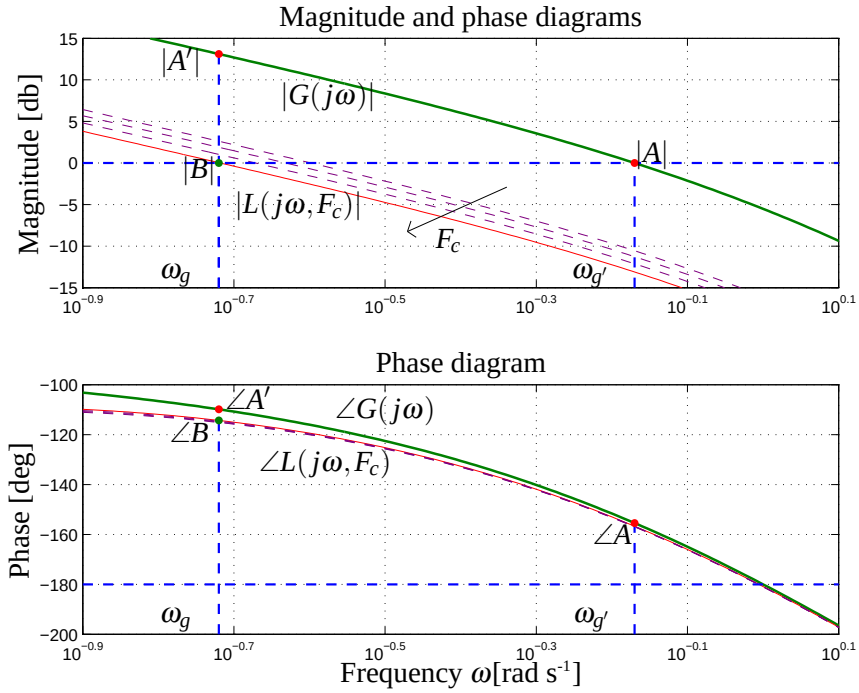

Figure 2.7: Example 2. The Bode plots of $G(j\omega)$ and $L(j\omega,F_c)$ for $F_c = [4:2:10]$ obtained using a Lag controller.

2.2.2 Design of Lag controllers

The Lag compensator (2.6) can be used to solve the Design Problem *A* such that the magnitude of the plant is attenuated until the phase margin specification is satisfied. The effects of the undesired phase shift of the loop gain are reduced by the design procedure, which is described below.

Step 1. *Draw the Bode plots of $G(j\omega)$ and calculate the phase margin ϕ_G of the uncompensated system.*

Step 2. *Determine the compensated gain crossover frequency.* The gain crossover frequency ω_g of the compensated system is chosen such that the following relation holds

$$\angle G(j\omega_g) = -\pi + \phi_m + F_c, \tag{2.13}$$

where F_c is a correction term that can be chosen in the range $[5^\circ, 10^\circ]$.

Step 3. *Calculate the parameter α.* From the definition of phase margin, the desired phase margin ϕ_m can be achieved at ω_g by modifying the magnitude of $G(j\omega)$ such that

$$|L(j\omega_g)| = 1 \quad \text{or} \quad |L(j\omega_g)|_{db} = 0db, \tag{2.14}$$

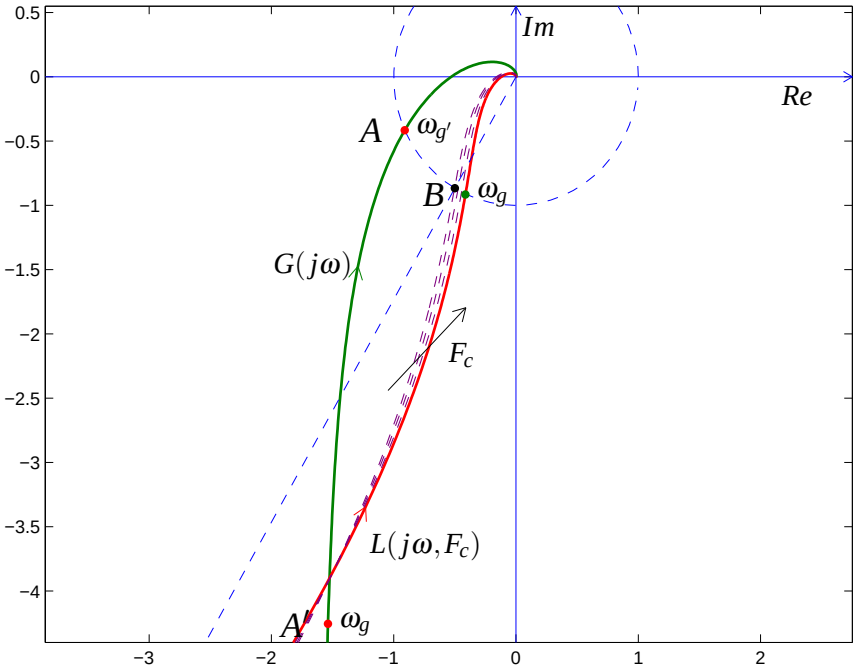

Figure 2.8: Example 2. The Nyquist plots of $G(j\omega)$ and $L(j\omega,F_c)$ for $F_c = [4:2:10]$ obtained using a Lag controller.

where $L(j\omega_g) = C_{Lag}(j\omega_g)G(j\omega_g)$ is the loop gain frequency response. For all frequencies greater than about $4z_c$, $|C_{Lag}(j\omega)| \simeq \alpha$. From (2.14), α can be calculated using the following relation

$$\alpha = \frac{1}{|G(j\omega_g)|}. \tag{2.15}$$

The term F_c in (2.13) is required to compensate the small phase of $C_{Lag}(j\omega)$ at ω_g.

Step 4. *Calculate z_c and p_c.* The value of z_c can be chosen a decade below ω_g. This is usually enough to ensure a magnitude of $C_{Lag}(j\omega)$ equal to α at frequency ω_g. It follows that z_c and p_c can be determined using the following relations

$$|z_c| \leq \frac{\omega_g}{10}, \qquad\qquad p_c = \alpha z_c. \tag{2.16}$$

From (2.16), it follows that $\tau = -\frac{1}{p_c}$.

Example 2. Given the plant $G(s) = \frac{5.3}{s(s+1)(s+2)(s+3)}$, which includes the gain and the integrations terms needed to satisfy the steady-state requirements, design a Lag controller to meet a phase margin $\phi_m \geq 50^\circ$.

Solution: The phase margin of $G(j\omega)$ is $\phi_G = 26.8^\circ$, see the green lines in Fig. 2.7 and 2.8. The chosen gain crossover frequency ω_g of the compensated system is 0.192rad s^{-1}. At that frequency

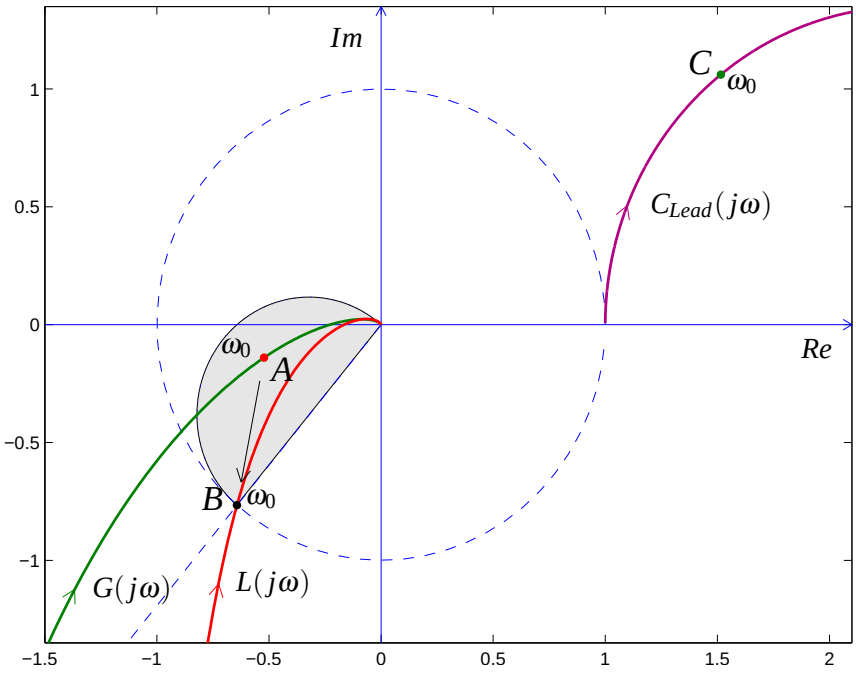

Figure 2.9: The point A is brought to point B by a Lead controller (solution of Example 1 using Inversion Formulae method).

$\angle G(j\omega_g) = -110^\circ$ and the relation (2.13) holds for $F_c = 10^\circ$. From (2.15) and (2.16) $\alpha = 0.236$, $z_c = -0.0241$, $p_c = -0.0045$ and $\tau = 220.7$. The loop gain crossover frequency $L(j\omega)$ is shown in red in Fig. 2.7 and 2.8. The purple lines denote the loop gain crossover frequencies for $F_c = [4:2:8]^\circ$.

2.3 The Inversion Formulae method

The graphical and numerical solutions of the Design Problems A and B by using Lead and Lag networks and Inversion Formulae method can be found in [4]-[7].

2.3.1 Graphical solution

Referring to the block diagram shown in Fig. 1.1 and to the Design Problems A and B, let $B = M_B e^{j\varphi_B}$ the point through which the loop gain frequency response $L(j\omega)$ has to pass to satisfy the given dynamic requirements (Fig. 2.9), that is

$$L(j\omega_0) = C(j\omega_0)G(j\omega_0) = B, \tag{2.17}$$

where ω_0 is the desired frequency of $L(j\omega)$ at point B. The point B can be expressed in the following

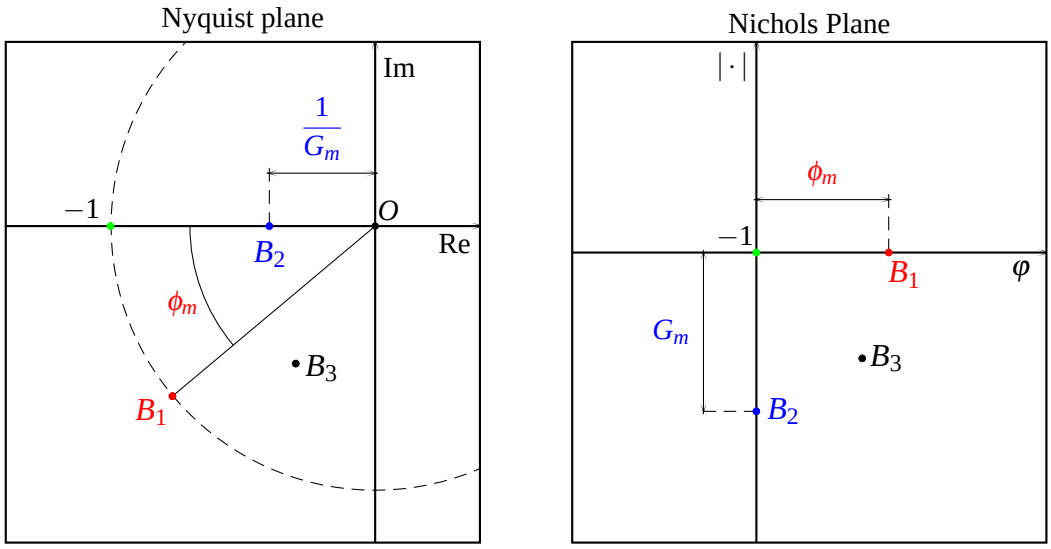

Figure 2.10: Position of point B on the Nyquist and Nichols planes w.r.t. the design specifications.

way on the base of design specifications

$$B = \begin{cases} B_1 = e^{j(\pi+\phi_m)} & \text{specification on } \phi_m \\ B_2 = -\dfrac{1}{G_m} & \text{specification on } G_m \\ B_3 = M_3\, e^{j\,\varphi_3} & \text{medley specification} \end{cases} \tag{2.18}$$

The medley specification denotes explicitly the position of point B_3 through which $L(j\omega)$ has to pass. The position of points B_1, B_2, B_3 on the Nyquist and the Nichols planes are shown in Fig. 2.10. Relation (2.17) can also be expressed as

$$C \cdot A = B, \tag{2.19}$$

where $A = M_A\, e^{j\,\varphi_A}$ and $C = M\, e^{j\varphi}$ are the points of $G(j\omega)$ and $C(j\omega)$ at frequency ω_0, see Fig. 2.9. We say that point A can be brought to point B by using the compensator $C(s)$ if a set of positive parameters of $C(s)$ exists such that (2.17) and (2.19) hold. This happens when $M = M_B/M_A$ and $\varphi = \varphi_B - \varphi_A$.

Let us define *admissible domain $\mathscr{D}_B$ of the compensator $C(s)$ with respect to B* as the set of all the points $A \in \mathbb{C}$ that can be brought to B by the controller.

The Lead and Lag regulators (2.1) and (2.6) can be expressed by the following unified frequency response

$$C(j\omega) = \frac{1 + j\,\tau_1\omega}{1 + j\,\tau_2\omega}, \tag{2.20}$$

and the admissible domain $\mathscr{D}_B$ of Lead and Lag controllers can be expressed as

$$\mathscr{D}_B = \left\{ A \in \mathbb{C} \,\middle|\, \exists\, \tau_1, \tau_2 > 0, \exists\, \omega \geq 0 : C(j\omega) \cdot A = B \right\}.$$

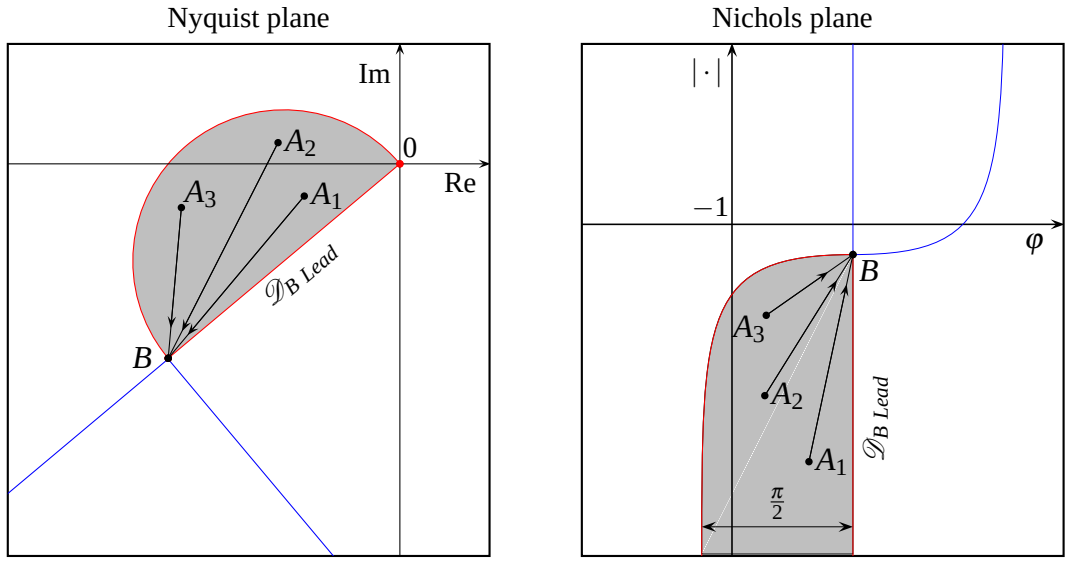

Figure 2.11: Admissible domain $\mathscr{D}_B$ of Lead compensator in the Nyquist and Nichols planes.

The shape of $\mathscr{D}_B$ for Lead and Lag compensators in the Nyquist and Nichols planes are shown in gray in Fig. 2.11 and 2.12.

Definition 1 (*Lead-Lag Inversion Formulae*). *Given two points $A = M_A e^{j\varphi_A}$ and $B = M_B e^{j\varphi_B}$ of the complex plane $\mathbb{C}$, the Lead-Lag* Inversion Formulae *$P(A,B)$ and $Q(A,B)$ are defined as follows*

$$\boxed{\begin{aligned} P(A,B) &= \frac{M-\cos\varphi}{\sin\varphi}, \\ Q(A,B) &= \frac{\cos\varphi-\dfrac{1}{M}}{\sin\varphi}, \end{aligned}} \tag{2.21}$$

where $M = \frac{M_B}{M_A}$ and $\varphi = \varphi_B - \varphi_A$, see [2], [4] and [14].

Tuning procedure

The main steps of the proposed method for the solution of Design Problems *A* and *B* are illustrated below.

Step 1. *Determine the point $B = M_B e^{j\varphi_B}$.* This point is completely determined by the design specifications, see (2.18).

Step 2. *Draw the admissible domain $\mathscr{D}_B$.* The domains $\mathscr{D}_B$ of Lead and/or Lag compensators in the Nyquist and Nichols planes are shown in Fig. 2.11 and 2.12.

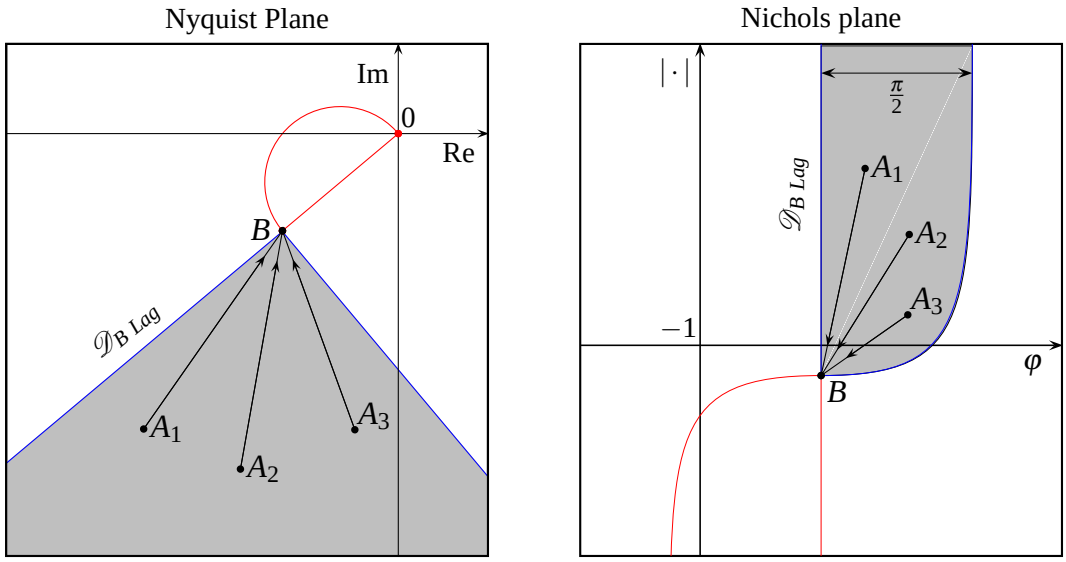

Figure 2.12: Admissible domain $\mathscr{D}_B$ of Lag compensator in the Nyquist and Nichols planes.

Step 3. *Plot the frequency response $G(j\omega)$ of the plant.* Let $A = G(j\omega_0) = M_A e^{j\varphi_A}$ be a point of $G(j\omega)$ belonging to $\mathscr{D}_B$. This point is completely defined by the design requirements if the frequency ω_0 of $L(j\omega)$ in point B is a explicit design specification (i.e. the gain or the phase crossover frequency). The point A can be brought to point B by a Lead or Lag controller if only if $A \in \mathscr{D}_B$. If there are no intersection points between $G(j\omega)$ and $\mathscr{D}_B$ the problem has no solutions.

Step 4. *Design the parameters of the compensator.* The values of τ_1 and τ_2 in (2.1) or (2.6) can be obtained by using the *Inversion Formulae* with $P(A,B) = \tau_1\omega$ and $Q(A,B) = \tau_2\omega$, that is

$$\tau_1 = \frac{M - \cos\varphi}{\omega \sin\varphi}, \qquad \tau_2 = \frac{\cos\varphi - \frac{1}{M}}{\omega \sin\varphi}. \tag{2.22}$$

Using the forms of Lead and Lag networks (2.1) and (2.6) as function of classical parameters α and τ, equations (2.22) lead to

$$\alpha = \frac{M_g \cos\varphi_g - 1}{M_g\,(M_g - \cos\varphi_g)}, \qquad \tau = \frac{M_g - \cos\varphi_g}{\omega_g \sin\varphi_g}, \tag{2.23}$$

$$\alpha = \frac{M_g\,(\cos\varphi_g - M_g)}{1 - M_g \cos\varphi_g}, \qquad \tau = \frac{M_g \cos\varphi_g - 1}{\omega_g M_g \sin\varphi_g}, \tag{2.24}$$

for Lead and Lag regulators respectively.

Proof: The frequency responses of Lead an Lag compensators (2.1) and (2.6) can be written as

$$C(j\omega) = \frac{1 + jP(\omega)}{1 + jQ(\omega)} = Me^{j\varphi}, \tag{2.25}$$

where $P(\omega)=\tau_1\omega$, $Q(\omega)=\tau_2\omega$, $M=M(j\omega)$ and $\varphi=\varphi(\omega)$. Equation (2.25) can be expressed in matrix form as

$$\begin{bmatrix}1 & -M\cos\varphi\\ 0 & M\sin\varphi\end{bmatrix}\begin{bmatrix}P(\omega)\\ Q(\omega)\end{bmatrix}=\begin{bmatrix}M\sin\varphi\\ M\cos\varphi-1\end{bmatrix}. \tag{2.26}$$

Solving (2.26) with respect to $P(\omega)$ and $Q(\omega)$ one directly obtain the Inversion Formulae (2.21). As a consequence, (2.22) can be obtained by using the *Inversion Formulae* with $P(A,B)=\tau_1\omega$ and $Q(A,B)=\tau_2\omega$. □

Numerical examples

Let us consider the same numerical examples solved in Sec. 2.2 by using the classical method.

Solution of Example 1: The design specification $\phi_m=50^\circ$ defines the position of the point $B=M_Be^{j\varphi_B}$, i.e. $M_B=1$ and $\varphi_B=230^\circ$. The admissible domain $\mathscr{D}_B$ of the Lead compensator is shown in gray in Fig. 2.9. The point $A=G(j\omega_0)$ can be chosen in the admissible domain $\mathscr{D}_B$. A comparison with the classical solution can be performed by choosing $\omega_0=\omega_g=2$ rad s^{-1}. It follows that $M_A=0.54$, $\varphi_A=-165$, $M=\frac{M_B}{M_A}=1.85$ and $\varphi=\varphi_B-\varphi_A=35^\circ$. Substituting the values of M, φ and $\omega=\omega_g$ in (2.22), one obtains $\tau_1=0.892$ and $\tau_2=0.241$. The loop gain frequency response $L(j\omega)$ is shown in red in Fig. 2.9. Notice that $L(j\omega)$ passes exactly through point B.
The corresponding MATLAB® instructions to solve analytically the given problem by using the Inversion Formulae method are shown in Algorithm 1.

Algorithm 1 Solution of Example 1 in MATLAB®

```
s=tf('s');
G=25/(s*(s+1)*(s+10));
wg=2;
PM=50*pi/180;
C=evalfr(G,j*wg);
M=1/abs(C);
phi=PM-(pi+angle(C));
if (sin(phi)<0)|(cos(phi)<0)|M<1/cos(phi),
   disp('No solutions with a Lead network');
   return
end
tau1=(M-cos(phi))/(wg*sin(phi));
tau2=(cos(phi)-1/M)/(wg*sin(phi));
```

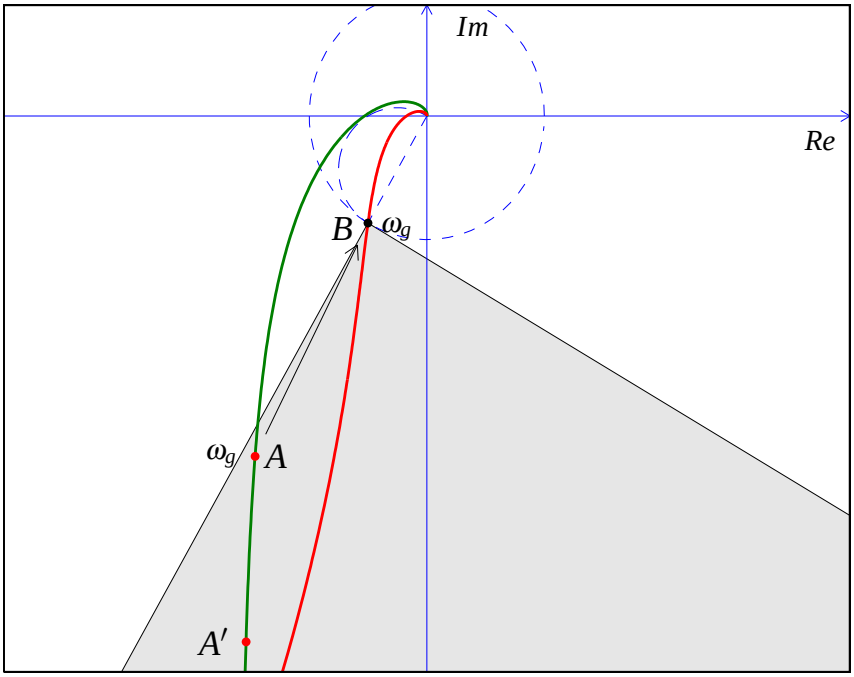

Figure 2.13: The point A is brought to point B by a Lag controller (solution of Example 2 using Inversion Formulae method).

Solution of Example 2: The phase margin $\phi_m = 55^\circ \geq 50^\circ$ defines the point $B = M_B e^{j\varphi_B}$: $M_B = 1$ and $\varphi_B = 235^\circ$. The admissible domain $\mathscr{D}_B$ is shown in gray in Fig. 2.13. The point $A = G(j\omega_0)$ can be chosen on the plot of $G(j\omega)$ (the green line in Fig. 2.13) and in the admissible domain $\mathscr{D}_B$. We choose $\omega_0 = \omega_g = 0.27$. It follows that $M_A = 3.12$, $\varphi_A = -118^\circ$, $M = \frac{M_B}{M_A} = 0.321$ and $\varphi = \varphi_B - \varphi_A = -2.06^\circ$. Substituting the values of M, φ and $\omega = \omega_g$ in (2.22), one obtains $\tau_1 = 69.9$ and $\tau_2 = 218$.

The loop gain frequency response $L(j\omega)$ is shown in red in Fig. 2.13. Notice that $L(j\omega)$ passes exactly through point B.

2.3.2 Numerical solution

The numerical solutions of the Design Problems A and B can be directly obtained by (2.22) and (2.25), with

$$\textit{i-a)} \quad M(\omega_g) = M_g = 1/\ |G(j\omega_g)|\ ,$$

$$\textit{ii-a)} \quad \varphi(\omega_g) = \varphi_g = \phi_m - \pi - \arg G(j\omega_g),$$

for the solution of the Design Problem A, and

$$\textit{i-b)} \quad M(\omega_p) = M_p = 1/(\ G_m\,|G(j\omega_p)|\ ),$$

$$\textit{ii-b)} \quad \varphi(\omega_p) = \varphi_p = -\pi - \arg G(j\omega_p),$$

for the solution of the Design Problem *B*. The solutions are acceptable for the design of Lead compensator if and only if

$$0 < \varphi < \frac{\pi}{2} \quad \text{and} \quad M > \frac{1}{\cos\varphi}, \tag{2.27}$$

are and they are acceptable for the design of Lag controller if and only if

$$-\frac{\pi}{2} < \varphi < 0 \quad \text{and} \quad M < \cos\varphi. \tag{2.28}$$

The proof can be easily obtained by the polar expression of the frequency response of the plant and the regulator, and the use of the Inversion Formulae (2.21).

On a educational environment the following questions can be given to students in written test.

Question 1. Given the plant $G(s) = k\dfrac{s+10}{s(s^2+2s+10)}$, design the gain k and a phase-correction network that satisfies the following static and dynamic specifications:

- velocity constant equal to 0.5;
- phase margin equal to 45°;
- gain crossover frequency equal to 3 rad/sec.

Find also the range of phase margins that are achievable at the crossover frequency 3 rad/sec with this phase-correction network. Also, determine the range of phase margins that at this gain crossover frequency ensures closed-loop stability.

The DC gain K must be selected so as to satisfy the specification on the velocity constant:

$$K_v = \lim_{s\to 0} sC(s)\,G(s) = K,$$

so that $K = 0.5$. In order to select the right compensation structure, we compute $M(\omega_g)$ and $\varphi(\omega_g)$:

$$\begin{aligned} M(\omega_g) &= \frac{1}{|G(3\,j)|} = 6\sqrt{\frac{37}{109}} \simeq 3.4957, \\ \varphi(\omega_g) &= \phi_m - (\pi + \text{arc}G(3\,j)) \\ &= \frac{7}{4}\pi - \arctan(3/10) + \arctan 6 \simeq 18.84^\circ. \end{aligned}$$

Since the conditions (2.27) are both satisfied, a Lead network may be used. A simple computation, that can even be carried out in closed-form with pen and paper, shows that

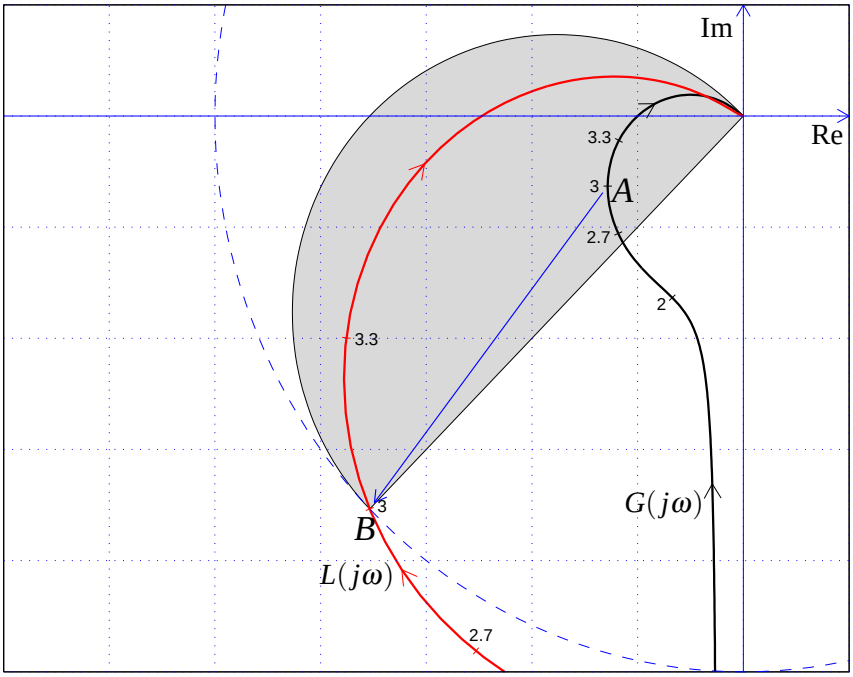

Figure 2.14: Graphical representation on the Nyquist of solution of Question 1.

$$\alpha = \frac{3\cdot 85\cdot\sqrt{2}-109}{36\cdot 37-3\cdot 85\sqrt{2}} \simeq 0.2590,$$
$$\tau = \frac{12\cdot 37-85\sqrt{2}}{3\cdot 29\sqrt{2}} \simeq 2.6317\,\text{sec}.$$

The corresponding MATLAB® instructions are shown in Algorithm 2, and the required compensator that satisfies all the specifications is given by

$$C_{\text{Lead}}(s) = 0.5\,\frac{1+2.6317\,s}{1+0.6817\,s}.$$

A graphical plot on the Nyquist plane of the frequency response $G(j\omega)$ is shown with the black line in Fig. 2.14, where A denotes the point of $G(j\omega)$ at frequency $\omega_g = 3$ rad/sec. Notice that A belongs to the admissible domain of Lead controller shown in grey in the plot. The compensator $C_{\text{Lead}}(s)$ has been designed such that $L(j\omega)$ shown with red line passes through point $B = e^{j(\phi_m+\pi)}$ at frequency ω_g.

The smallest phase margin achievable with a Lead network at the gain crossover frequency $\omega_g = 3$ rad/sec is

$$\phi_{\text{m min}} = \pi + \arg G(j\omega_g) = \frac{\pi}{2} + \arctan\frac{3}{10} - \arctan 6 \simeq 26.1616^\circ,$$

and the largest phase margin is

$$\begin{aligned}\phi_{\text{m max}} &= \pi + \arg G(j\omega_g) + \arccos(|G(j\omega_g)|) \\ &= \frac{\pi}{2} + \arctan\frac{3}{10} - \arctan 6 + \arccos\frac{1}{6}\sqrt{\frac{109}{37}} \simeq 99.54^\circ.\end{aligned}$$

Algorithm 2 Solution of Question 1 in MATLAB®

```
s=tf('s');
G=0.5*(s+10)/(s*(s^2+2*s+10));
wg=3;
PM=pi/4;
C=evalfr(G,j*wg);
M=1/abs(C);
phi=PM-(pi+angle(C));
if (sin(phi)<0)|(cos(phi)<0)|M<1/cos(phi),
   disp('No solutions with a Lead network');
   return
end
alpha=(M*cos(phi)-1)/(M*(M-cos(phi)));
tau=(M-cos(phi))/(wg*sin(phi));
```

Question 2. Given the same plant of Question 1, design a phase-correction network that satisfies the following specifications:

- velocity error equal to 0.1;
- phase margin equal to 60°;
- gain crossover frequency equal to 1 rad/sec.

Find also the range of phase margins that are achievable at this crossover frequency with this phase-correction network.

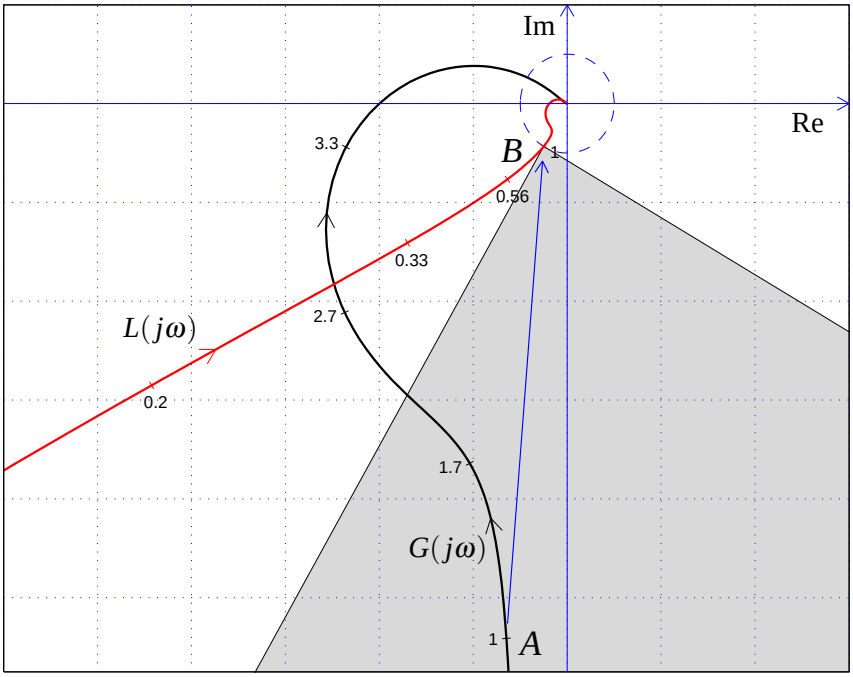

Figure 2.15: Design of a Lag network on the Nyquist plane to meet the specifications of Question 2.

Since the velocity error is equal to $e_v = 1/K_v$ and $K_v = K$ as shown in Question 1, it is found that $K = 10$. In order to select the right compensation structure, we compute $M(\omega_g)$ and $\varphi(\omega_g)$:

$$\begin{aligned} M(\omega_g) &= = \frac{1}{10}\sqrt{\frac{85}{101}} \simeq 0.0917 < 1, \\ \varphi(\omega_g) &= -\frac{\pi}{6} - \arctan(1/10) + \arctan\frac{2}{9} \simeq -23.18^\circ. \end{aligned}$$

Since (2.24) are satisfied, a Lag network can be used to solve the problem. The Lag controller is characterised by the parameters $\alpha = 0.0829$ and $\tau = 25.3559$ sec by simply replacing $M(\omega_g)$ and $\varphi(\omega_g)$ thus found into (2.24). The smallest phase margin achievable with a Lag network at the gain crossover frequency $\omega_g = 1$ rad/sec is

$$\phi_{\text{m min}} = \pi + \arg G(j\omega_g) - \arccos\frac{1}{|G(j\omega_g)|} \simeq -1.55^\circ,$$

and the largest phase margin is

$$\phi_{\text{m max}} = \pi + \arg G(j\omega_g) \simeq 83.18^\circ.$$

The graphical interpretation of the network design is shown in Fig. 2.15. The designed Lag controller brings the point $A = G(j\omega_g)$ to the desired point $B = e^{j240^\circ}$. The gray area denotes the set of points that

can be brought to B by a Lag network. If $A = G(j\omega_g)$ is not within this area, the problem cannot be solved with this type of network.

Question 3. Let $K = 10$. Find the interval of gain margins achieved using a Lag network at the phase crossover frequency $\omega_p = 4$ rad/sec that guarantee asymptotic stability of the closed loop.

A simple computation shows that

$$\begin{aligned} M(\omega_p) &= \frac{2}{G_m\sqrt{29}}, \\ \varphi(\omega_p) &= -\frac{\pi}{2} + \arctan\frac{2}{5} + \arctan\frac{4}{3}, \end{aligned}$$

from which it follows that

$$\alpha = \frac{52 - \frac{20}{G_m}}{145\,G_m - 52}, \qquad \tau = \frac{145\,G_m - 52}{56}.$$

It follows that

$$C(s) = \frac{56 + \left(52 - \frac{20}{G_m}\right)s}{56 + (145\,G_m - 52)\,s}.$$

The characteristic polynomial is

$$\begin{aligned} &(145\,G_m - 52)\,s^4 + (290\,G_m - 48)\,s^3 \\ &+(112 + 1450G_m - \frac{200}{G-m})\,s^2 + (6320 - \frac{2000}{G_m})\,s + 5600 = 0. \end{aligned}$$

The asymptotic stability of the closed loop can at this point be studied using the Routh criterion on this polynomial. Such study will lead to a set of intervals for G_m that guarantee asymptotic stability of the closed-loop.

2.4 Evaluations on the methods

The classical design procedure based on the Bode diagrams is still one of the most widely used in educational environment. However the method is based on trial-and-error procedure, the specifications are not exactly satisfied and the repetition of the same steps could discourage the students. The two different design procedures for the design of Lead and Lag controllers are difficult to remember. Moreover they are based only on the design of the magnitude of the regulators, while the phase is designed by rule of thumb. In this way the two parameters of the regulators are used to satisfy only a design requirement, that is the given margin specification, while the gain crossover frequency is automatically determined by the design procedure.

The main advantage of the Inversion Formulae method is that both the magnitude and the phase of the controller are designed to exactly meet the given margin specification at a given crossover frequency.

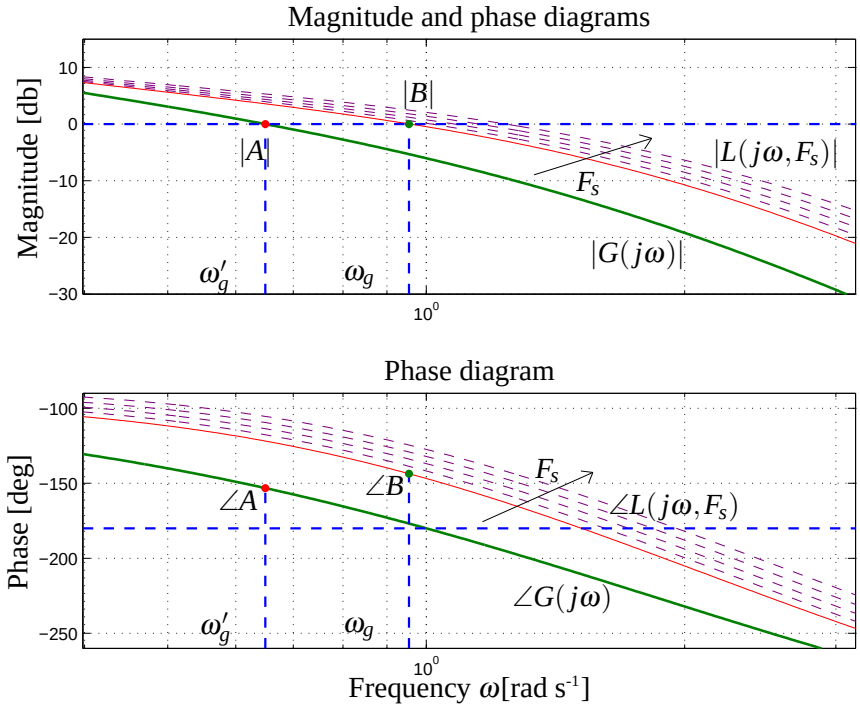

Figure 2.16: Example 3. The Bode plots of $G(j\omega)$ and the closed-loop frequency responses $L(j\omega,F_s)$ for $F_s = [10:5:30]^\circ$.

This can be done numerically, using very simple formulae, or graphically on Bode, Nyquist or Nichols planes. It is well known that in the process of learning the graphical representation of a numerical solution makes it easier to understand and easier to recall. The drawing and the comparison of the same function plotted in different diagrams, i.e. the loop gain frequency response on the Bode, the Nyquist and the Nichols diagrams, have a great educational value. They emphasize some properties hidden in a single representation and lead to a deeper knowledge of the concepts. Moreover the design procedure is the same for the two types of regulators, the feasibility of the design procedure can be checked a priori on the base of the concept of the admissible domain, the method can be employed in all forms of written questions and exercises.

Moreover in some cases the classical method is not able to solve the problem with a single compensator, while this is possible with the Inversion Formulae method. Let us consider the following example.

Example 3. Given the plant of example 2 $G(s) = \frac{5}{s(s+1)(s+2)(s+3)}$ which includes the gain and the required integrators terms to satisfy the steady-state specification, design a Lead network to satisfy a phase margin equal to 50°.

Solution: The uncompensated phase margin is 26.8°, and the gain crossover frequency is $\omega'_g =$

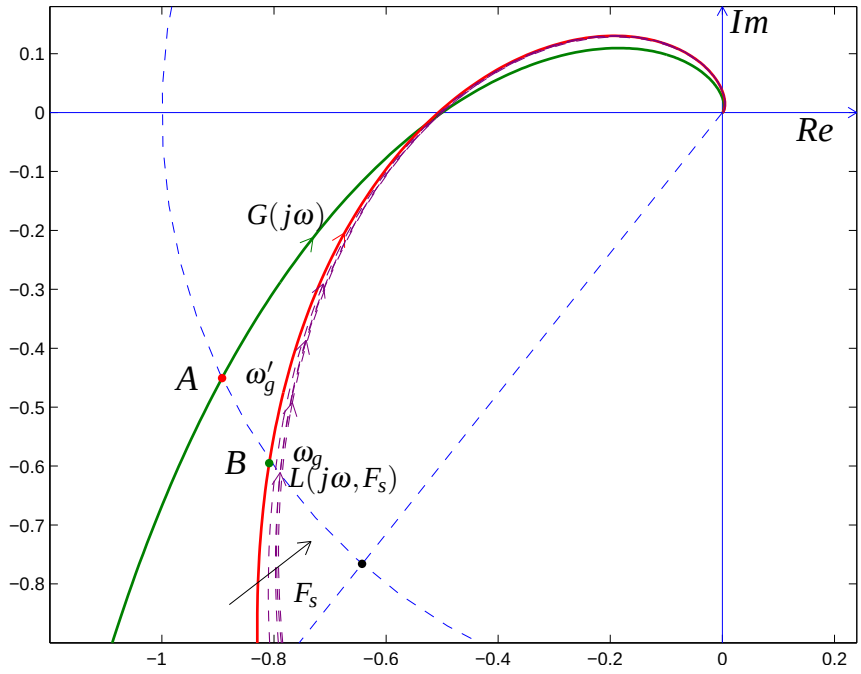

Figure 2.17: Example 3. The Nyquist plots of $G(j\omega)$ and the closed-loop frequency responses $L(j\omega,F_s)$ for $F_s = [10:5:30]^\circ$.

0.6496 see the green curves in Fig. 2.16 and 2.17. The value $\alpha = 0.29$, calculated using (2.7) and (2.8) when $F_s = 10^\circ$, leads to design the following compensator

$$C_{Lead}(s) = \frac{1.937s+1}{0.566s+1}. \tag{2.29}$$

The corresponding loop gain frequency response is shown in red in Fig. 2.16 and 2.17, the gain crossover frequency is $\omega_g = 0.955$. Notice that the phase margin of the compensated system is only 36.1°. This can be increased choosing an higher value of F_s but the compensated phase margin is still too low. The plots of the compensated loop gain frequency responses $L(j\omega,F_s) = G(j\omega)C_{Lead}(j\omega,F_s)$ for $F_s \in [15^\circ : 5^\circ : 30^\circ]$ are shown in purple in Fig. 2.16 and 2.17.

The Example 3 can be exactly solved using the Inversion Formulae method. The point A is chosen in the admissible domain of Lead controller at $\omega_g = 0.9550$, that is the gain crossover frequency obtained by the classical solution. The compensator which exactly solves the problem is

$$C_{Lead}(s) = \frac{1.66s+1}{0.202s+1}.$$

The corresponding loop gain crossover frequency is the red curve in Fig. 2.18 and 2.19. Notice that ω_g is a free parameter when the Inversion Formulae method is used. That is each frequency $\omega_g \in (\omega_{min},\omega_{max})$, that corresponds to a point of $G(j\omega)$ placed in the admissible domain of the controller, leads to a feasible

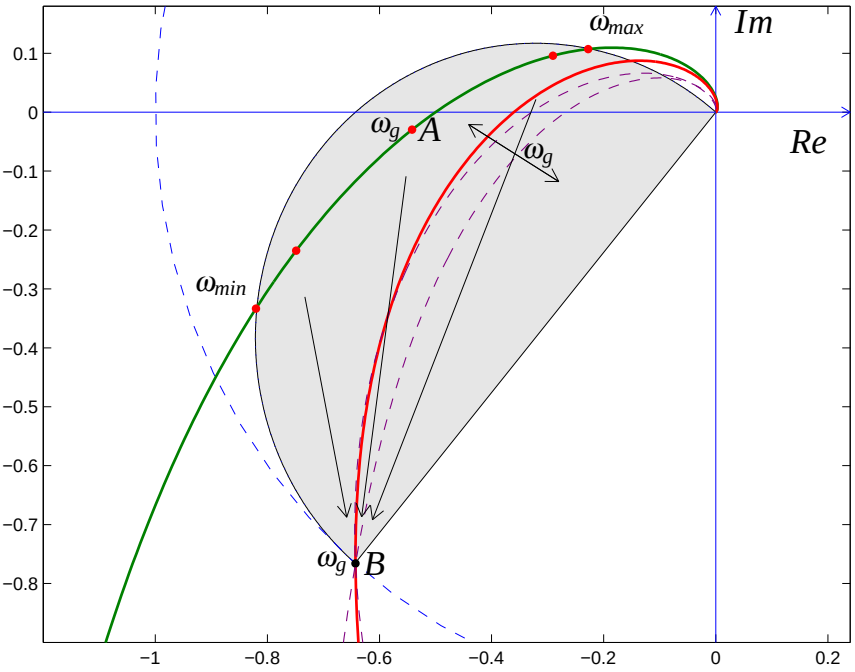

Figure 2.18: Example 3. Solution of Example 3 using the Inversion Formulae method, ω_g is a free parameter.

solution. An open research problem is to find a criterion to choose the gain crossover frequency ω_g when this is not a given design requirement.

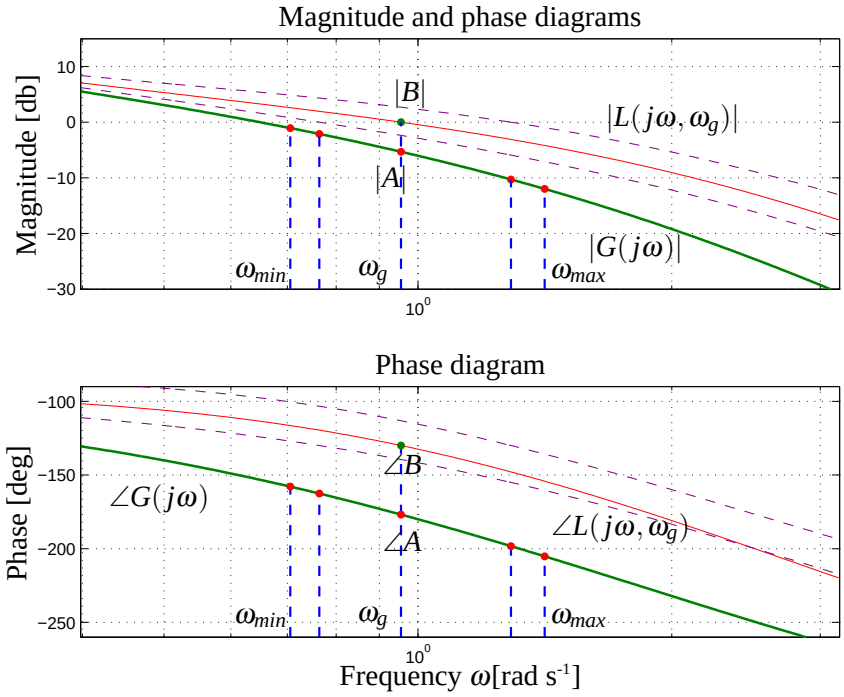

Figure 2.19: Example 3: graphical representation on the Bode diagrams of the solution using the Inversion Formulae method, ω_g is a free parameter.

Chapter 3

Lead-Lag networks

The Lead-Lag compensator has a richer dynamic structure compared to the structure of Lead and Lag networks, since it is characterized by a second-order transfer function, with two poles and two zeros. The form of the regulator that has been considered in this thesis has an unity static gain and is characterized by three degrees of freedom. As known, PID controllers are the most widely used networks in industry because of their simplicity. However in some cases Lead-Lag controllers, compared with PID regulators, lead to a better tradeoff between the static accuracy, system stability and insensibility to disturbance in frequency domain [21]. Moreover the recent literature shows a renewed interest in the design of this type of controllers [22]-[24]. In particular, they are utilized for classical loop shaping and weighting functions for automated controller synthesis algorithms, [24].

Within the context of exact design with frequency domain specifications, the first order Lead and Lag networks can satisfy only specifications on either the phase margin and the gain crossover frequency or on the gain margin and on the phase crossover frequency. The use of Lead-Lag compensators – also known as *notch compensators* – is particularly important. Indeed, there are cases in which a Lead-Lag compensator can satisfy the control specifications whereas a simple Lead or Lag network cannot. For example when the frequency response of the plant at the desired gain crossover frequency is such that its magnitude is greater than 1 and the difference between its argument and the desired phase margin is an angle greater than $\pi/2$ and smaller than π. Similar considerations hold with requirements on the gain margin and phase crossover frequency. On the other hand, the degree of freedom of the extra parameter in the transfer function of the second-order Lead-Lag compensator can be exploited to satisfy an additional requirement/specification, for example on the other margin.

In this chapter it is described how the Inversion Formulae method has been extended to Lead-Lag controllers to meet three frequency specifications, such as the phase and gain margins and the gain crossover frequency specifications, by analytic and graphical solutions, see [8], [10]-[12]. As in the case of Lead and Lag regulators, the solution can be carried out by determining directly the parameters of the

compensator as a function of the specifications and by making use of the Nyquist or Nichols plots. In this way, the advantages of analytic and graphic procedures are combined together to deliver a method that outperforms the classic techniques based on trial-and-error considerations. Differently from the method in [25], in which the parameters of the compensator are determined using a graphic construction on a special design chart, the approach presented in this chapter enables the parameters of the compensator to be computed *exactly* using simple formulae.

3.1 Lead-Lag compensators: the general structure

Consider a Lead-Lag compensator described by the transfer function

$$C_{LL}(s) = \frac{s^2 + 2\,\gamma\delta\,\omega_n s + \omega_n^2}{s^2 + 2\,\delta\,\omega_n s + \omega_n^2}, \tag{3.1}$$

where γ, δ and ω_n are real and positive. When $\gamma\delta < 1$ and/or $\delta < 1$ the zeros and/or the poles of the Lead-Lag compensator $C_{LL}(s)$ are complex conjugate with negative real part. The compensator $C_{LL}(s)$ has a unity static gain $C_{LL}(0) = 1$ which does not change the static behavior (i.e., the steady-state performance) of the controlled system. The frequency response $C_{LL}(j\omega)$ of the compensator $C_{LL}(s)$ is

$$C_{LL}(j\omega) = \frac{\omega_n^2 - \omega^2 + j\,2\,\gamma\delta\,\omega_n\omega}{\omega_n^2 - \omega^2 + j\,2\delta\,\omega_n\,\omega}, \tag{3.2}$$

which, for $\omega \neq \omega_n$, can be written as

$$C_{LL}(j\omega) = \frac{1 + j\,P(\omega)}{1 + j\,Q(\omega)} \tag{3.3}$$

where

$$P(\omega) = \frac{2\gamma\delta\,\omega\,\omega_n}{\omega_n^2 - \omega^2}, \qquad Q(\omega) = \frac{2\delta\,\omega\,\omega_n}{\omega_n^2 - \omega^2}. \tag{3.4}$$

Due to assumptions that γ, δ and ω_n are real and positive, functions $P(\omega)$ and $Q(\omega)$ satisfy

$$\begin{cases} P(\omega) > 0,\ Q(\omega) > 0 & \text{when} \quad \omega < \omega_n, \\ P(\omega) < 0,\ Q(\omega) < 0 & \text{when} \quad \omega > \omega_n. \end{cases} \tag{3.5}$$

The parameter γ is the gain of $C_{LL}(j\omega)$ at frequency $\omega = \omega_n$. From (5.4) and (3.3) we get:

$$\gamma = C_{LL}(j\omega_n) = \frac{P(\omega)}{Q(\omega)}\Big|_{\omega\neq\omega_n}. \tag{3.6}$$

The gain γ is the minimum (or maximum) amplitude of $C_{LL}(j\omega)$. The Nyquist and Bode diagrams of $C_{LL}(j\omega)$ for $\omega_n = 1$ and for different values of the parameters δ and γ are shown in Fig. 3.1 and Fig. 3.2. The Nyquist diagrams of Fig. 3.1 satisfy a property which is based in the following definition.

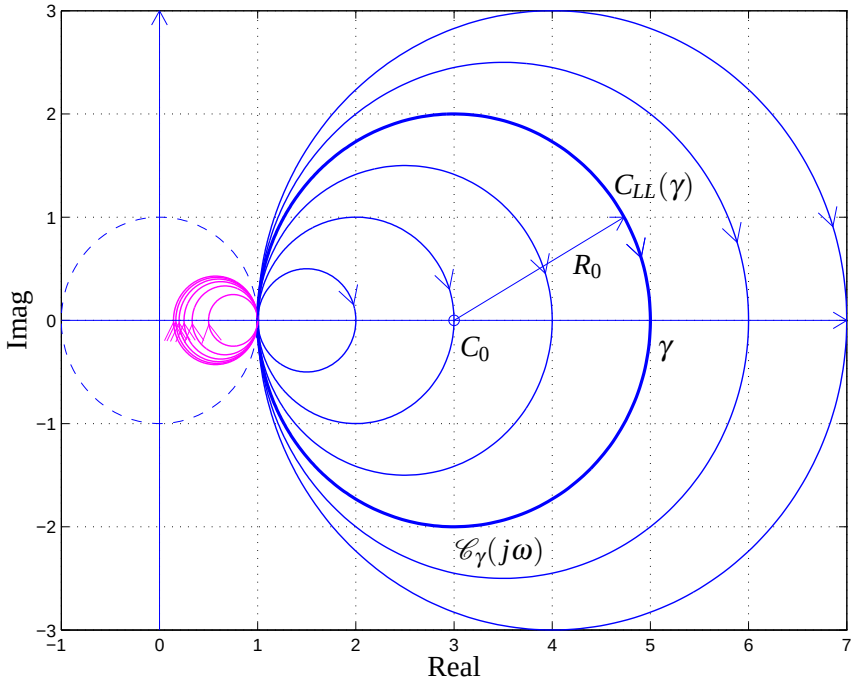

Figure 3.1: Nyquist diagrams of function $C_{LL}(j\omega)$ when $\omega_n = 1$, ($\delta = 1.5$, $\gamma = [2:1:7]$, blue lines) and ($\delta = 1.5$, $\gamma = 1./[2:1:7]$, magenta lines). The thick blue line is for $\delta = 1.5$ and $\gamma = 5$.

Definition 1 *Let $\mathscr{C}(\gamma)$ denote the set of all the Lead-Lag compensators $C_{LL}(s)$ as defined in (3.1) characterized by the same parameter γ, that is*

$$\mathscr{C}(\gamma) = \left\{ C_{LL}(s) \text{ as in } (3.1) \;\middle|\; \delta > 0, \omega_n > 0 \right\}. \tag{3.7}$$

Moreover, let $\mathscr{C}_\gamma(s) \in \mathscr{C}(\gamma)$ denote one element of $\mathscr{C}(\gamma)$ chosen arbitrarily.

Property 1 *The shape of the frequency response $\mathscr{C}_\gamma(j\omega)$ of $\mathscr{C}_\gamma(s)$ on the Nyquist plane is a circle with center C_0 and radius R_0*

$$C(\gamma) = C_0 + R_0 e^{j\theta}, \qquad C_0 = \frac{\gamma+1}{2}, \qquad R_0 = \frac{|\gamma-1|}{2} \tag{3.8}$$

where $\theta \in [0, 2\pi]$, see Fig. 3.1. The intersections of $\mathscr{C}_\gamma(j\omega)$ with the real axis occur at points 1 and γ. The shape does not depend on $\delta > 0$ and $\omega_n > 0$.

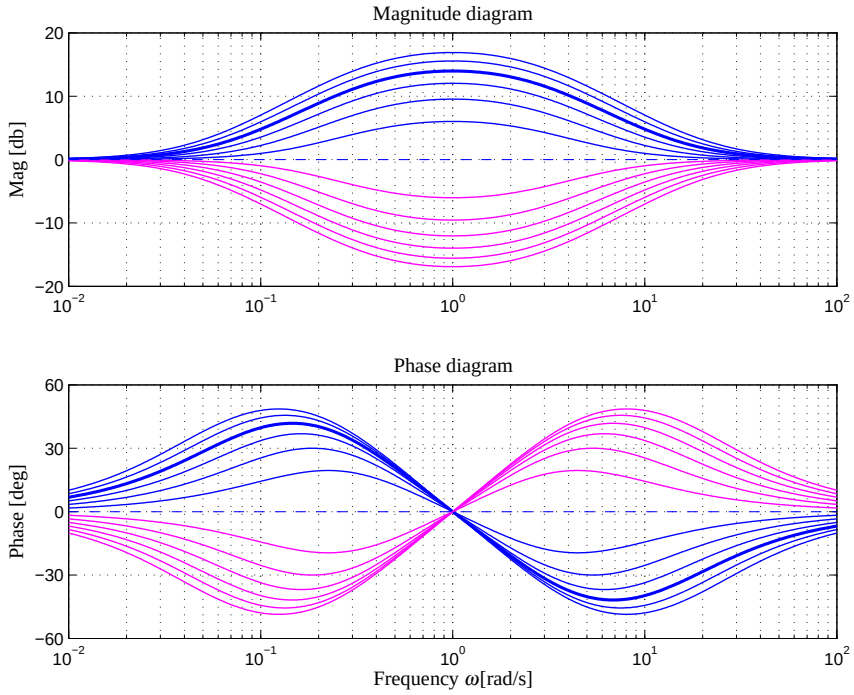

Figure 3.2: Bode diagrams of function $C_{LL}(j\omega)$ when $\omega_n = 1$, ($\delta = 1.5$, $\gamma = [2:1:7]$, blue lines) and ($\delta = 1.5$, $\gamma = 1./[2:1:7]$, magenta lines). The thick blue line is for $\delta = 1.5$ and $\gamma = 5$.

Proof: One can easily verify that the distance $d = |\mathscr{C}_\gamma(j\omega) - C_0|$ of the generic point $\mathscr{C}_\gamma(j\omega)$ from the center C_0 is constant and equal to R_0:

$$\begin{aligned} d^2 = |\mathscr{C}_\gamma(j\omega) - C_0|^2 &= \left| \frac{\omega_n^2 - \omega^2 + j\,2\gamma\delta\omega_n\omega}{\omega_n^2 - \omega^2 + j2\delta\omega_n\omega} - \frac{\gamma+1}{2} \right|^2 \\ &= \left| \frac{2(\omega_n^2 - \omega^2 + j\,2\gamma\delta\omega_n\omega) - (\gamma+1)(\omega_n^2 - \omega^2 + j2\delta\omega_n\omega)}{2(\omega_n^2 - \omega^2 + j2\delta\omega_n\omega)} \right|^2 \\ &= \left| \frac{(1-\gamma)[(\omega_n^2 - \omega^2) - j\,2\gamma\delta\omega_n\omega)]}{2(\omega_n^2 - \omega^2 + j2\delta\omega_n\omega)} \right|^2 = \left| \frac{\gamma-1}{2} \right|^2 = R_0^2. \end{aligned}$$

Variations of ω_n and δ modify the distribution of the frequency ω on the Nyquist diagram of $\mathscr{C}_\gamma(j\omega)$, but they do not change the diagram shape, which only depends on γ. □

Remark 1 *The considered Lead-Lag compensator $C_{LL}(s)$ in (3.1) is a general form which encompasses the classical form $C_r(s)$ with real poles and real zeros*

$$C_r(s) = \frac{(1+\tau_1 s)(1+\tau_2 s)}{(1+\alpha\tau_1 s)(1+\frac{\tau_2}{\alpha}s)} \tag{3.9}$$

with $0 < \tau_1 < \tau_2$ and $0 < \alpha < 1$. Details on the relations that link the parameters of the general and the classical forms $C_{LL}(s)$ and $C_r(s)$ are given in Appendix A.

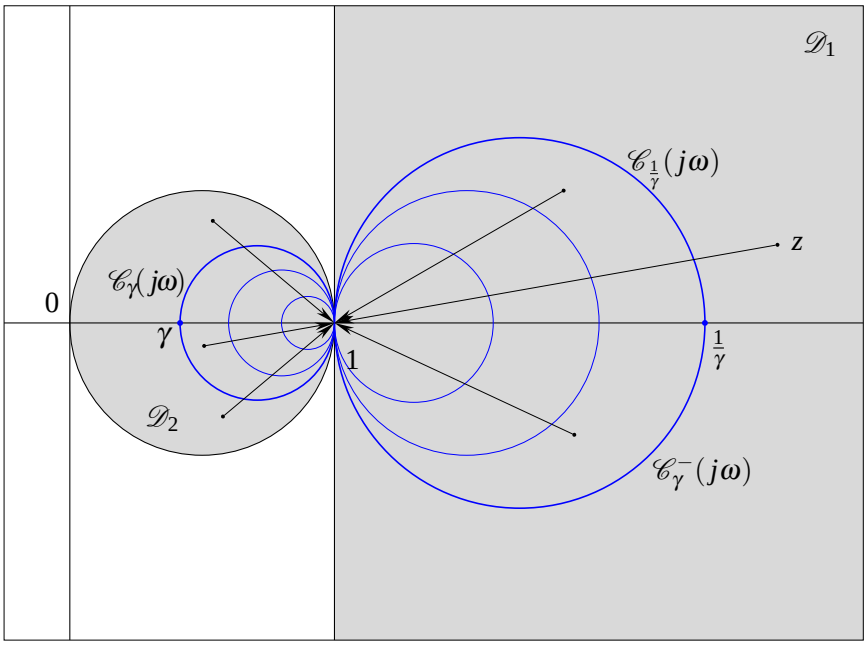

Figure 3.3: Admissible domain $\mathscr{D} = \mathscr{D}_1 \cup \mathscr{D}_2$ of Lead-Lag compensators $C_{LL}(s)$ on the Nyquist plane.

3.2 Inversion Formulae method for the design of Lead-Lag compensators

The concepts introduced in chapter 2 for the graphical and the numerical design of Lead and Lag regulators are here recalled and extended to the design of Lead-Lag compensators.

Definition 2 **($\mathscr{D}$)** *Let us define the* "admissible domain of a Lead-Lag compensator $C_{LL}(s)$" *as*

$$\mathscr{D} = \{z \in \mathbb{C} \,|\, \exists\, \gamma, \delta, \omega_n > 0, \exists\, \omega \geq 0 : \; C_{LL}(j\omega) \cdot z = 1\}.$$

Loosely speaking, the *admissible domain* $\mathscr{D}$ can be interpreted as the set of all the points $z \in \mathbb{C}$ that "can be moved" to point 1 on the Nyquist plane by pre-multiplication with the frequency response $C_{LL}(j\omega)$, where $C_{LL}(s)$ is as in (3.1), for some $\omega \geq 0$ and for suitable values of the parameters $\gamma, \delta, \omega_n > 0$, see Fig. 3.3. It can be easily verified that domain $\mathscr{D}$ is given by $\mathscr{D} = \mathscr{D}_1 \cup \mathscr{D}_2$ where

$$\mathscr{D}_1 = \left\{ z = M e^{j\varphi} \;\middle|\; -\frac{\pi}{2} < \varphi < \frac{\pi}{2},\, M > \frac{1}{\cos\varphi} \right\},$$

$$\mathscr{D}_2 = \left\{ z = M e^{j\varphi} \;\middle|\; -\frac{\pi}{2} < \varphi < \frac{\pi}{2},\, 0 < M < \cos\varphi \right\}.$$

Domain $\mathscr{D}_1$ is obtained when $\gamma > 1$ and domain $\mathscr{D}_2$ is obtained when $0 < \gamma < 1$. The shape of $\mathscr{D} = \mathscr{D}_1 \cup \mathscr{D}_2$ on the Nyquist plane is shown in Fig. 3.3, see [4].

Definition 3 *Let $\mathscr{C}^-(\gamma)$ denote the set of Lead-Lag compensators defined as*

$$\mathscr{C}^-(\gamma) = \left\{ \frac{1}{C_{LL}(s)} \;\middle|\; C_{LL}(s) \in \mathscr{C}(\gamma) \right\}, \tag{3.10}$$

with $\mathscr{C}(\gamma)$ defined in (4.10). Moreover, let $\mathscr{C}^-_\gamma(s) \in \mathscr{C}^-(\gamma)$ denote one element of the set $\mathscr{C}^-(\gamma)$ chosen arbitrarily.

Property 2 *Given $\gamma > 0$, the two sets $\mathscr{C}^-(\gamma)$ and $\mathscr{C}(\frac{1}{\gamma})$ coincide, i.e.,*

$$\mathscr{C}^-(\gamma) = \mathscr{C}(\tfrac{1}{\gamma}) \tag{3.11}$$

and the frequency responses $\mathscr{C}^-_\gamma(j\omega)$ and $\mathscr{C}_{\frac{1}{\gamma}}(j\omega)$ of $\mathscr{C}^-_\gamma(s)$ and $\mathscr{C}_{\frac{1}{\gamma}}(s)$ on the Nyquist plane have the same shape, see Fig. 3.3. The property holds also on the Nichols plane.

Proof: Each element $\mathscr{C}^-_\gamma(s)$ of $\mathscr{C}^-(\gamma)$ also belongs to $\mathscr{C}(\frac{1}{\gamma})$. In fact, from (4.10) and (3.10), it follows that

$$\mathscr{C}^-_\gamma(s) = \frac{s^2 + 2\delta\omega_n s + \omega_n^2}{s^2 + 2\gamma\delta\omega_n s + \omega_n^2} = \frac{s^2 + 2(\frac{1}{\gamma})\overline{\delta}\omega_n s + \omega_n^2}{s^2 + 2\overline{\delta}\omega_n s + \omega_n^2} \in \mathscr{C}(\tfrac{1}{\gamma}),$$

where $\overline{\delta} = \gamma\delta$. In the same way it can be easily proved that each element $\mathscr{C}_{\frac{1}{\gamma}}(s)$ of $\mathscr{C}(\frac{1}{\gamma})$ also belongs to $\mathscr{C}^-(\gamma)$, and therefore $\mathscr{C}^-(\gamma)$ and $\mathscr{C}(\frac{1}{\gamma})$ coincide. Moreover, the shape of the Nyquist diagrams of $\mathscr{C}^-_\gamma(s)$ and $\mathscr{C}_{\frac{1}{\gamma}}(s)$ depend only on γ and therefore they coincide. The extension of this property to Nichols diagrams is straightforward. □

From (4.9) and (3.11) it follows that the Nyquist diagram of $\mathscr{C}^-_\gamma(s)$ is a circle whose center $C_0 = (\gamma+1)/(2\gamma)$ lies on the real axis, whose radius is $R_0 = |\gamma-1|/(2\gamma)$ and its intersections with the real axis occur at points $a = 1$ and $b = \frac{1}{\gamma}$, see Fig. 3.3.

Definition 4 ($\mathscr{D}_B$) *Given a point $B \in \mathbb{C}$, let us define the* "admissible domain of the Lead-Lag compensator $C_{LL}(s)$ to point *B" as*

$$\mathscr{D}_B = \{A \in \mathbb{C} \mid \exists\, \gamma, \delta, \omega_n > 0, \exists\, \omega \geq 0 :\; C_{LL}(j\omega)\cdot A = B\}.$$

Domain $\mathscr{D}_B$ is the set of all the points A of the complex plane that can be moved to point B using the compensator $C_{LL}(s)$. One can easily verify that $\mathscr{D}_B$ can be expressed as $\mathscr{D}_B = \mathscr{D}_{B1} \cup \mathscr{D}_{B2}$ where

$$\mathscr{D}_{B1} = \left\{ A = M_A e^{j\varphi_A} \;\middle|\; -\frac{\pi}{2} + \varphi_B < \varphi_A < \frac{\pi}{2} + \varphi_B,\; M_A > \frac{M_B}{\cos(\varphi_A - \varphi_B)} \right\},$$

and

$$\mathscr{D}_{B2} = \left\{ A = M_A e^{j\varphi_A} \;\middle|\; -\tfrac{\pi}{2} + \varphi_B < \varphi_A < \tfrac{\pi}{2} + \varphi_B,\; 0 < M_A < M_B \cos(\varphi_A - \varphi_B) \right\},$$

see Fig. 3.4.

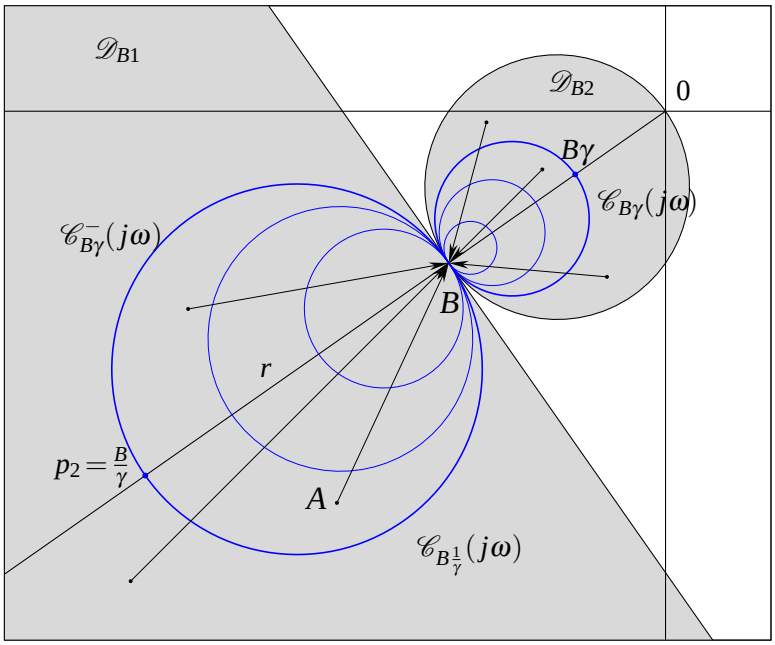

Figure 3.4: Admissible domain $\mathscr{D}_B = \mathscr{D}_{B1} \cup \mathscr{D}_{B2}$ on the Nyquist plane.

Definition 5 *Given $B \in \mathbb{C}$, let $\mathscr{C}_B(\gamma)$ and $\mathscr{C}^{-}_B(\gamma)$ denote the sets of Lead-Lag compensators $C_{LL}(s)$ defined as*

$$\mathscr{C}_B(\gamma) = \left\{ B \cdot C_{LL}(s) \mid C_{LL}(s) \in \mathscr{C}(\gamma) \right\} \tag{3.12}$$

$$\mathscr{C}^{-}_B(\gamma) = \left\{ \frac{B}{C_{LL}(s)} \;\middle|\; C_{LL}(s) \in \mathscr{C}(\gamma) \right\} \tag{3.13}$$

with $\mathscr{C}(\gamma)$ defined in (4.10). Moreover, let $\mathscr{C}_{B\gamma}(s) \in \mathscr{C}_B(\gamma)$ and $\mathscr{C}^{-}_{B\gamma}(s) \in \mathscr{C}^{-}_B(\gamma)$ denote particular elements of the two sets $\mathscr{C}_B(\gamma)$ and $\mathscr{C}^{-}_B(\gamma)$ chosen arbitrarily.

Property 3 *Given $\gamma > 0$, the two sets $\mathscr{C}^{-}_B(\gamma)$ and $\mathscr{C}_B(\frac{1}{\gamma})$ coincide, i.e.,*

$$\mathscr{C}^{-}_B(\gamma) = \mathscr{C}_B(\tfrac{1}{\gamma}), \tag{3.14}$$

and the Nyquist diagram of the frequency responses $\mathscr{C}^{-}_{B\gamma}(j\omega)$ and $\mathscr{C}_{B\frac{1}{\gamma}}(j\omega)$ of $\mathscr{C}^{-}_{B\gamma}(s)$ and $\mathscr{C}_{B\frac{1}{\gamma}}(s)$ have the same shape. The intersections p_1 and p_2 of $\mathscr{C}^{-}_{B\gamma}(j\omega)$ with the straight line r passing through points 0 and B are $p_1 = B$ and $p_2 = \frac{B}{\gamma}$. The corresponding graphical representation is shown in Fig. 3.4.

Proof: Property 3 follows directly from Property 2 because $\mathscr{C}^{-}_B(\gamma) = B \cdot \mathscr{C}^{-}(\gamma) = B \cdot \mathscr{C}(\frac{1}{\gamma})$. □

The following property shows how the Inversion Formulae (2.21) introduced for the design of first order Lead and Lag networks can be efficiently employed in the design of a Lead-Lag compensators.

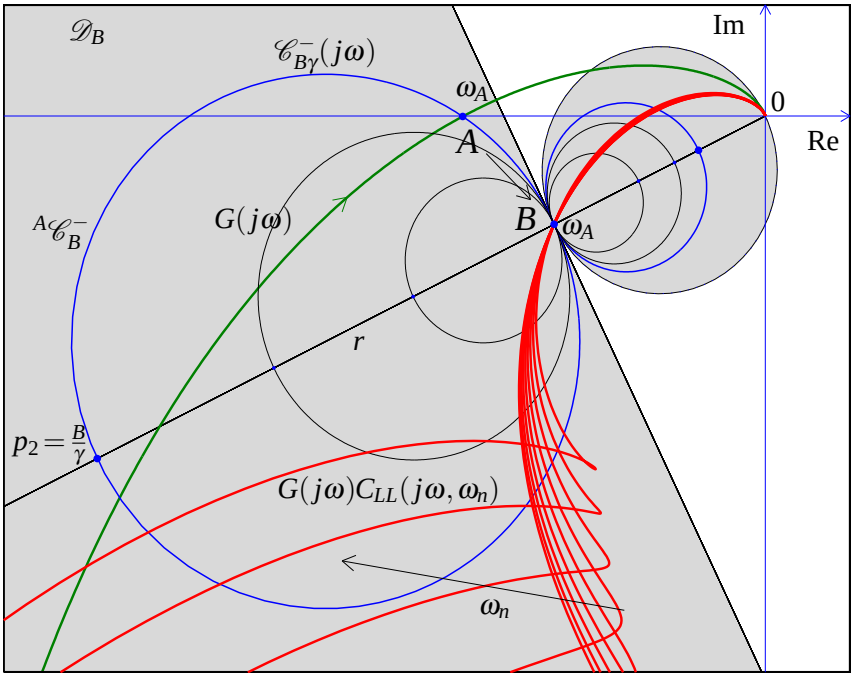

Figure 3.5: Design of the Lead-Lag compensators $C_{LL}(j\omega,\omega_n)$ moving point A to point B.

Property 4 ***(From** A **to** B**).*** *Given a point $B \in \mathbb{C}$ and chosen a point A of the frequency response $G(j\omega)$ at frequency ω_A belonging to the admissible domain $\mathscr{D}_B$, i.e. $A = G(j\omega_A) \in \mathscr{D}_B$, the set $C_{LL}(s,\omega_n)$ of all the Lead-Lag compensators $C_{LL}(s)$ that move point A to point B is obtained from (3.1) using*

$$\gamma = \frac{P}{Q} > 0, \qquad \delta = Q\frac{\omega_n^2 - \omega_A^2}{2\omega_n\omega_A} > 0, \tag{3.15}$$

for all $\omega_n > 0$ such that $\delta > 0$ and with $P = P(A,B)$ and $Q = Q(A,B)$ obtained using (2.21).

Proof: For $\omega = \omega_A$, (3.4) can be rewritten as

$$\gamma = \frac{P(\omega_A)}{Q(\omega_A)}, \qquad \delta = Q(\omega_A)\frac{\omega_n^2 - \omega_A^2}{2\omega_n\omega_A}.$$

Substituting in (3.1) one obtains

$$C_{LL}(s,\omega_n) = \frac{s^2 + P\frac{\omega_n^2-\omega_A^2}{\omega_A}s + \omega_n^2}{s^2 + Q\frac{\omega_n^2-\omega_A^2}{\omega_A}s + \omega_n^2},$$

where $P = P(\omega_A)$ and $Q = Q(\omega_A)$. The frequency response of $C_{LL}(s,\omega_n)$ at frequency ω_A is equal to the constant value

$$C_{LL}(j\omega_A,\omega_n) = C_{LL}(j\omega_A) = \frac{1+jP}{1+jQ}. \tag{3.16}$$

From (2.19) it is evident that $A = G(j\omega_A) = M_A e^{j\varphi_A}$ can be moved to $B = M_B e^{j\varphi_B}$ if and only if

$$C_{LL}(j\omega_A) = M e^{j\varphi} = \frac{M_B}{M_A} e^{j(\varphi_B - \varphi_A)}. \tag{3.17}$$

From (3.20) and (5.14) we obtain the complex equation

$$(M\cos\varphi + jM\sin\varphi)(1 + jQ) = 1 + jP,$$

which is equivalent to the following linear system

$$\begin{bmatrix} 1 & -M\cos\varphi \\ 0 & M\sin\varphi \end{bmatrix} \begin{bmatrix} P \\ Q \end{bmatrix} = \begin{bmatrix} M\sin\varphi \\ M\cos\varphi - 1 \end{bmatrix}.$$

Solving for P and Q, one directly obtains (2.21)

$$P = \frac{\begin{vmatrix} M\sin\varphi & -M\cos\varphi \\ M\cos\varphi - 1 & M_0\sin\varphi \end{vmatrix}}{M\sin\varphi} = \frac{M - \cos\varphi}{\sin\varphi},$$

$$Q = \frac{\begin{vmatrix} 1 & M\sin\varphi \\ 0 & M\cos\varphi - 1 \end{vmatrix}}{M\sin\varphi} = \frac{\cos\varphi - \dfrac{1}{M}}{\sin\varphi}.$$

The assumption that A belongs to the admissible domain $\mathscr{D}_B$ ensures that there exist admissible Lead-Lag controllers $C_{LL}(s,\omega_n)$ moving point A to point B which are characterized by positive parameters γ, δ and ω_n, see Definition 4. All the admissible values of ω_n are those that satisfy $\delta > 0$ in (3.15). □

From (3.15) and (2.21) it follows that the gain γ of $C_{LL}(s,\omega_n)$ at $\omega = \omega_n$ is

$$\gamma = \frac{P}{Q} = \frac{M - \cos\varphi}{\cos\varphi - \frac{1}{M}}. \tag{3.18}$$

Note that γ does not depend on ω_A and ω_n, but only on the position of A and B.

Property 5 *Given two points A and B such that $A \in \mathscr{D}_B$, the gain γ in (3.15) can be graphically determined as shown in Fig. 3.5:*

1) *draw the unique circle ${}^{A}\mathscr{C}_B^-$ that passes through points A and B having its diameter on the straight line r which passes through points* 0 *and B;*
2) *the circle ${}^{A}\mathscr{C}_B^-$ intersects the straight line r at points $p_1 = B$ and $p_2 = B/\gamma$;*
3) *the gain γ is equal to the modulus of point B over the modulus of point p_2: $\gamma = |B|/|p_2|$.*

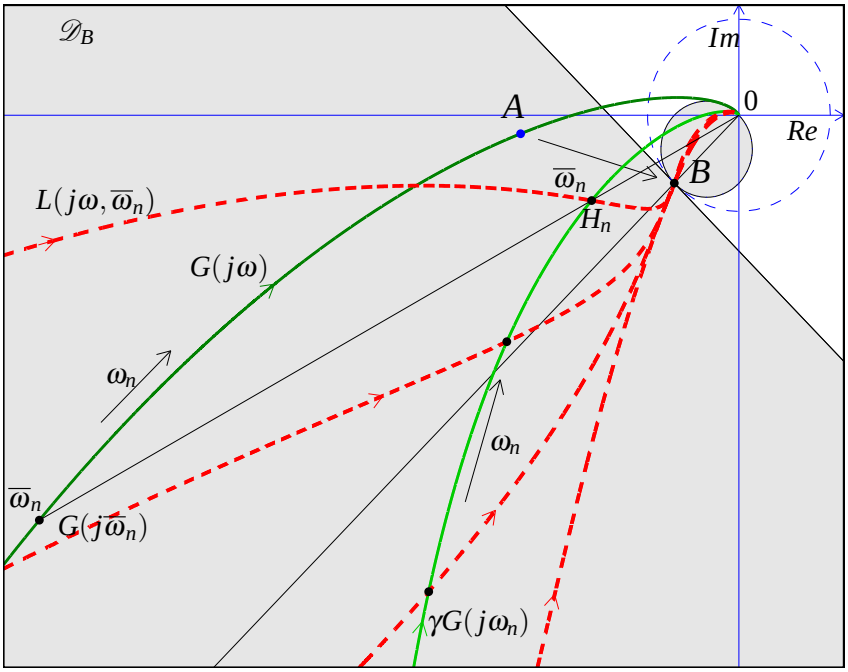

Figure 3.6: The Nyquist plots of the set of $L(j\omega,\omega_n)$ passing on B and graphical interpretation of $\gamma G(j\omega)$.

Proof: It follows directly from Property 3 because the circle ${}^{A}\mathscr{C}_B^-$ on the Nyquist plane coincides with the frequency response $\mathscr{C}_{B\gamma}^-(j\omega)$ of $\mathscr{C}_{B\gamma}^-(s) \in \mathscr{C}_B^-(\gamma)$ and because the intersections of these functions with the straight line r occur at points B and $p_2 = B/\gamma$. □

From Prop. (4), the set of all the compensators (3.1) that bring the point A at frequency ω_A to the point B can be expressed as

$$C(s,\omega_n) = \frac{s^2 + \frac{P(A,B)}{\omega_A}(\omega_n^2 - \omega_A^2)s + \omega_n^2}{s^2 + \frac{Q(A,B)}{\omega_A}(\omega_n^2 - \omega_A^2)s + \omega_n^2}. \tag{3.19}$$

In this way all the loop gain frequency responses $L(j\omega,\omega_n) = G(j\omega)C(j\omega,\omega_n)$, for $\omega_n \in (0,\omega_A)$, pass thought the required point B at frequency ω_A, see Fig. 3.6. However the choice of the parameter ω_n influences heavily the close-loop performances and stability [26]. Compensators $C(s,\omega_n)$ satisfy the following Properties 6 and 7.

Property 6 *All the frequency responses $C(j\omega,\omega_n)$, for $\omega_n \in (0,\omega_A)$, have the same parameter γ and the same shape on the Nyquist diagram: a circle with center $C_0 = \frac{\gamma+1}{2}$ and radius $R_0 = \frac{|\gamma-1|}{2}$ (see Fig. 3.7). The value of parameter ω_n modifies the distribution of the frequencies ω on the Nyquist diagram, except*

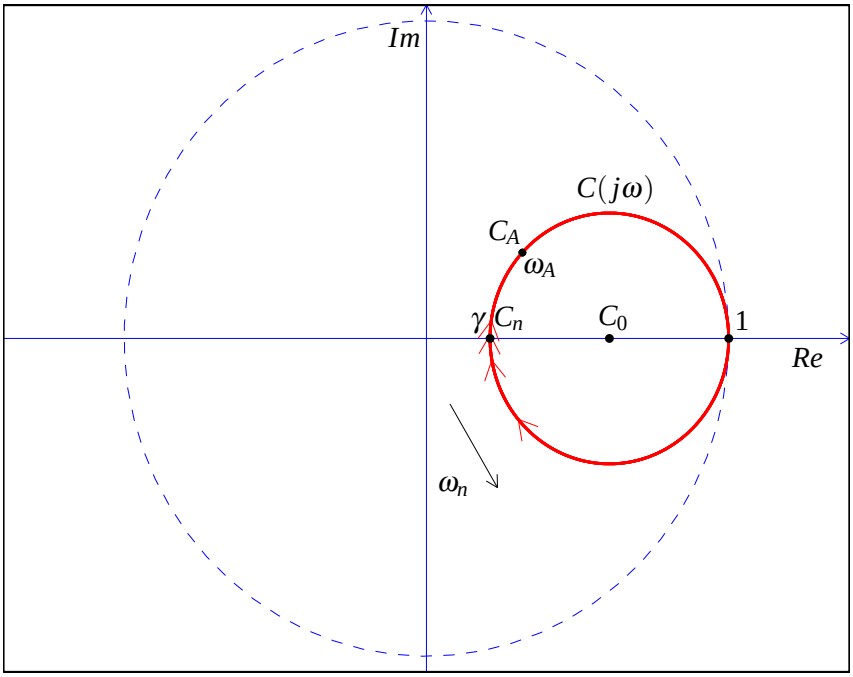

Figure 3.7: The Nyquist diagrams of $C(j\omega,\omega_n)$ on variations of ω_n.

for frequency ω_A corresponding to the point $C_A = C(j\omega_A,\omega_n)$, which is constant and does not depend on ω_n:

$$C_A = C(j\omega_A,\omega_n) = \frac{1+jP(A,B)}{1+jQ(A,B)} = C(j\omega_A). \tag{3.20}$$

Similarly, the Bode diagrams of $C(j\omega,\omega_n)$ when $\omega_n \in (0,\omega_A)$ are shown in Fig. 3.8: the blue highlighted points $C_n(\omega_n)$ denote the magnitudes and the phases of $C(j\omega,\omega_n)$ at frequency ω_n. Only point C_A does not change its magnitude and its phase when ω_n varies.

Property 7 *Given the loop gain frequency response $L(j\omega,\overline{\omega}_n) = G(j\omega)C(j\omega,\overline{\omega}_n)$ for a particular value $\overline{\omega}_n \in (0,\omega_A)$, the point $H_n = L(j\omega_n,\overline{\omega}_n)|_{\omega=\omega_n}$ is $H_n = \gamma G(j\overline{\omega}_n)$. Point H_n can be graphically determined on the Nyquist plane as the point $\gamma G(j\overline{\omega}_n)$ where function $L(j\omega,\overline{\omega}_n)$ intersects the straight line passing through points $G(j\overline{\omega}_n)$ and 0. So, for $\omega_n \in (0,\omega_A)$, the function $\gamma G(j\omega_n)$ is the locus of all the points of the loop gain frequency responses $L(j\omega,\omega_n) = C(j\omega,\omega_n)G(j\omega)$ at frequency $\omega = \omega_n$, see Fig. 3.6.*

The proof follows directly from Prop. 6 and from the fact that, for every $\omega_n \in (0,\omega_A)$, it is

$$L(j\omega_n,\omega_n) = C(j\omega_n,\omega_n)G(j\omega_n) = \gamma G(j\omega_n). \tag{3.21}$$

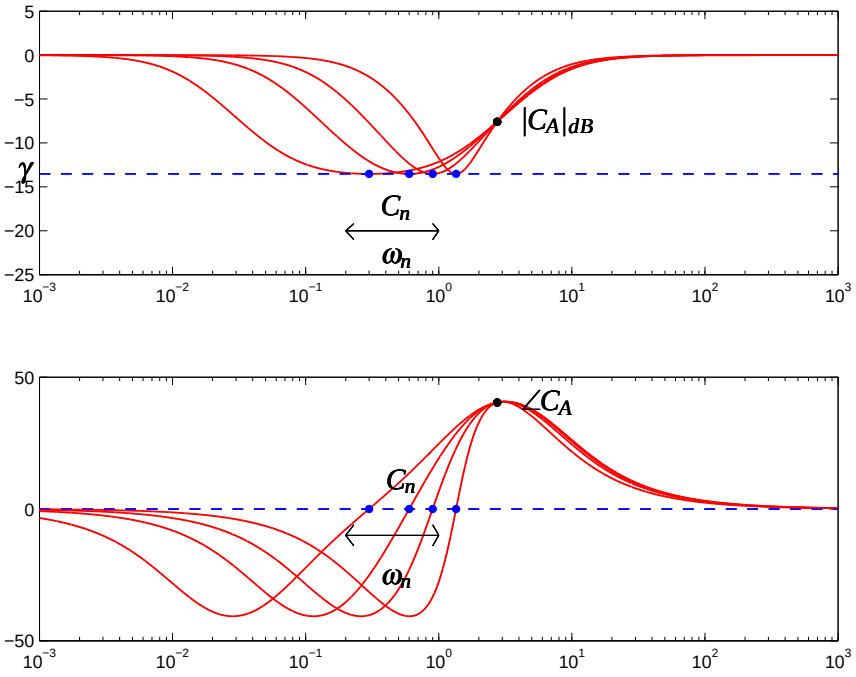

Figure 3.8: The Bode diagrams of $C(j\omega,\omega_n)$ on variations of ω_n.

3.3 Synthesis of Lead-Lag compensators

In this section the Design Problems concerning the synthesis of Lead-Lag compensators $C_{LL}(s)$ based on the following design specifications will be addressed, see Tab. 1.1: ***A)*** phase margin ϕ_m and gain crossover frequency ω_g; ***B)*** gain margin G_m and phase crossover frequency ω_p; ***C)*** phase margin ϕ_m, gain margin G_m and gain crossover frequency ω_g; ***D)*** phase margin ϕ_m, gain margin G_m and phase crossover frequency ω_p; ***E)*** phase margin ϕ_m and gain margin G_m.

Design Problem A: (ϕ_m,ω_g). Given the transfer function $G(s)$ and the design specifications on the phase margin ϕ_m and on the gain crossover frequency ω_g, design the Lead-Lag compensator $C_{LL}(s)$ such that the loop gain transfer function $C_{LL}(j\omega)G(j\omega)$ passes through point $B_g = e^{j(\pi+\phi_m)}$ for $\omega=\omega_g$.

Solution A: *Let $A_g = G(j\omega_g)$ denote the value of $G(j\omega)$ at the desired gain crossover frequency $\omega=\omega_g$ and let $B_g = e^{j(\pi+\phi_m)}$ denote the point corresponding to the desired phase margin ϕ_m. The set $C_g(s,\omega_n)$ of all the compensators $C_{LL}(s)$ which solve Design Problem A is obtained from (3.1) using the parameters*

$$\gamma = \frac{P_g}{Q_g} > 0, \qquad \delta = Q_g \frac{\omega_n^2-\omega_g^2}{2\omega_n\omega_g} > 0 \tag{3.22}$$

for all $\omega_n > 0$ such that $\delta > 0$ and with $P_g = P(A_g,B_g)$ and $Q_g = Q(A_g,B_g)$ obtained using (2.21).

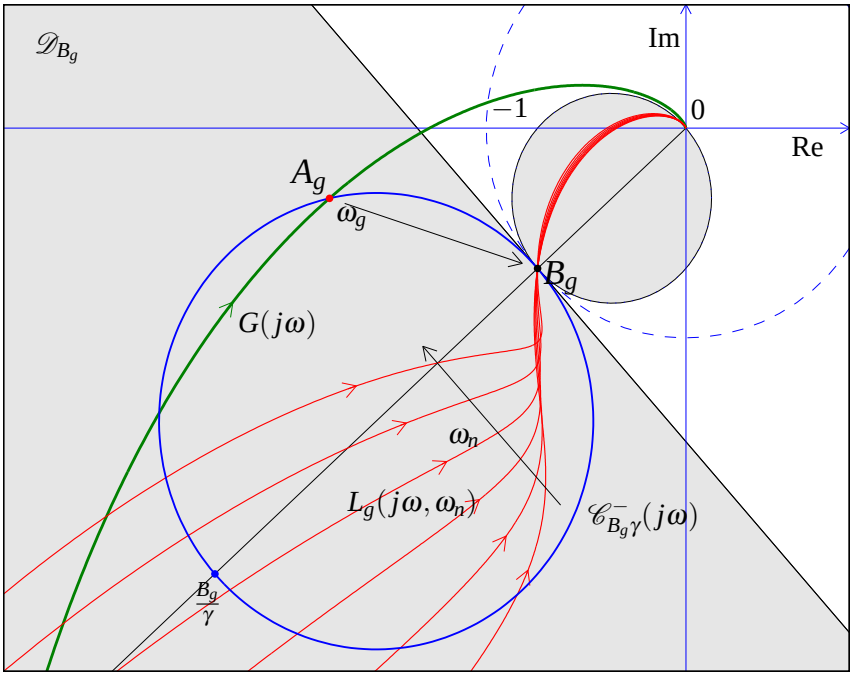

Figure 3.9: Graphical solution of Design Problem A on the Nyquist plane.

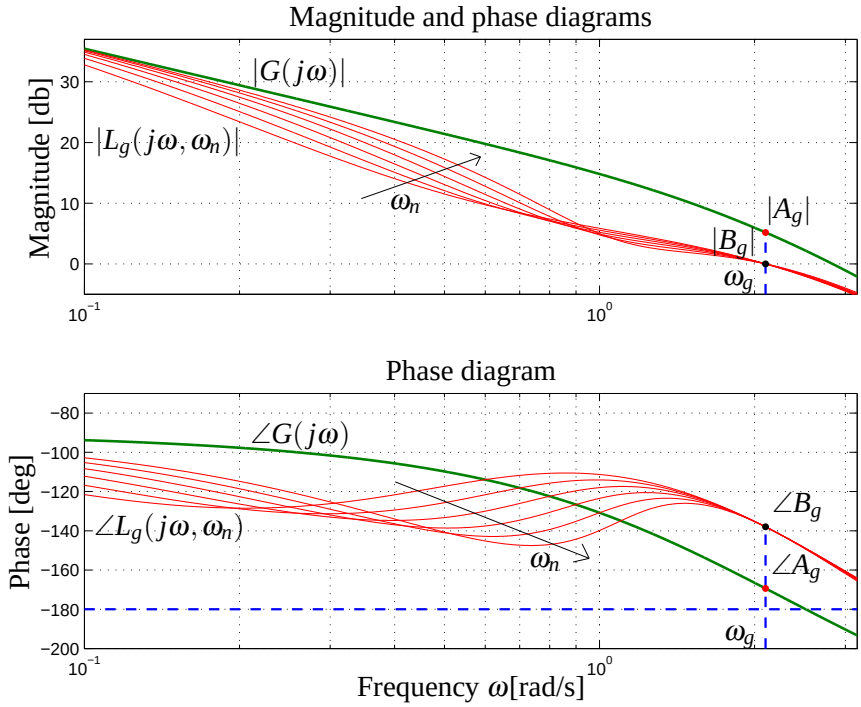

Figure 3.10: Graphical representation of the solution of Design Problem A on the Bode diagrams.

Proof: The design specifications on the phase margin ϕ_m and gain crossover frequency ω_g can be satisfied if and only if the loop gain frequency response $C_{LL}(j\omega)G(j\omega)$ at $\omega=\omega_g$ is equal to B_g, that is if and only if $B_g = C_{LL}(j\omega_g)\cdot A_g$. According to Definition 4, Design Problem A has a solution only if point A_g belongs to the admissible domain $\mathscr{D}_{B_g}$, see the grey region in Fig. 3.9. The parameters (3.22) of all the compensators $C_g(s,\omega_n)$ which move point A_g to point B_g are obtained from Property 4 when $\omega_A=\omega_g$, $A=A_g$ and $B=B_g$. □

Examples of the loop gain frequency response $L_g(j\omega,\omega_n)=C_g(j\omega,\omega_n)G(j\omega)$ obtained from (3.22) for different values of ω_n are plotted in red in Fig. 3.9 and 3.10. The blue circle $\mathscr{C}^-_{B_g\gamma}(j\omega)$ represents the frequency response of all the functions $\mathscr{C}^-_{B_g\gamma}(s)\in\mathscr{C}^-_{B_g}(\gamma)$ with $\gamma=P_g/Q_g$ given in (3.22). The free parameter ω_n of $C_g(s,\omega_n)$ can be used to satisfy an additional constraint such as, for example, a desired gain margin G_m as required in Design Problem C.

Design Problem B: (G_m,ω_p). Given the transfer function $G(s)$ and design specifications on the gain margin G_m and phase crossover frequency ω_p, design the Lead-Lag compensator $C_{LL}(s)$ such that $C_{LL}(j\omega)G(j\omega)$ passes through point $B_p=-1/G_m$ for $\omega=\omega_p$.

Solution B: *Let $A_p=G(j\omega_p)$ denote the value of $G(j\omega)$ at the desired phase crossover frequency $\omega=\omega_p$ and let $B_p=-1/G_m=M_{B_p}e^{j\varphi_{B_p}}$ denote the point corresponding to the desired gain margin G_m. The set $C_p(s,\omega_n)$ of all the compensators $C_{LL}(s)$ which solve the Design Problem B is obtained from (3.1) using*

$$\gamma=\frac{P_p}{Q_p}>0,\qquad \delta=Q_p\frac{\omega_n^2-\omega_p^2}{2\omega_n\omega_p}>0, \tag{3.23}$$

for all $\omega_n>0$ such that $\delta>0$ and with $P_p=P(A_p,B_p)$ and $Q_p=Q(A_p,B_p)$ obtained using (2.21).

Proof: The design specifications on the gain margin G_m and phase crossover frequency ω_p are satisfied if and only if $B_p=C_{LL}(j\omega_p)\cdot A_p$. According to Definition 2, Design Problem B has a solution only if A_p belongs to $\mathscr{D}_{B_p}$, see the grey region in Fig. 3.11. The parameters (3.23) of all the compensators $C_p(s,\omega_n)$ which move A_p to B_p are obtained from Property 4 when $\omega_A=\omega_p$, $A=A_p$ and $B=B_p$. □

The loop gain frequency responses $L_p(j\omega,\omega_n)=C_p(j\omega,\omega_n)G(j\omega)$ obtained from (3.23) for different values of ω_n are plotted in red in Fig. 3.11 and 3.12. The blue circle $\mathscr{C}^-_{B_p\gamma}(j\omega)$ in Fig. 3.11 represents the frequency response of all the functions $\mathscr{C}^-_{B_p\gamma}(s)\in\mathscr{C}^-_{B_p}(\gamma)$ with $\gamma=P_p/Q_p$ given in (3.23). The free parameter ω_n of $C_p(s,\omega_n)$ can be used to satisfy, for example, a constraint on ϕ_m.

Design Problem C: $(\phi_m\ ,\ G_m\ ,\ \omega_g)$. Given the transfer function $G(s)$ and design specifications on the phase margin ϕ_m, gain margin G_m and gain crossover frequency ω_g, design a Lead-Lag compensator $C_{LL}(s)$ such that $C_{LL}(j\omega)G(j\omega)$ passes through $B_g=e^{j(\pi+\phi_m)}$ for $\omega=\omega_g$ and $B_p=-1/G_m$.

Solution C: *Let $A_g=G(j\omega_g)$ denote the value of $G(j\omega)$ at the desired gain crossover frequency*

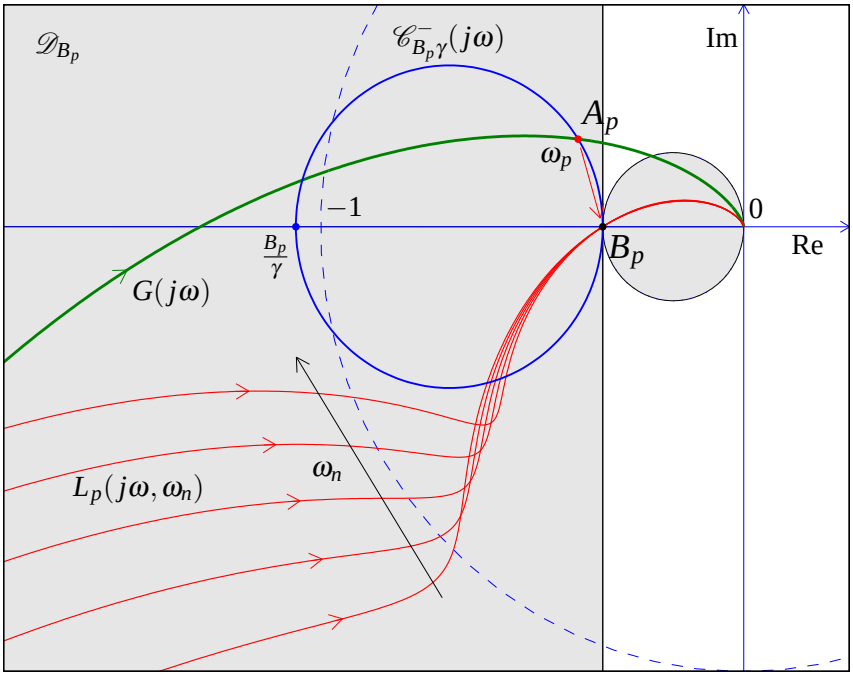

Figure 3.11: Graphical solution of Design Problem B on the Nyquist plane.

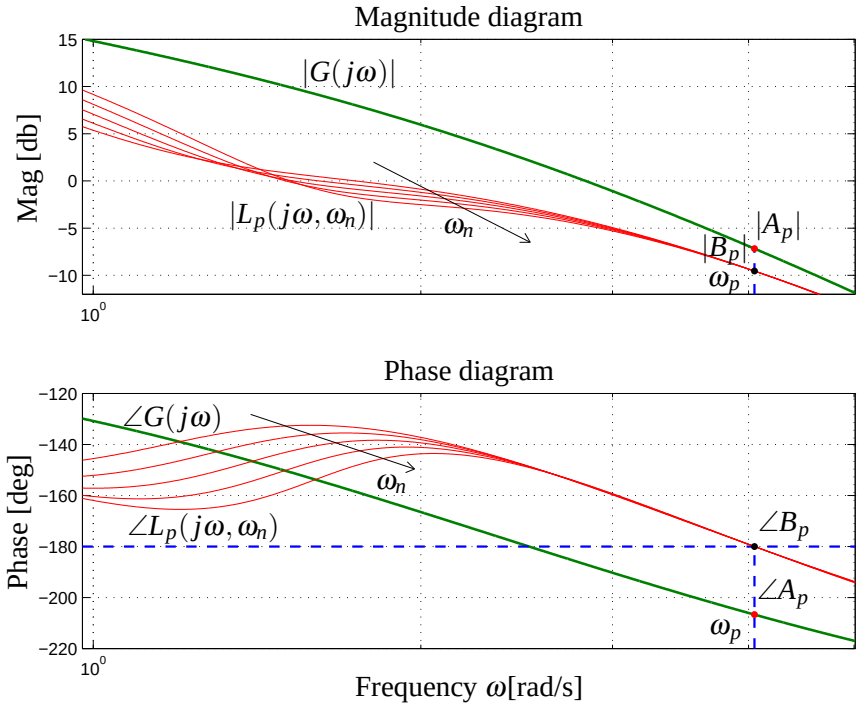

Figure 3.12: Graphical representation of the solution of Design Problem B on the Bode diagrams.

$\omega=\omega_g$, and let $B_g=e^{j(\pi+\phi_m)}$ and $B_p=-1/G_m=M_{B_p}e^{j\varphi_{B_p}}$ denote the complex points corresponding to the desired phase margin ϕ_m and gain margin G_m, respectively. The set $C_g(s,\omega_p)$ of all the Lead-Lag compensators $C_{LL}(s)$ which solve Design Problem C is obtained from (3.1) using

$$\gamma=\frac{P_g}{Q_g}>0, \qquad \delta=Q_g\frac{\omega_n^2-\omega_g^2}{2\omega_n\omega_g}>0, \tag{3.24}$$

$$\omega_n=\sqrt{\frac{Q_p\,\omega_p-Q_g\,\omega_g}{\frac{Q_p}{\omega_p}-\frac{Q_g}{\omega_g}}}>0, \tag{3.25}$$

where the coefficients $P_g=P(A_g,B_g)$, $Q_g=Q(A_g,B_g)$, $P_p=P(A_p,B_p)$ and $Q_p=Q(A_p,B_p)$ are obtained using the inversion formulae (2.21) with $A_p=G(j\omega_p)=M_{A_p}(\omega_p)e^{j\varphi_{A_p}(\omega_p)}$, for all the frequencies ω_p satisfying

$$\gamma=\gamma_p(\omega_p), \tag{3.26}$$

where $\gamma_p(\omega_p)=P_p/Q_p$ is defined as

$$\gamma_p(\omega_p)=\frac{\frac{M_{B_p}}{M_{A_p}(\omega_p)}-\cos(\varphi_{B_p}-\varphi_{A_p}(\omega_p))}{\cos(\varphi_{B_p}-\varphi_{A_p}(\omega_p))-\frac{M_{A_p}(\omega_p)}{M_{B_p}}}. \tag{3.27}$$

A solution $C_g(s,\omega_p)$ of Design Problem C exists only if: 1) the set S_{ω_p} of all the ω_p satisfying (3.26) is not empty; 2) $A_g\in\mathscr{D}_{B_g}$ and $A_p\in\mathscr{D}_{B_p}$; 3) ω_n and δ in (3.24) and (3.25) are real and positive.

Proof: The design specifications completely define the position of points B_g, A_g and B_p. According to Solution A, the Lead-Lag compensators $C_g(s,\omega_n)$ which move point $A_g\in\mathscr{D}_{B_g}$ to point B_g are obtained using the parameters γ and δ in (3.24). The free parameter ω_n can now be used to force the loop gain frequency response $C_g(j\omega,\omega_n)G(j\omega)$ to pass through point B_p. This condition can be satisfied only if a frequency ω_p exists such that $C_g(s,\omega_n)$ moves point $A_p=G(j\omega_p)\in\mathscr{D}_{B_p}$ to point B_p, that is only if

$$\gamma=\frac{P_p}{Q_p}=\frac{P(A_p,B_p)}{Q(A_p,B_p)}. \tag{3.28}$$

This relation does not depend on ω_n, but only on the design specifications ϕ_m, G_m and ω_g. Substitution of (2.21), $M=\frac{M_B}{M_A}$ and $\varphi=\varphi_B-\varphi_A$ into (3.28) yields (3.26)-(4.14). The frequencies $\omega_p\in S_{\omega_p}$ satisfying (3.26) are acceptable only if the compensator $C_p(s,\omega_n)$ obtained using Solution B is equal to $C_g(s,\omega_n)$. This condition is satisfied only if the two compensators share the same δ, that is only if

$$\delta=Q_g\frac{\omega_n^2-\omega_g^2}{2\omega_n\omega_g}=Q_p\frac{\omega_n^2-\omega_p^2}{2\omega_n\omega_p}>0. \tag{3.29}$$

Solving (3.29) with respect to ω_n leads to (3.25). □

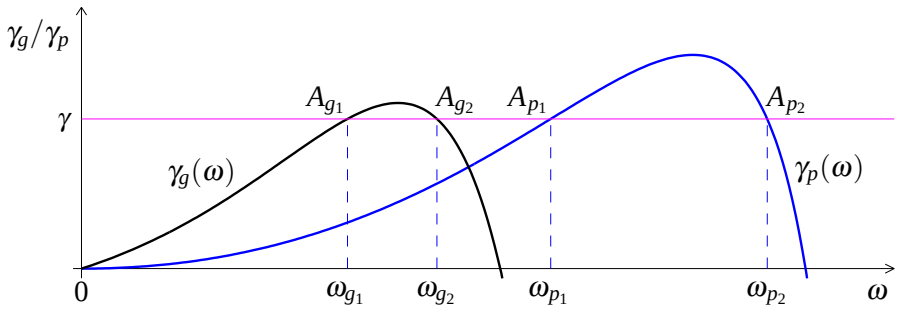

Figure 3.13: Functions $\gamma_p(\omega)$ (blue line) and $\gamma_g(\omega)$ (black line).

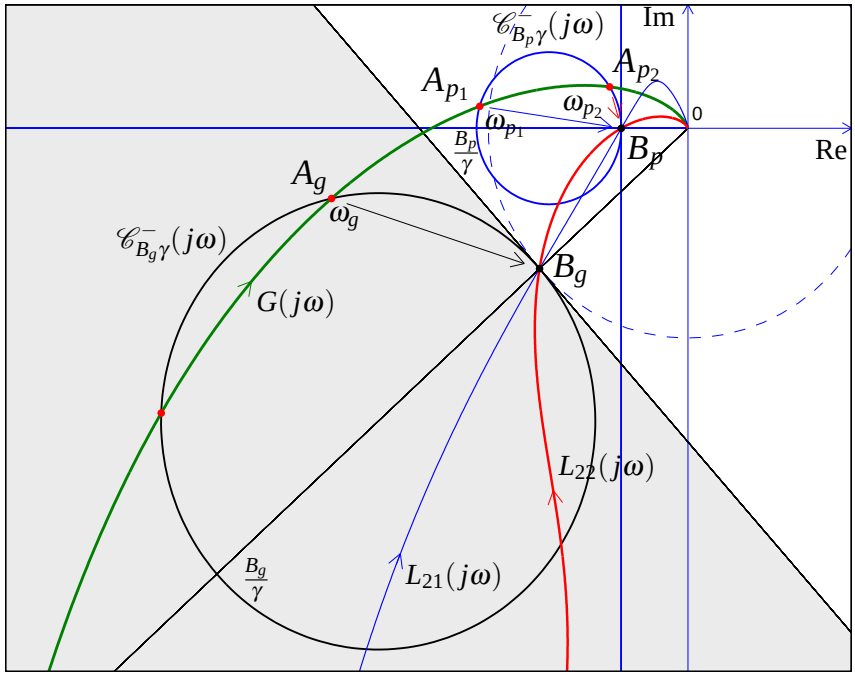

Figure 3.14: Graphical solution of Design Problem C on the Nyquist plane.

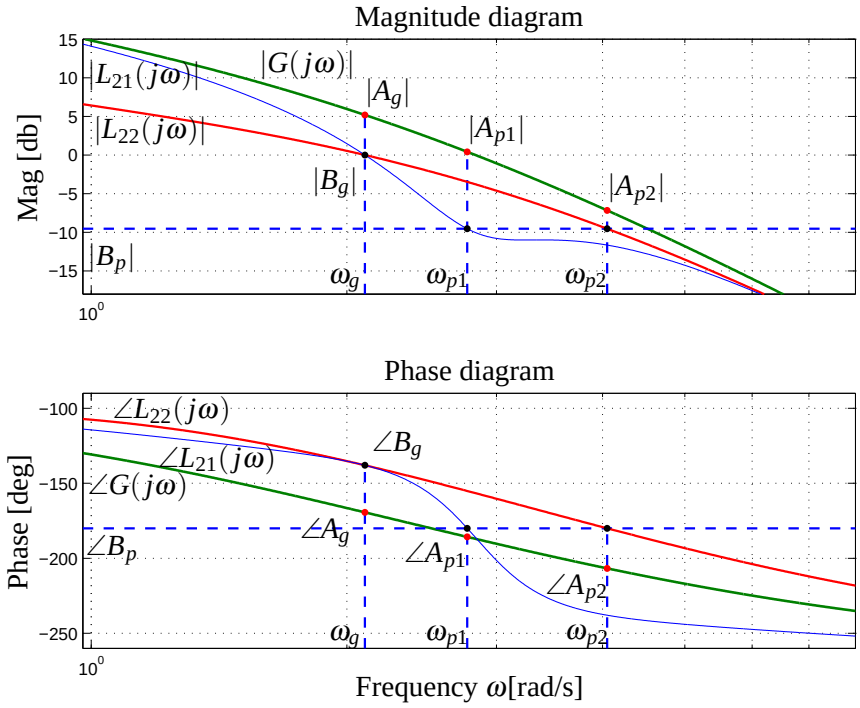

Figure 3.15: Graphical representation of the solution of Design Problem C on the Bode diagrams.

The solution of (3.26) can also be obtained graphically by plotting $\gamma_p(\omega)$ and by finding all the frequencies $\omega_p \in S_{\omega_p}$ for which $\gamma_p(\omega_p)$ intersects the horizontal line γ, see Fig. 3.13. In the example of Fig. 3.13 it is $S_{\omega_p} = \{\omega_{p1},\ \omega_{p2}\}$ and therefore there are two solutions: $C_g(s,\omega_{p1})$ and $C_g(s,\omega_{p2})$. The corresponding loop gain frequency responses $L_{21}(j\omega) = C_g(j\omega,\omega_{p1})G(j\omega)$ (thin blue line) and $L_{22}(j\omega) = C_g(j\omega,\omega_{p2})G(j\omega)$ (red line) on the Nyquist and the Bode diagrams are shown in Fig. 3.14 and 3.15. Both solutions satisfy the design specifications and are acceptable because $\delta > 0$ and $\omega_n > 0$.

Property 8 *The frequencies $\omega_p \in S_{\omega_p}$ satisfying (3.26) can be graphically determined on the Nyquist plane as shown in Fig. 3.14:*

1) *draw the circle $\mathscr{C}^-_{B_g\gamma}(j\omega)$ on the Nyquist plane passing through points A_g and B_g with its diameter on the segment $(B_g, \frac{B_g}{\gamma})$;*

2) *determine the gain γ of the Lead-Lag compensators $C_g(s,\omega_p)$ as described in Property 5 when $A = A_g$ and $B = B_g$;*

3) *draw the circle $\mathscr{C}^-_{B_p\gamma}(j\omega)$ having its diameter on the segment $(B_p, \frac{B_p}{\gamma})$;*

4) *the intersections A_{pi} of $\mathscr{C}^-_{B_p\gamma}(j\omega)$ with $G(j\omega)$ correspond to the frequencies ω_{pi} belonging to the set S_{ω_p}.*

Proof: The circles $\mathscr{C}^-_{B_g\gamma}(j\omega)$ (black line) and $\mathscr{C}^-_{B_p\gamma}(j\omega)$ (blue line) shown in Fig. 3.14 represent, respectively, the frequency responses of $\mathscr{C}^-_{B_g\gamma}(s) \in \mathscr{C}^-_{B_g}(\gamma)$ and $\mathscr{C}^-_{B_p\gamma}(s) \in \mathscr{C}^-_{B_p}(\gamma)$ with $\gamma = P_g/Q_g = P_p/Q_p$ given in (3.26) and (3.28). These two circles can be easily determined on the Nyquist plane because A_g, B_g and B_p are known (they follow from the design specifications) and γ is given by the graphical construction described in Property 5. A frequency ω_p satisfying (3.26) exists only if

$$G(j\omega_p)C_\gamma(j\omega_p) = B_p, \tag{3.30}$$

where $C_\gamma(s)$ is the Lead-Lag compensator (3.1) with the value of γ determined as described above. Relation (5.34) can be rewritten as

$$G(j\omega) = \frac{B_p}{C_\gamma(j\omega)} = \mathscr{C}^-_{B_p\gamma}(j\omega), \tag{3.31}$$

with $\omega = \omega_p$, and therefore it can be solved graphically on the Nyquist plane by finding the intersections ω_p of $G(j\omega)$ with $\mathscr{C}^-_{B_p\gamma}(j\omega)$. □

Design Problem D: (ϕ_m , G_m , ω_p). Given the transfer function $G(s)$ and the design specifications on the phase margin ϕ_m, gain margin G_m and phase crossover frequency ω_p, design a Lead-Lag compensator $C_{LL}(s)$ such that $C_{LL}(j\omega)G(j\omega)$ passes through point $B_p = -1/G_m$ for $\omega = \omega_p$ and passes through point $B_g = e^{j(\pi+\phi_m)}$.

Solution D: *The given design specifications completely define the points* $A_p = G(j\omega_p)$, $B_g = e^{j(\pi+\phi_m)}$ *and* $B_p = -1/G_m = M_{B_p}e^{j\varphi_{B_p}}$. *The set* $C_p(s,\omega_g)$ *of all the Lead-Lag compensators* $C_{LL}(s)$ *which solve Design Problem D is obtained from (3.1) using*

$$\gamma = \frac{P_p}{Q_p} > 0, \qquad \delta = Q_p\frac{\omega_n^2 - \omega_p^2}{2\omega_n\omega_p} > 0, \tag{3.32}$$

$$\omega_n = \sqrt{\frac{Q_p\,\omega_p - Q_g\,\omega_g}{\frac{Q_p}{\omega_p} - \frac{Q_g}{\omega_g}}} > 0, \tag{3.33}$$

where $P_p = P(A_p,B_p)$, $Q_p = Q(A_p,B_p)$, $P_g = P(A_g,B_g)$ *and* $Q_g = Q(A_g,B_g)$ *are obtained using (2.21) with* $A_g = G(j\omega_g) = M_{A_g}(\omega_g)e^{j\varphi_{A_g}(\omega_g)}$, *for all the frequencies* ω_g *satisfying*

$$\gamma = \gamma_g(\omega_g), \tag{3.34}$$

where $\gamma_g(\omega_g) = P_g/Q_g$ *is defined as*

$$\gamma_g(\omega_g) = \frac{\frac{M_{B_g}}{M_{A_g}(\omega_g)} - \cos(\varphi_{B_g} - \varphi_{A_g}(\omega_g))}{\cos(\varphi_{B_g} - \varphi_{A_g}(\omega_g)) - \frac{M_{A_g}(\omega_g)}{M_{B_g}}}. \tag{3.35}$$

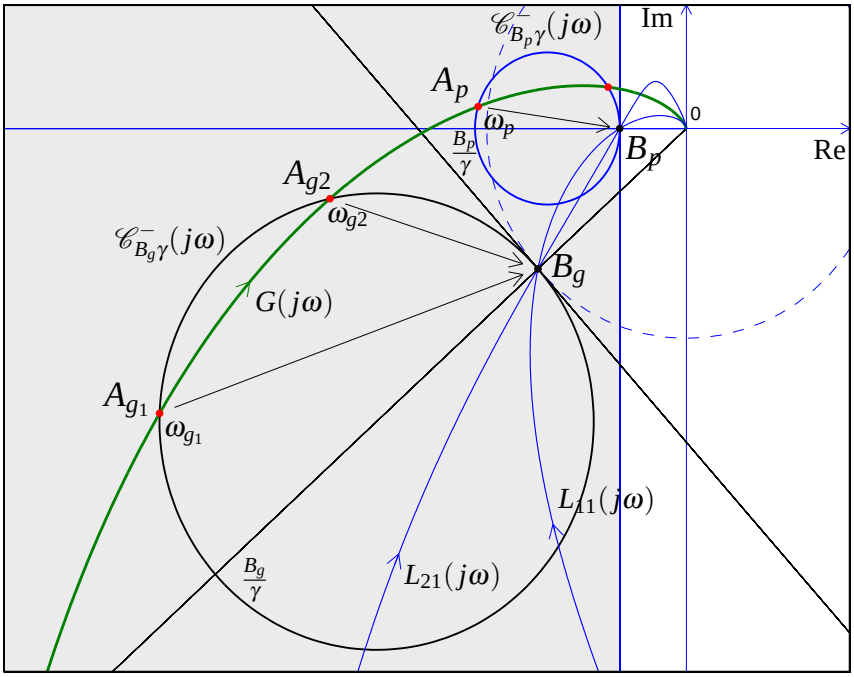

Figure 3.16: Graphical solution of Design Problem D on the Nyquist plane.

A solution $C_p(s,\omega_g)$ of Design Problem D exists only if: 1) the set S_{ω_g} of all the ω_g satisfying $\gamma=\gamma_g(\omega_g)$ is not empty; 2) $A_p\in\mathscr{D}_{B_p}$ and $A_g\in\mathscr{D}_{B_g}$; 3) ω_n and δ in (3.33) are real and positive.

Proof: The proof is similar to that of Solution C. The positions of $B_g=e^{j(\pi+\phi_m)}$, $B_p=-1/G_m$ and $A_p=G(j\omega_p)$ are directly determined by the given design specifications. The parameters γ and δ in (3.32) define the structure of the Lead-Lag compensators $C_p(s,\omega_n)$ which move $A_p\in\mathscr{D}_{B_p}$ to B_p. The loop gain $C_p(j\omega,\omega_n)G(j\omega)$ passes through B_g only if a frequency ω_g exists such that $C_p(s,\omega_n)$ moves $A_g=G(j\omega_g)\in\mathscr{D}_{B_g}$ to B_g, that is only if the relation $\gamma=\frac{P_g}{Q_g}=\gamma_g(\omega_g)$ given in (3.34) holds. The frequencies $\omega_g\in S_{\omega_g}$ satisfying (3.34) are acceptable only if (3.29) holds. From this relation one directly obtains (3.33). □

The graphical solution of (3.34) can be obtained, see Fig. 3.13, by plotting $\gamma_g(\omega)$ (the black line) and by finding all the frequencies $\omega_g\in S_{\omega_g}$ where $\gamma_g(\omega_g)$ intersects the horizontal line γ. In Fig. 3.13 it is $S_{\omega_g}=\{\omega_{g1},\ \omega_{g2}\}$. The corresponding loop gain frequency responses $L_{11}(j\omega)=C_g(j\omega,\omega_{g1})G(j\omega)$ and $L_{21}(j\omega)=C_g(j\omega,\omega_{g2})G(j\omega)$ on the Nyquist and Bode diagrams are the thin blue lines shown in Fig. 3.16 and 3.17. These solutions are acceptable only if $\delta>0$ and $\omega_n>0$ in (3.32) and (3.33).

Property 9 *The frequencies $\omega_g\in S_{\omega_g}$ satisfying (3.34) can be graphically determined on the Nyquist plane as follows, see Fig. 3.16:*

1) draw the circle $\mathscr{C}^{-}_{B_p\gamma}(j\omega)$ on the Nyquist plane passing through points A_p and B_p with its diameter

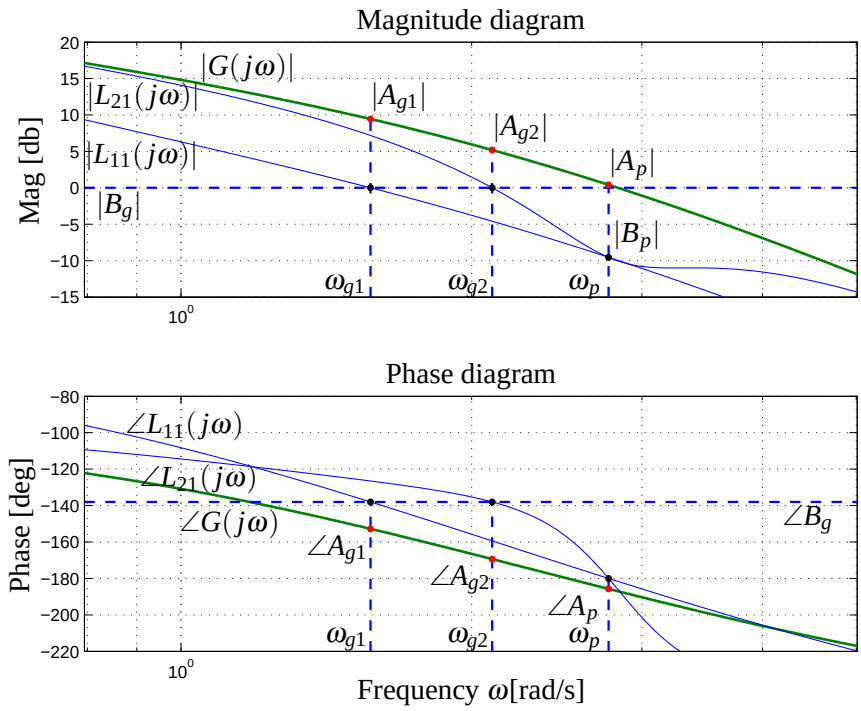

Figure 3.17: Graphical representation of the solution of Design Problem D on the Bode diagrams.

on the segment $(B_p, \frac{B_p}{\gamma})$*;*

2) *determine* γ *as described in Property 5 when* $A = A_p$ *and* $B = B_p$*;*

3) *draw the circle* $\mathscr{C}^-_{B_g\gamma}(j\omega)$ *having its diameter on the segment* $(B_g, \frac{B_g}{\gamma})$*;*

4) *the points* A_{gi} *where circle* $\mathscr{C}^-_{B_g\gamma}(j\omega)$ *intersects* $G(j\omega)$ *correspond to the frequencies* $\omega_{gi} \in S_{\omega_g}$.

This graphical construction holds because a frequency ω_g satisfies (3.34) only if

$$G(j\omega_g)C_\gamma(j\omega_g) = B_g. \tag{3.36}$$

This relation can be rewritten as

$$G(j\omega) = \frac{B_g}{C_\gamma(j\omega)} = \mathscr{C}^-_{B_g\gamma}(j\omega), \tag{3.37}$$

with $\omega = \omega_g$, and can be solved graphically on the Nyquist plane by finding the intersections ω_g of $G(j\omega)$ with $\mathscr{C}^-_{B_g\gamma}(j\omega)$.

Let us now consider the following Design Problem E which is a relaxed version of Design Problem C and Design Problem D.

Design Problem E: (ϕ_m , G_m , γ) Given the transfer function $G(s)$ and the design specifications on the phase margin ϕ_m and gain margin G_m, design a Lead-Lag compensator $C_{LL}(s)$ such that the loop gain transfer function $C_{LL}(j\omega)G(j\omega)$ passes through points $B_g = e^{j(\pi+\phi_m)}$ and $B_p = -1/G_m$ for a value of γ chosen arbitrarily.

Solution E: *Let $B_g = e^{j(\pi+\phi_m)}$ and $B_p = -1/G_m = M_{B_p} e^{j\varphi_{B_p}}$ denote the points corresponding to the desired phase margin ϕ_m and gain margin G_m. The set $C_\gamma(s,\omega_g,\omega_p)$ of all the compensators $C_{LL}(s)$ which solve Design Problem E is obtained as follows:*

a) *find all the pairs $(\omega_g,\ \omega_p) \in S_{\gamma\omega}$ of frequencies which solve*

$$\gamma = \gamma_g(\omega_g) = \gamma_p(\omega_p), \tag{3.38}$$

where $\gamma > 0$ is chosen arbitrarily, $S_{\gamma\omega}$ is the set of all the pairs $(\omega_g,\ \omega_p)$ satisfying (3.38), and $\gamma_g(\omega_g)$ and $\gamma_p(\omega_p)$ are defined in (3.35) and (4.14) with $A_g = G(j\omega_g) = M_{A_g}(\omega_g)\, e^{j\varphi_{A_g}(\omega_g)}$ and $A_p = G(j\omega_p) = M_{A_p}(\omega_p)\, e^{j\varphi_{A_p}(\omega_p)}$, respectively.

b) *for each pair $(\omega_g,\ \omega_p) \in S_{\gamma\omega}$ compute*

$$\omega_n = \sqrt{\frac{P_p\,\omega_p - P_g\,\omega_g}{\frac{P_p}{\omega_p} - \frac{P_g}{\omega_g}}} = \sqrt{\frac{Q_p\,\omega_p - Q_g\,\omega_g}{\frac{Q_p}{\omega_p} - \frac{Q_g}{\omega_g}}} > 0, \tag{3.39}$$

and

$$\delta = Q_g \frac{\omega_n^2 - \omega_g^2}{2\omega_n\omega_g} = Q_p \frac{\omega_n^2 - \omega_p^2}{2\omega_n\omega_p} > 0, \tag{3.40}$$

where the coefficients $P_g = P(A_g(\omega_g), B_g)$, $Q_g = Q(A_g(\omega_g), B_g)$, $P_p = P(A_p(\omega_p), B_p)$ and $Q_p = Q(A_p(\omega_p), B_p)$ are obtained using the inversion formulae (2.21).

A solution $C_\gamma(s,\omega_g,\omega_p)$ of Design Problem E exists only if: 1) γ satisfies

$$0 < \gamma < \min\left[\max(\gamma_g(\omega_g)), \max(\gamma_p(\omega_p))\right] \tag{3.41}$$

2) $S_{\gamma\omega}$ is not empty; 3) points $A_g(\omega_g)$ and $A_p(\omega_p)$ belong, respectively, to the admissible domains $\mathscr{D}_{B_g}$ and $\mathscr{D}_{B_p}$; 4) parameters ω_n in (3.39) and δ in (3.40) are real and positive.

Proof: The design specifications on the phase margin ϕ_m and gain margin G_m completely define the position of points B_g and B_p on the complex plane. A solution $C_\gamma(s,\omega_g,\omega_p)$ exists only if the frequencies ω_g and ω_p satisfy (5.34) and (3.36), that is only if they satisfy (3.38) where $\gamma_g(\omega_g) = P_g/Q_g$ and $\gamma_p(\omega_p) = P_p/Q_p$. For each value of γ satisfying (3.41), one can find the set $S_{\gamma\omega}$ of all the solutions (ω_g,ω_p) of (3.38). This relation does not depend on δ and ω_n, but only on the frequencies (ω_g,ω_p) and points (B_g, B_p). Each solution $(\omega_g,\omega_p) \in S_{\gamma\omega}$ corresponds to an acceptable regulator $C_\gamma(s,\omega_g,\omega_p)$ only if ω_n and δ given in (3.39) and (3.40) are real and positive. The expressions of ω_n and δ in (3.39) and (3.40) are

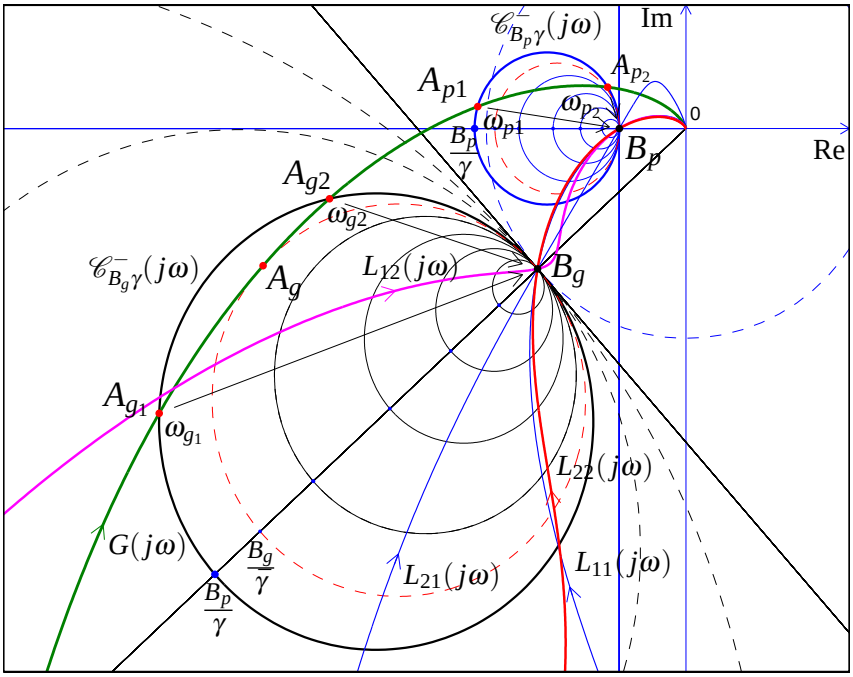

Figure 3.18: Graphical solution of Design Problem E on the Nyquist plane.

obtained as described in the Solution of Design Problem C by taking into account (3.38), $P_g = \gamma Q_g$ and $P_p = \gamma Q_p$. □

The numerical solution of (3.38) can be obtained graphically by plotting $\gamma_g(\omega)$ and $\gamma_p(\omega)$ and by finding, for each admissible value of γ, all the pairs $(\omega_g, \omega_p) \in S_{\omega_g}$ where $\gamma_g(\omega_g)$ and $\gamma_p(\omega_p)$ intersect the horizontal line γ, see Fig. 3.13. In the example of Fig. 3.13 there are four different solutions: $S_{\gamma\omega} = \{(\omega_{g1}, \omega_{p1}), (\omega_{g1}, \omega_{p2}), (\omega_{g2}, \omega_{p1}), (\omega_{g2}, \omega_{p2})\}$. The loop gain frequency responses $L_{11}(s)$, $L_{12}(s)$, $L_{21}(s)$ and $L_{22}(s)$ of these four solutions on the Nyquist plane are shown in Fig. 3.18. These solutions are acceptable only if $\delta > 0$ and $\omega_n > 0$ given in (3.39) and (3.40) are satisfied.

The solution of the Design Problem E can also be performed graphically on the Nyquist and Nichols planes. Five different graphical representations are now described.

a) $G(j\omega)$**-graphical representation on Nyquist plane**. The frequencies $(\omega_g, \omega_p) \in S_{\omega_g}$ can also be determined on the Nyquist plane using the graphical construction shown in Fig. 3.18:

1) given points B_g and B_p and a desired value for $\gamma > 0$, draw the circles $\mathscr{C}^-_{B_g\gamma}(j\omega)$ and $\mathscr{C}^-_{B_p\gamma}(j\omega)$ having their diameters on the segments $(B_g,\ B_g/\gamma)$ and $(B_p,\ B_p/\gamma)$;

2) if the frequency response $G(j\omega)$ does not intersect both circles $\mathscr{C}^-_{B_g\gamma}(j\omega)$ and $\mathscr{C}^-_{B_p\gamma}(j\omega)$, the chosen value of γ is not acceptable.

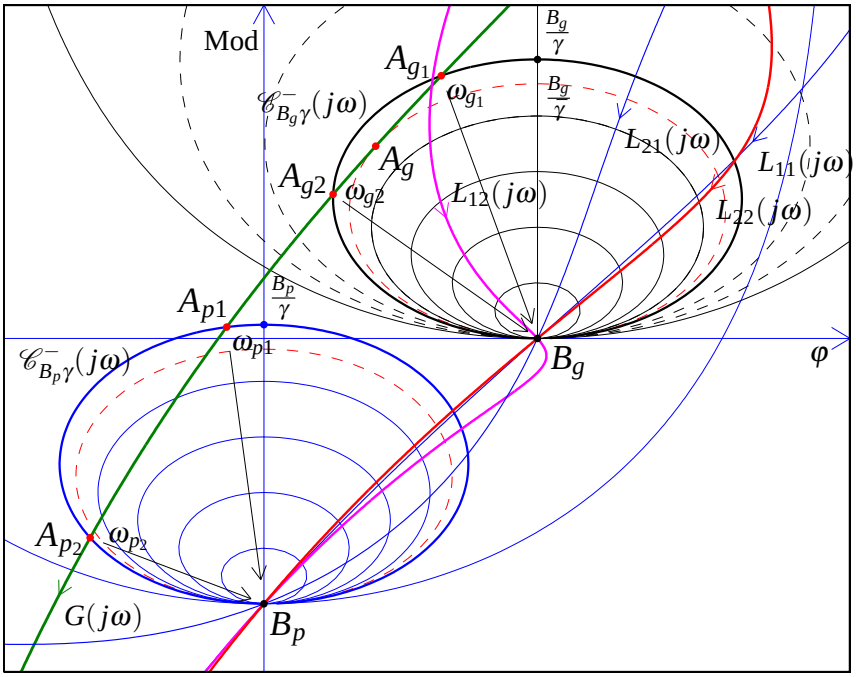

Figure 3.19: $G(j\omega)$-graphical representation on Nichols plane.

3) otherwise, each pair (ω_g, ω_p) corresponding to the intersections of $G(j\omega)$ with circles $\mathscr{C}^-_{B_g\gamma}(j\omega)$ and $\mathscr{C}^-_{B_p\gamma}(j\omega)$ is a possibile solution for Design Problem E.

This graphical construction hinges on the fact that ω_g and ω_p satisfy relation (3.38) only if $G(j\omega_g)C_\gamma(j\omega_g) = B_g$ and $G(j\omega_p)C_\gamma(j\omega_p) = B_p$. These relations can be rewritten as

$$\begin{cases} G(j\omega)|_{\omega=\omega_g = \frac{B_g}{C_\gamma(j\omega_g)}} = \mathscr{C}^-_{B_g\gamma}(j\omega)\Big|_{\omega=\omega_g} \\ G(j\omega)|_{\omega=\omega_p = \frac{B_p}{C_\gamma(j\omega_p)}} = \mathscr{C}^-_{B_p\gamma}(j\omega)\Big|_{\omega=\omega_p} \end{cases} \tag{3.42}$$

These relations can be solved graphically on the Nyquist plane by finding the frequencies (ω_g, ω_p) where $G(j\omega)$ intersects $\mathscr{C}^-_{B_g\gamma}(j\omega)$ and $\mathscr{C}^-_{B_p\gamma}(j\omega)$.

Using the graphical construction of Fig. 3.18 it is also easy to determine the maximum value $\bar{\gamma}$ of parameter γ for which a solution of Design Problem E exists: it is the value for which the circle $\mathscr{C}^-_{B_g\bar{\gamma}}(j\omega)$ is tangent to $G(j\omega)$, see the dashed red circles and point A_g in Fig. 3.18.

b) $G(j\omega)$**-graphical representation on Nichols plane**. The graphical construction described above can be carried out also on the Nichols plane, see Fig. 3.19. The shapes of $\mathscr{C}^-_{B_g\gamma}(j\omega)$ and $\mathscr{C}^-_{B_p\gamma}(j\omega)$ on the Nichols plane are not circles, but the intersection points A_{g1}, A_{g2}, A_{p1}, A_{p2} with $G(j\omega)$ can still be determined. An advantage of working on the Nichols plane is that $\mathscr{C}^-_{B_g\gamma}(j\omega)$ and $\mathscr{C}^-_{B_p\gamma}(j\omega)$ have the same shape and the same dimension. In fact, these functions differ for just a constant, $\mathscr{C}^-_{B_p\gamma}(j\omega) =$

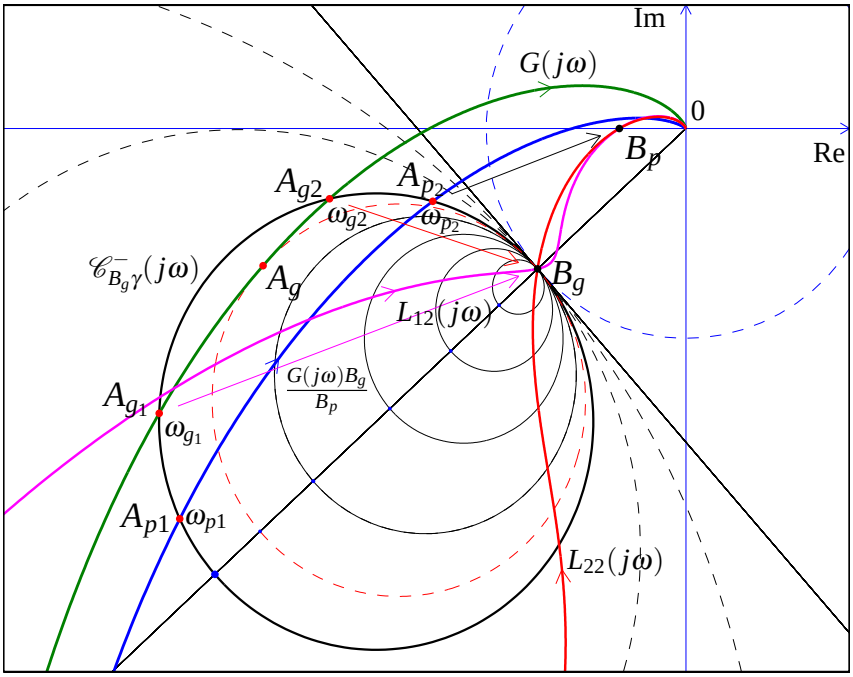

Figure 3.20: $\mathscr{C}^-_{B_g\gamma}(j\omega)$-graphical representation on Nyquist plane.

$(B_p/B_g)\mathscr{C}^-_{B_g\gamma}(j\omega)$, and therefore they differ for just a translation on the Nichols plane.

c) $\mathscr{C}^-_{B_g\gamma}(j\omega)$**-graphical representation on Nyquist plane**. Multiplying the second equation of system (3.42) by the constant B_g/B_p one obtains

$$\begin{cases} G(j\omega)|_{\omega=\omega_g} = \mathscr{C}^-_{B_g\gamma}(j\omega)\Big|_{\omega=\omega_g} \\ \dfrac{G(j\omega)B_g}{B_p}\Big|_{\omega=\omega_p} = \mathscr{C}^-_{B_g\gamma}(j\omega)\Big|_{\omega=\omega_p} \end{cases} \tag{3.43}$$

It is evident that these relations can be solved graphically on the Nyquist plane by finding the frequencies (ω_g, ω_p) where $\mathscr{C}^-_{B_g\gamma}(j\omega)$ intersects $G(j\omega)$ and $G(j\omega)B_g/B_p$. A graphical representation of (3.43) on the Nyquist plane is shown in Fig. 3.20: the intersections of $\mathscr{C}^-_{B_g\gamma}(j\omega)$ with $G(j\omega)$ provide the frequencies ω_{g1}, ω_{g2}, etc.; the intersections of $\mathscr{C}^-_{B_g\gamma}(j\omega)$ with $G(j\omega)B_g/B_p$ provide the frequencies ω_{p1}, ω_{p2}, etc. The loop gain transfer functions $L_{12}(j\omega)$ and $L_{22}(j\omega)$ corresponding to solutions $(\omega_{g1}, \omega_{p2})$ and $(\omega_{g2}, \omega_{p2})$ are shown in magenta and in red in Fig. 3.20.

d) $\mathscr{C}_\gamma(j\omega)$**-graphical representation on the Nyquist plane**. Using simple mathematical manipulations,

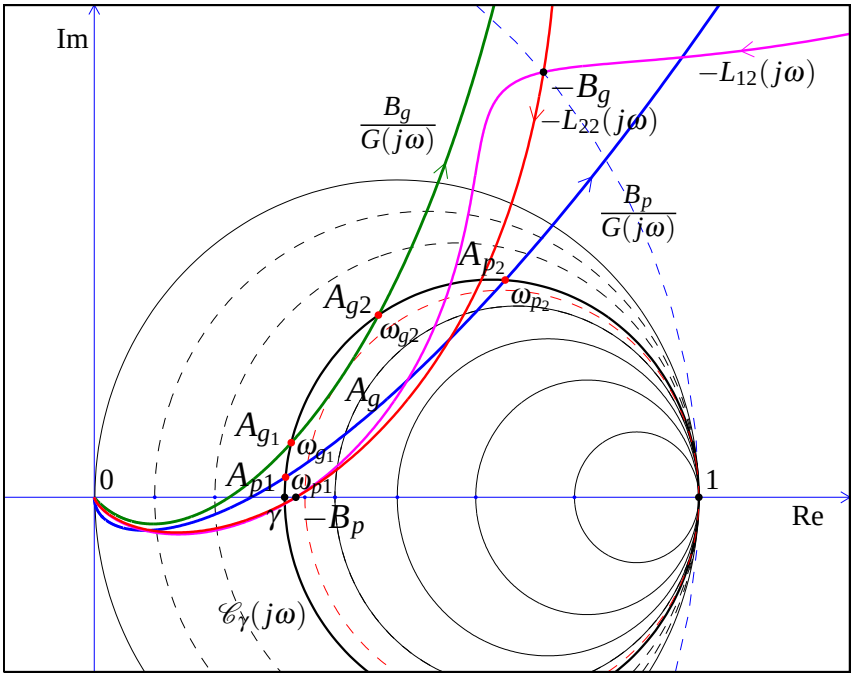

Figure 3.21: $\mathscr{C}_\gamma(j\omega)$-graphical representation on the Nyquist plane.

system (3.42) can be rewritten as

$$\begin{cases} \left.\dfrac{B_g}{G(j\omega)}\right|_{\omega=\omega_g} = \mathscr{C}_\gamma(j\omega)\big|_{\omega=\omega_g} \\ \left.\dfrac{B_p}{G(j\omega)}\right|_{\omega=\omega_g} = \mathscr{C}_\gamma(j\omega)\big|_{\omega=\omega_p} \end{cases} \tag{3.44}$$

These equations can be solved graphically on the Nyquist plane by finding the frequencies (ω_g, ω_p) where $\mathscr{C}_\gamma(j\omega)$ intersects $B_g/G(j\omega)$ and $B_p/G(j\omega)$. A graphical representation of (3.44) on the Nyquist plane is shown in Fig. 3.21. The intersections with $B_g/G(j\omega)$ provide the frequencies ω_{g1}, ω_{g2}, etc. and the intersections with $B_p/G(j\omega)$ provide ω_{p1}, ω_{p2}, etc. Note that in Fig. 3.21 the points $-B_g$ and $-B_p$, and the two loop gain frequency responses $-L_{12}(s)$ and $-L_{22}(s)$ have also been reported: the relative position of these points and functions with respect to point 1 is the same of points B_g and B_p and $L_{12}(s)$ and $L_{22}(s)$ with respect to -1.

e) $\mathscr{C}_\gamma(j\omega)$-graphical representation on Nichols plane. Equations (3.44) can be solved graphically on the Nichols plane as well, as shown in Fig. 3.22. In this case the shapes of $\mathscr{C}_\gamma(j\omega)$ are not circles, but the graphical representation is more precise for small values of the modulus. This graphical representation is similar to the one presented in [25] for the solution of Design Problems C and D. From the solution

of the Design Problem E directly follows the solution of a second version of the Design Problem D.

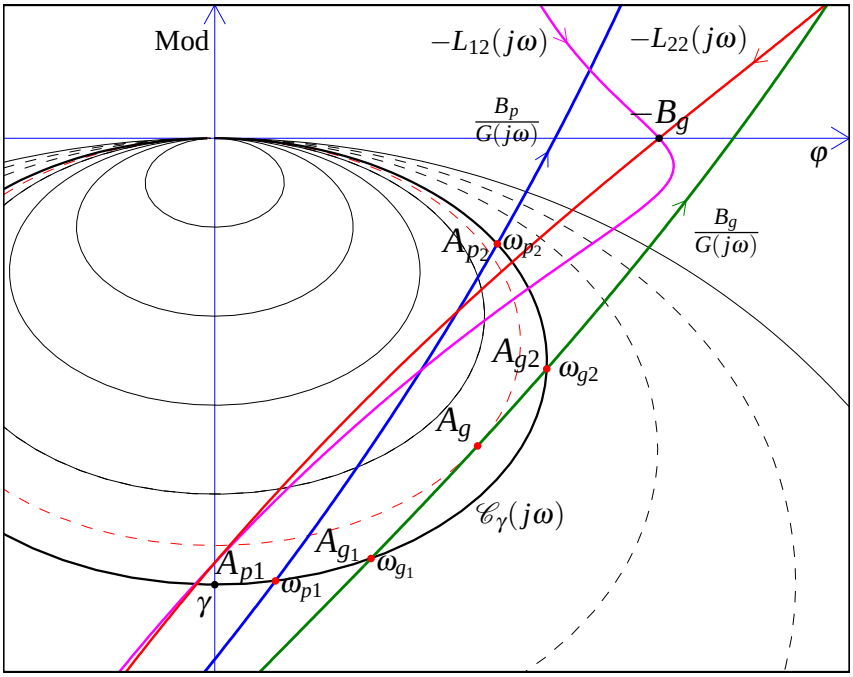

Figure 3.22: $\mathscr{C}_\gamma(j\omega)$-graphical representation on Nichols plane.

Design Problem D': (G_m , ω_p , ϕ_m). Given the control scheme of Fig. 1.1 and the transfer function $G(s)$, design a compensator $C_{LL}(s)$ which satisfies the gain margin G_m, the phase crossover frequency ω_p and the maximum allowable phase margin ϕ_m.

Solution D': *The value of* $\gamma = \frac{P_p}{Q_p}$ *can be determined as in Design Problem D.1 by points* $B_p = -1/G_m$ *and* $A_p = G(j\omega_p)$. *The gain* γ *completely defines the shape of circle* $\mathscr{C}_{B\frac{1}{\gamma}}(j\omega)$. *The maximum value* $\bar{\phi}_m$ *of the phase margin* ϕ_m *can be graphically determined moving point* $B_g = e^{j(\pi+\phi_m)}$ *on the unit circle until* $\mathscr{C}_{B\frac{1}{\gamma}}(j\omega)$ *is tangent to function* $G(j\omega)$. *The frequency* ω_g *of the tangent point substituted in (3.39) and (3.40) provides the parameters* ω_n *and* δ *of the compensator* $C(s)$.

3.4 Numerical examples

Example 1. All the graphical representations from Fig. 3.9 to Fig. 3.22 used in the solutions of Design Problems A, B, C, D and E refer to the system

$$G(s) = \frac{40(s+1)}{s(s+1.5)^2(s+3)}$$

with the following design specifications: phase margin $\phi_m = 42^\circ$, gain margin $G_m = 3$, gain crossover frequency $\omega_g = 2.1$ and phase crossover frequency $\omega_p = 4.05$. The modulus and the phase of points

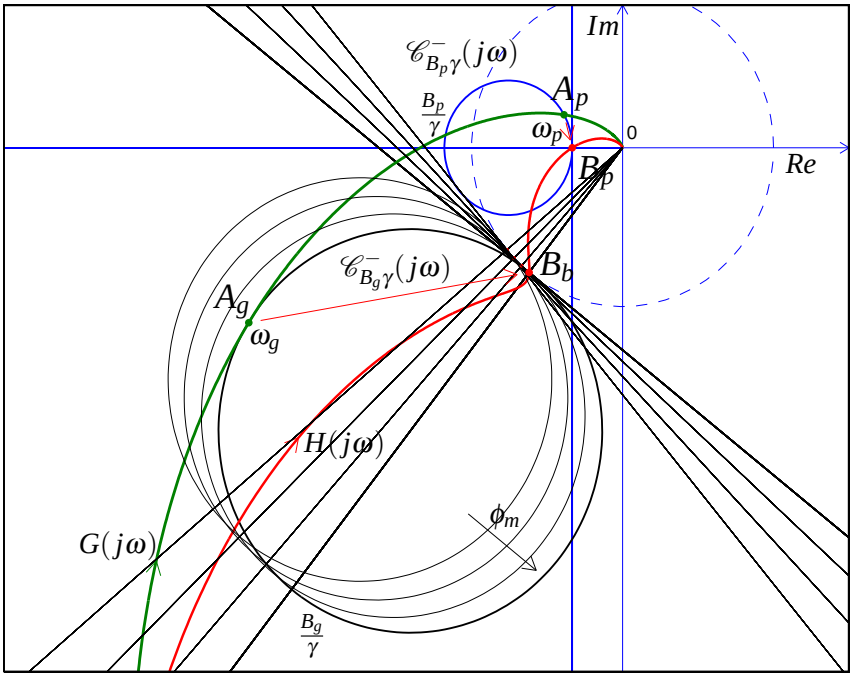

Figure 3.23: Graphical solution of Design Problem D'.

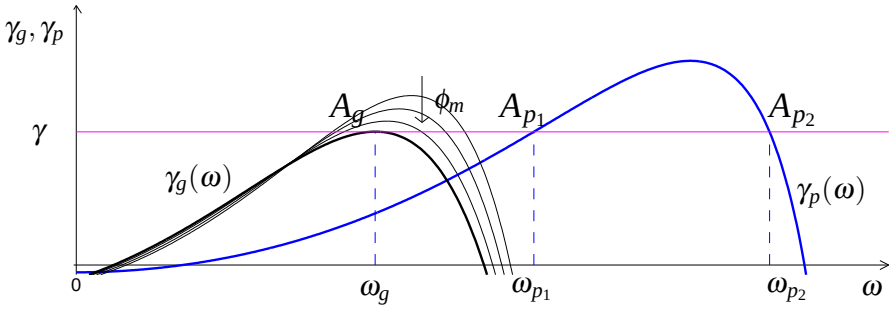

Figure 3.24: Design problem D': function $\gamma_p(\omega)$ (blue line) and functions $\gamma_g(\omega)$ (black lines) for $\phi_m = \{40, 44, 48, 51.75\}$.

$B_g = M_{B_g} e^{j\varphi_{B_g}} = e^{j(\pi+\phi_m)}$ and $B_p = M_{B_p} e^{j\varphi_{B_p}} = -1/G_m$ are $M_{B_g} = 1$, $\varphi_{B_g} = 222^\circ$, $M_{B_p} = 0.333$ and $\varphi_{B_p} = 180^\circ$. The value of γ obtained in (3.22), (3.23), (3.26), (3.32) and used in Design Problem E is

$$\gamma = \frac{P_g}{Q_g} = \frac{Q_p}{P_p} = 0.315.$$

The frequencies ω_{g1}, $\omega_{g2} = \omega_g$, $\omega_{p1} = \omega_p$ and ω_{p2} (3.26), (3.34) and (3.38) are $\omega_{g1} = 1.57$, $\omega_{g2} = 2.1$, $\omega_{p1} = 2.77$ and $\omega_{p2} = 4.05$. The corresponding points $A_{g1} = G(j\omega_{g1})$, $A_{g2} = A_g = G(j\omega_{g2})$, $A_{p1} = A_p = G(j\omega_{p1})$ and $A_{p2} = G(j\omega_{p2})$ on the frequency response $G(j\omega)$ are

$$A_{g1} = 2.97\,e^{-j152.7^\circ}, \quad A_{g2} = 1.82\,e^{-j169.4^\circ},$$
$$A_{p1} = 1.05\,e^{j174.3^\circ}, \quad A_{p2} = 0.44\,e^{j153.3^\circ}.$$

Let us now consider the solutions of the previously described Design Problems separately.

Design Problem A: (ϕ_m, ω_g). The parameters P_g, Q_g and γ corresponding to A_g and B_g are $P_g = -0.5824$, $Q_g = -1.8491$ and $\gamma = P_g/Q_g = 0.315$. The set of regulators $C_g(s,\omega_n)$ satisfying Design Problems A are

$$C_g(s,\omega_n) = \frac{s^2 + P_g\frac{\omega_g^2-\omega_n^2}{\omega_g}s + \omega_n^2}{s^2 + Q_g\frac{\omega_g^2-\omega_n^2}{\omega_g}s + \omega_n^2}, \tag{3.45}$$

for $0 < \omega_n < \omega_g = 2.1$. The loop gain transfer function $L_g(j\omega,\omega_n) = C_g(s,\omega_n)G(j\omega)$ for $\omega_n = \{0.6 : 0.1 : 1.1\}$ is represented by red lines in Fig. 3.9 and 3.10.

Design Problem B: (G_m, ω_p). The parameters P_p, Q_p and γ corresponding to A_p and B_p are $P_p = -0.295$, $Q_p = -0.937$ and $\gamma = P_p/Q_p = 0.315$. The set of regulators $C_p(s,\omega_n)$ satisfying the Design Problems B are

$$C_p(s,\omega_n) = \frac{s^2 + P_p\frac{\omega_p^2-\omega_n^2}{\omega_p}s + \omega_n^2}{s^2 + Q_p\frac{\omega_p^2-\omega_n^2}{\omega_p}s + \omega_n^2}, \tag{3.46}$$

for $0 < \omega_n < \omega_p = 4.05$. The loop gain transfer function $L_p(j\omega,\omega_n) = C_p(s,\omega_n)G(j\omega)$ is represented by red lines in Fig. 3.11 and 3.12 for $\omega_n = \{1.2 : 0.1 : 1.6\}$.

Design Problem C: (ϕ_m, G_m, ω_g). The parameters P_g, Q_g and γ corresponding to A_g and B_g are $P_g = -0.582$, $Q_g = -1.849$ and $\gamma = P_g/Q_g = 0.315$. The two solutions of (3.26) are $S_{\omega_p} = \{\omega_{p1},\omega_{p2}\} = \{2.77, 4.05\}$. Substitution into (3.24) and (3.25) yields $\delta = -0.571$ and $\omega_n = 2.85$ when $\omega = \omega_{p1}$; $\delta = 5.14$ and $\omega_n = 0.37$ when $\omega = \omega_{p2}$. Only the second solution where $\delta > 0$ is acceptable:

$$C_g(s,\omega_{p2}) = \frac{s^2 + 1.186\,s + 0.134}{s^2 + 3.765s + 0.134}. \tag{3.47}$$

The corresponding loop gain transfer function $L_{22}(j\omega) = C_g(s,\omega_{p2})G(j\omega)$ is plotted in red in Fig. 3.14 and 3.15.

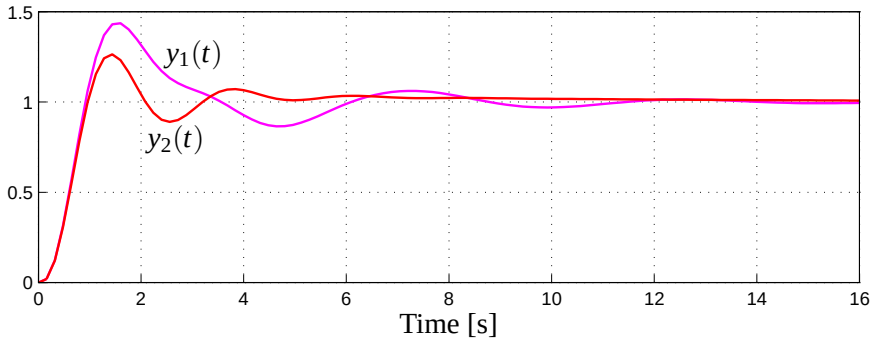

Figure 3.25: Step responses $y_1(t)$ (magenta line) and $y_2(t)$ (red line) of the closed loop system when, respectively, regulators $C_\gamma(s,\omega_{g1},\omega_{p2})$ in (3.48) and $C_g(s,\omega_{p2})$ in (3.47) are used.

Design Problem D: (ϕ_m, G_m, ω_p). The parameters which correspond to points A_p and B_p are $P_p = -6.778$, $Q_p = -21.52$ and $\gamma = P_g/Q_g = 0.315$. The two solutions of (3.34) are $S_{\omega_g} = \{\omega_{g1},\omega_{g2}\} = \{1.57, 2.1\}$. Substitution into (3.32) and (3.33) yields $\delta = -8.82$ and $\omega_n = 4.13$ when $\omega = \omega_{g1}$; $\delta = -0.571$ and $\omega_n = 2.85$ when $\omega = \omega_{g2}$. Neither solution is acceptable because in both cases $\delta < 0$. The loop gain transfer functions $L_{11}(j\omega)$ and $L_{21}(j\omega)$ are the blue lines shown in Fig. 3.16 and 3.17.

Design Problem E: (ϕ_m, G_m, γ). Given B_g, B_p and γ, the four solutions $(\omega_{gi},\omega_{pj})$ of equation (3.38) can be graphically determined as shown in Fig. 3.13. By substitution into (3.39) and (3.40) one obtains only two acceptable and stable regulators $C_\gamma(s,\omega_g,\omega_p)$. The first one is obtained for $(\omega_{g1},\omega_{p2})$, $\delta = 1.691$ and $\omega_n = 1.338$:

$$C_\gamma(s,\omega_{g1},\omega_{p2}) = \frac{s^2+1.065s+1.791}{s^2+3.382s+1.791}. \tag{3.48}$$

The corresponding loop gain transfer function $L_{12}(j\omega) = C_\gamma(j\omega,\omega_{g1},\omega_{p2})G(j\omega)$ is shown on the Nyquist plane in Fig. 3.18 and on the Nichols plane in Fig. 3.19. The second acceptable solution $C_\gamma(s,\omega_{g2},\omega_{p2})$ is obtained for $(\omega_{g2},\omega_{p2})$, $\delta = 5.14$ and $\omega_n = 0.37$, and it coincides with the $C_g(s,\omega_{p2})$ given in (3.47). The other two solutions are not acceptable. The step responses $y_1(t)$ and $y_2(t)$ of the closed loop system when, respectively, regulators $C_\gamma(s,\omega_{g1},\omega_{p2})$ in (3.48) and $C_g(s,\omega_{p2})$ in (3.47) are used, are shown in Fig. 3.25.

Example 2. Given the plant

$$G(s) = \frac{1200(s+2)}{(s+1.5)^2(s+7)^2}, \tag{3.49}$$

solve the Design Problem D' to meet the following specifications: gain margin $G_m = 3$ and phase crossover frequency $\omega_p = 12.8$.

The maximum phase margin $\bar{\phi}_m$ which satisfies the Design Problem D can be graphically determined as shown in Fig. 3.23. The obtained value is $\bar{\phi}_m = 51.75^\circ$. When phase margin ϕ_m increases from 40° to

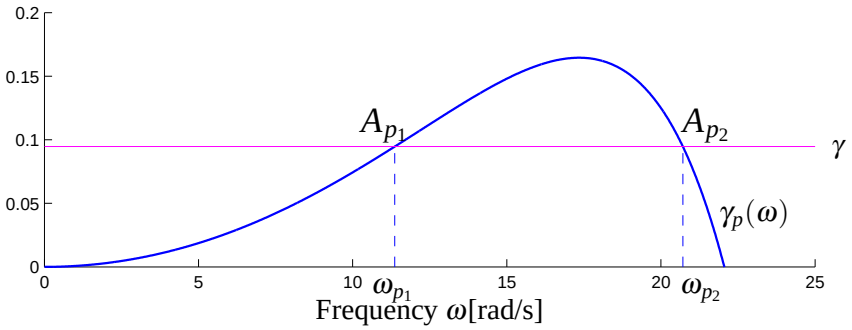

Figure 3.26: Example 3: function $\gamma_p(\omega)$ intersects the value γ at frequencies $\{\omega_{p1},\ \omega_{p2}\} = \{11.37, 20.71\}$.

$\bar{\phi}_m$, function $\gamma_g(\omega)$ modifies its shape as shown in Fig. 3.24.

Example 3. Let us consider the transfer function proposed in [25]:

$$G(s) = \frac{5000}{s(s+5)(s+10)}, \tag{3.50}$$

with the following design specifications: phase margin $\phi_m = 42^\circ$, gain crossover frequency $\omega_g = 9$ rad/s and gain margin $G_m = 4$. The synthesis of the Lead-Lag controllers $C_g(s, \omega_{p2})$ follows the lines described in Design Problem C. The modulus and the phase of $B_g = M_{B_g} e^{j\varphi_{B_g}} = e^{j(\pi+\phi_m)}$, $A_g = M_{A_g} e^{j\varphi_{A_g}} = G(j\omega_g)$ and $B_p = M_{B_p} e^{j\varphi_{B_p}} = -1/G_m$ are $M_{B_g} = 1$, $\varphi_{B_g} = 222^\circ$, $M_{A_g} = 4.01$, $\varphi_{A_g} = 167.1^\circ$, $M_{B_p} = 0.25$ and $\varphi_{B_p} = 180^\circ$. From A_g and B_g one obtains $P_g = -0.397$, $Q_g = -4.198$ and $\gamma = P_g/Q_g = 0.0946$. The two solutions of (3.26) are $S_{\omega_p} = \{\omega_{p1}, \omega_{p2}\} = \{11.37, 20.71\}$, see Fig. 3.26. Only the one corresponding to ω_{p2} is acceptable, and gives $\delta = 17.68 > 0$ and $\omega_n = 2.28$. The corresponding Lead-Lag regulator is

$$C_g(s, \omega_{p2}) = \frac{s^2 + 3.347\,s + 5.198}{s^2 + 35.36\,s + 5.198}. \tag{3.51}$$

The graphical constructions corresponding to the synthesis of the Lead-Lag compensator $C_g(s, \omega_{p2})$ on the Nyquist, Bode and Nichols planes are shown in Fig. 3.27-Fig. 3.29. The loop gain transfer function $L_2(j\omega) = C_g(j\omega, \omega_{p2})G(j\omega)$ is the red line shown in the figures.

Example 4. Given the plant $G(s) = \frac{K(s+10)}{s(s^2+2s+10)}$, design a Lead-Lag network that meets the following specifications: velocity constant $K_v = 0.1$; phase margin $\phi_m = 45^\circ$; gain margin $G_m = 3$; gain crossover frequency $\omega_g = 1$ rad/sec. First, notice that only a Lead-Lag network can simultaneously meet all the specifications, since a first order compensator has only two degree of freedom. The DC gain K included in $G(s)$ must be selected so as to satisfy the specification on the velocity constant:

$$K_v = \lim_{s\to 0} s C_{\mathrm{LL}}(s)\, G(s) = K,$$

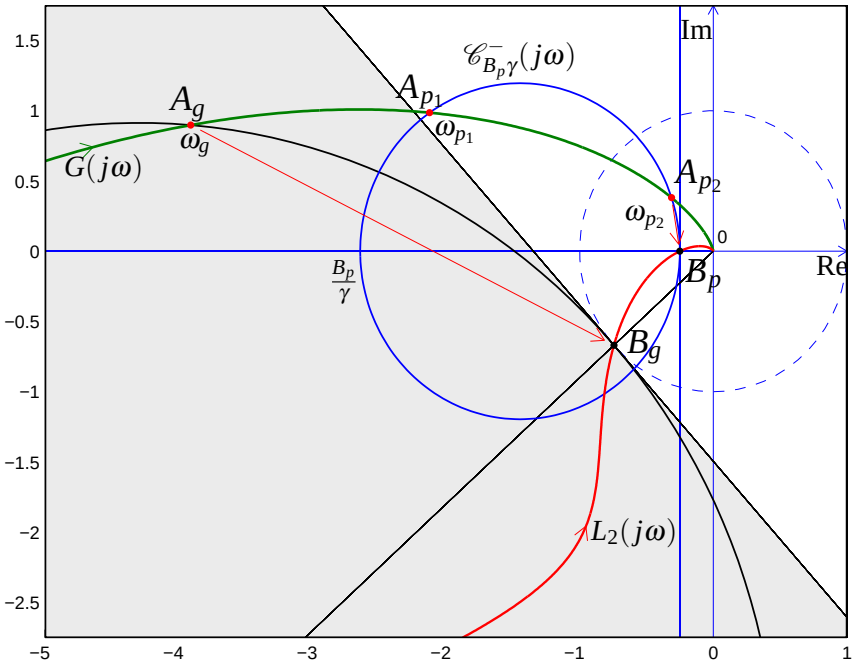

Figure 3.27: Example 3: synthesis and graphical interpretation of the Lead-Lag compensators $C_g(s, \omega_{p2})$ on the Nyquist plane.

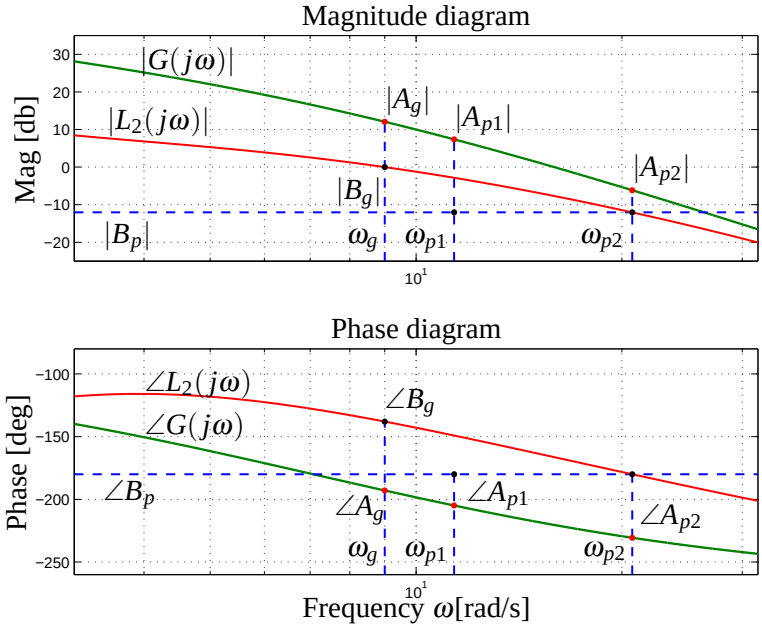

Figure 3.28: Example 3: graphical representation of the solution on the Bode diagrams.

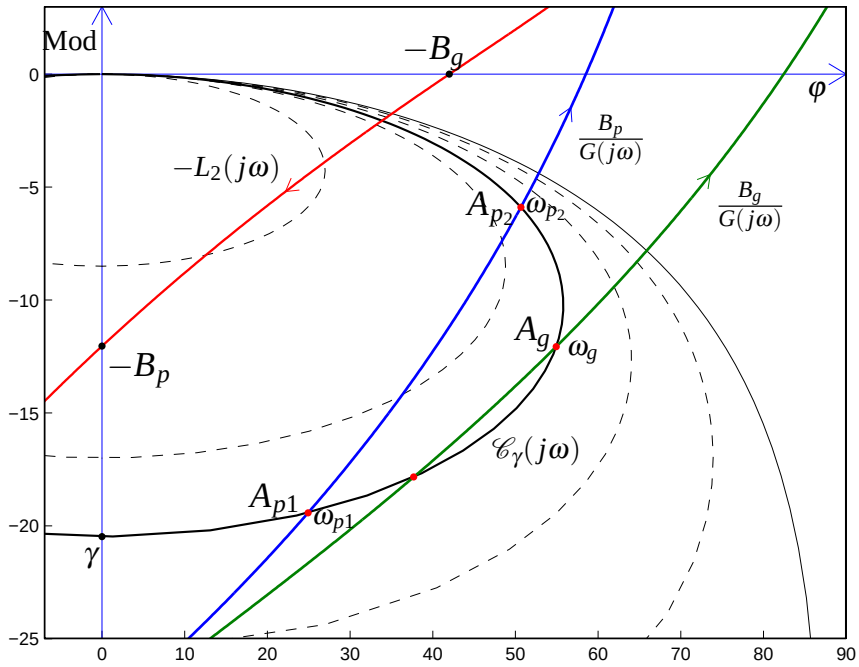

Figure 3.29: Example 3: Graphical determination on the Nichols plane of the frequencies $(\omega_{p1}, \omega_{p2})$ where $\mathscr{C}_\gamma(j\omega)$ intersects function $B_p/G(j\omega)$.

so that $K = 0.1$. The frequency response of the plant at $\omega = \omega_g$ is

$$G(j\omega_g) = \frac{10+j}{j\,(2\,j+9)}.$$

To meet the given phase margin and gain crossover frequency specisications, the magnitude M_g and the phase φ_g of the controller at frequency ω_g has to satisfy the following relations

$$\begin{aligned} M_g &= \frac{1}{K}\sqrt{\frac{85}{101}}, \\ \varphi_g &= \frac{\pi}{4} - \pi - (\arctan\frac{1}{10} - \frac{\pi}{2} - \arctan\frac{2}{9}) \\ &= \frac{3}{4}\pi - \arctan\frac{1}{10} + \arctan\frac{2}{9}. \end{aligned}$$

A simple goniometric calculation shows that

$$\cos\varphi_g = \frac{103}{2}\sqrt{\frac{2}{85\cdot 101}},$$

which leads to

$$\gamma = \frac{M_g - \cos\varphi_g}{\cos\varphi_g - M_g^{-1}} = \frac{170 - 103\sqrt{2}K}{103\sqrt{2}K - 202K^2}.$$

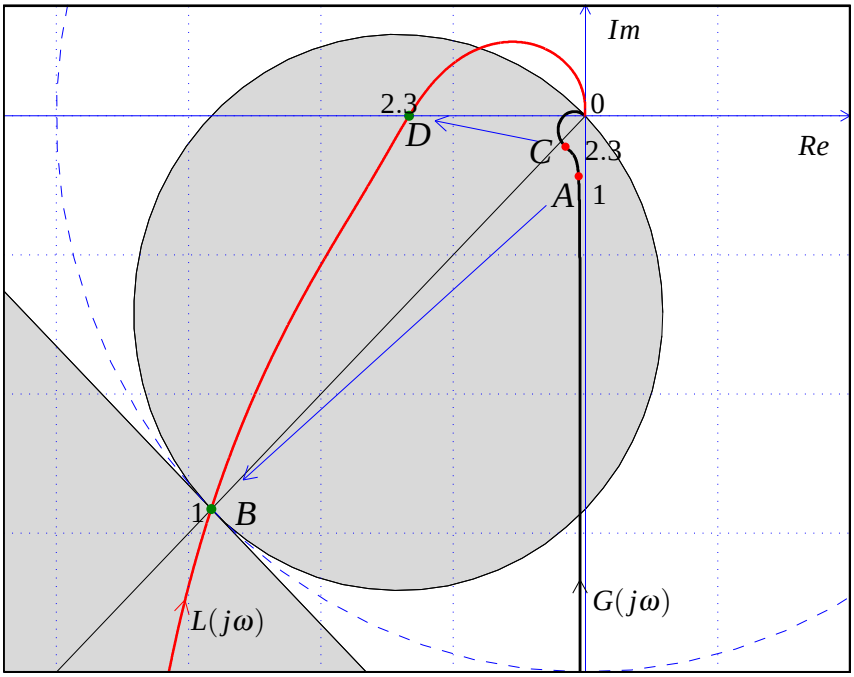

Figure 3.30: Graphical interpretation of the closed-form solution of Example 4.

We express $M_p = M(\omega_p)$ and $\varphi_p = \varphi(\omega_p)$ as a function of the phase crossover frequency ω_p, which is still unknown:

$$M_p = \frac{\omega_p \sqrt{4\,\omega_p^2 + (10 - \omega_p^2)^2}}{G_m \cdot K \sqrt{\omega_p^2 + 100}},$$

$$\cos\varphi_p = \frac{\omega_p\,(\omega_p^2 + 10)}{\sqrt{(100 + \omega_p^2)((10 - \omega_p^2)^2 + 4\,\omega_p^2)}}.$$

Plugging these expressions into (3.26), which can be rewritten as

$$\gamma = \frac{M_p - \cos\varphi_p}{\cos\varphi_p - M_p^{-1}},$$

yields the polynomial equation

$$\omega^6 - (16 + H + \gamma H)\omega^4 + 10\,(10 - H - \gamma H)\,\omega^2 + 100\,\gamma H^2 = 0,$$

where $H = G_m K$. This biquadratic equation has two positive solutions: $\omega_p' = 3.9591$ and $\omega_p'' = 2.3686$. Only the second solution leads to positive values of δ and ω_n. The corresponding values of the parameters of the Lead-Lag network are $\gamma = 12.3887$, $\delta = 1.6747$ and $\omega_n = 0.2980$. The graphical interpretation of the solution is represented in Fig. 3.30.

This example has shown the effectiveness of this design method from another perspective. In fact, even in the case of a plant with a reasonably rich dynamical structure, the design problem is found to admit a closed-form solution. Indeed, the 6th degree polynomial equation in ω_p is biquadratic, and is therefore solvable in finite terms. This leads to a "mathematically exact" solution of this design problem.

3.5 An open research problem to meet other design requirements

Using Inversion Formulae (2.21) and the Prop. 4 (From A to B), the set of all the compensators (3.19) exactly satisfies the given phase margin ϕ_m and the given gain crossover frequency ω_g specifications, which are very important indicators of system performance and robustness. The only necessary and sufficient condition required to employ a Lead-Lag controller to meet these requirements is that the point $A = G(j\omega_g)$ belongs to the admissible domain $\mathscr{D}_B$. As described in chapter 1, a very interesting research problem is to study how to choose the degree of freedom ω_n in (3.19) in order to improve the dynamical behavior of the control system. Let as consider two different design procedures to obtain a good settling time of the step response or a good resonance peak of the closed-loop system. These procedures could be an alternative to the procedure described in the solution of the Design Problem C to meet the gain margin specification G_m.

3.5.1 Requirement on a good settling time t_s

Design Problem F: Given the rational transfer function $G(s) = \frac{N(s)}{D(s)}$ and the design specifications on the phase margin ϕ_m and on the gain crossover frequency ω_g, design a Lead-Lag compensator $C_{LL}(s)$ such that the loop gain frequency response $C_{LL}(j\omega)G(j\omega)$ passes through point $B_g = e^{j(\pi+\phi_m)}$ at $\omega = \omega_g$ and the step response of the closed-loop system has a good settling time t_s.

Solution F: *From Prop. 4, design specifications on the phase margin ϕ_m and the gain crossover frequency ω_g can be exactly satisfied using the set of compensators $C_{LL}(s,\omega_n)$ described by (3.19), with $\omega_A = \omega_g$, $A = G(j\omega_g)$ and $B_g = e^{j(\pi+\phi_m)}$. It can be easily shown that the set of the closed-loop characteristic equations*

$$1 + G(s)C_{LL}(s,\omega_n) = 0 \tag{3.52}$$

can be expressed as follows

$$1 + \omega_n^2 \overline{G}(s) = 0, \tag{3.53}$$

where

$$\overline{G}(s) = \frac{D(s)(\omega_g + Q(A,B)s) + N(s)(\omega_g + P(A,B)s)}{\omega_g s(D(s)(s - Q(A,B)\omega_g) + N(s)(s - P(A,B)\omega_g))}$$

is a known function. Since (3.53) is linear in ω_n^2, the contour locus method can be applied. A good settling time t_s of the step response of the closed-loop system can be obtained choosing ω_n such to

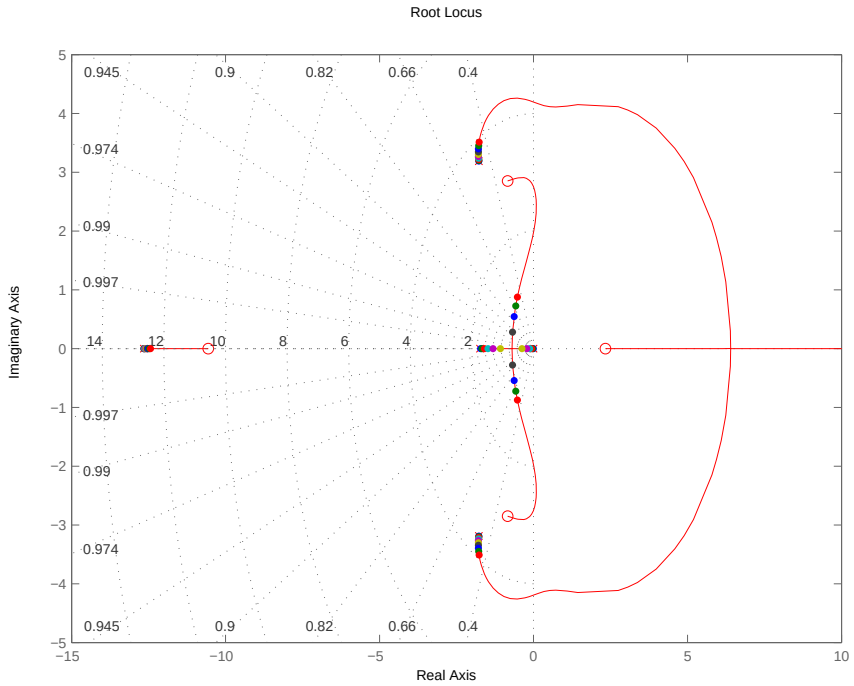

Figure 3.31: Root locus of $1+\omega_n^2\overline{G}(s)$ for $\omega_n^2 \in (0,\infty)$.

maximize the distance of the poles from the imaginary axis on the root locus of $\overline{G}(s)$ *when* $\omega_n^2 \in (0,\omega_A^2)$, *see Fig. 3.31.*

Numerical example. Given the plant

$$G(s) = \frac{200}{s(s+1)(s+10)}, \tag{3.54}$$

design the compensator $C_{LL}(s)$ that meets the design specifications of a phase margin $\phi_m = 45^\circ$ at gain crossover frequency $\omega_g = 2.75$ and such that the system step response has a good the settling time t_s.

Solution. The given design specifications define the points $B = e^{j225^\circ}$ and $A = G(j\omega_g) = 2.4e^{-j175^\circ} \in \mathscr{D}_B$, see Fig. 3.6. The set of compensators (3.19) that move the point A in B can be obtained using (2.21) and (4) with $P(A,B) = -0.531$ and $Q(A,B) = -2.52$. The Nyquist and the Bode plots of $C(j\omega,\omega_n)$ for $\omega_n \in \{0.3, 0.6, 0.9, 1.35\}$ are shown in Fig. 3.6-3.8 respectively. Function $\overline{G}(s)$ in (3.53) can be written as follows

$$\overline{G}(s) = \frac{-0.9174s^4 - 9.091s^3 + 1.826s^2 - 28.64s + 200}{s^5 + 17.94s^4 + 86.31s^3 + 269.4s^2 + 292.2s}.$$

The corresponding root locus is shown in Fig. 3.31, where the highlighted points are related to $\omega_n = 0.1 : 0.1 : 1$. A good settling time can be obtained placing the poles such to maximize their distance

from the imaginary axis. The minimum settling time $t_s = 1.72$s is given for $\omega_n = 0.3$.

3.5.2 Requirement on a good resonance peak

The complementary modulus margin M_c is equal to the inverse of the infinity-norm of the complementary sensitivity function $T(s)$, see [27]:

$$M_c = \|T(s)\|_\infty^{-1}, \quad \text{where} \quad T(s) = \frac{G(s)C(s)}{1+G(s)C(s)}.$$

The margin M_c can be graphically determined as the inverse of the modulus M of the constant M-circle tangent to the open loop frequency response $L(j\omega) = G(j\omega)C(j\omega)$. It follows that the margin M_c is an important performance indicator, since it is related to the resonance peak of the closed-loop system. Indeed if the type of the system is zero, M_c is equal to the static gain $L(0)$ over the resonance peak, if the type is greater than zero M_c is equal to the inverse of the resonance peak. Let us consider the following Design Problem proposed in [26].

Design Problem G: Given the plant $G(s)$ and design specifications on the phase margin ϕ_m and the gain crossover frequency ω_g, design a Lead-Lag compensator $C_{LL}(s)$ such that the loop gain frequency response $L(j\omega) = C_{LL}(j\omega)G(j\omega)$ is tangent in point $B_g = e^{j(\pi+\phi_m)}$ at frequency $\omega = \omega_g$ to the constant M-circle passing through point B_g.

Solution G: *Draw the controllable domain $\mathscr{D}_{B_g}$ with respect to $B_g = e^{j(\pi+\phi_m)}$ as shown in Fig. 3.32 and check if $A_g = G(j\omega_p)$ belongs to $\mathscr{D}_{B_g}$. If not the Design Problem has no acceptable solutions.*
Than determine the parameters $P_g = P(A_g, B_g)$, $Q_g = Q(A_g, B_g)$ using the Inversion Formulae (2.21).
The complementary modulus margin M_c related to the unique constant M-circle passing through B_g can be calculated employing the relation

$$M_c = \sqrt{2\cos(\pi+\phi_m)+2}. \tag{3.55}$$

The desired angle ψ of the loop gain frequency response $C(j\omega)G(j\omega)$ in B_g, see Fig. 3.32, can be obtained by using the following relation

$$\psi = \left|\arctan\left(-\frac{\cos\phi_m + c_c}{\sin\phi_m}\right)\right|, \tag{3.56}$$

where $c_c = -\frac{1}{1-M_c^2}$ is the position of the center of the constant M-circle on the real axis.

Once a point $A'_g = G(j\omega'_g)$ is chosen, where $\omega'_g = \omega_g + \Delta\omega$ and $\Delta\omega$ small, calculate δ and ω_n as follows

$$\delta = Q_g \frac{\omega_n^2 - \omega_g^2}{2\omega_n\omega_g}, \qquad \omega_n = \sqrt{\frac{-b \pm \sqrt{b^2-4ac}}{2a}}, \tag{3.57}$$

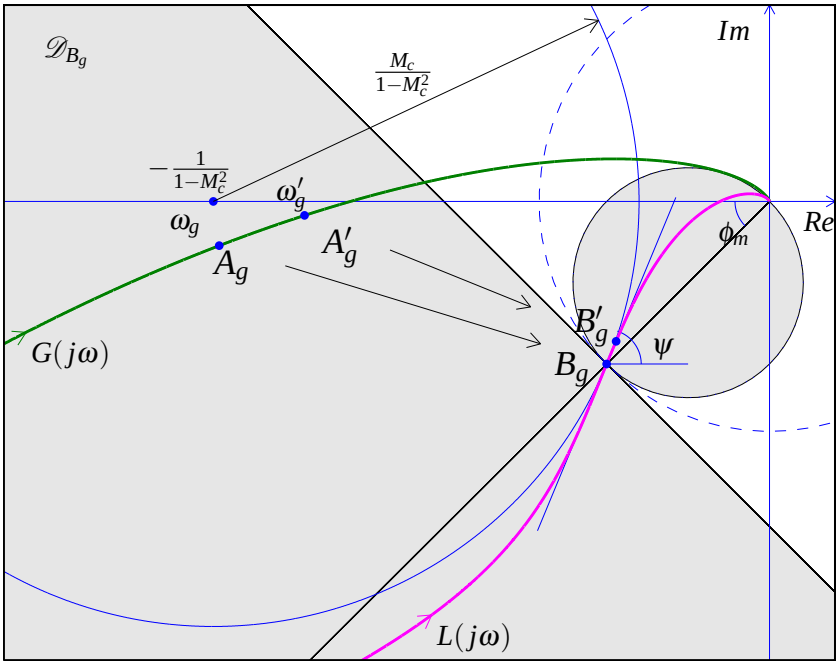

Figure 3.32: Solution of Design Problem G.

where

$$\begin{aligned}
a &= \alpha_1+\alpha_2-\alpha_3,\\
b &= \omega_g^2(\alpha_3-2\alpha_2)+\omega_g'^2(\alpha_3-2\alpha_1),\\
c &= \alpha_1\omega_g'^4+\omega_g^2(\alpha_2\omega_g^2-\alpha_3\omega_g'^2),\\
\alpha_1 &= Y_D+\tan\psi'(1-X_D),\\
\alpha_2 &= Q_g\tfrac{\omega_g'^2}{\omega_g^2}(Y_DQ_g+\tan\psi'(P_g-X_DQ_g)),\\
\alpha_3 &= (P_g-Q_g)\tfrac{\omega'_g}{\omega_g},\\
X_D &= Re(\tfrac{B_g}{A'_g}),\quad Y_D=Im(\tfrac{B_g}{A'_g}),\quad \psi'=\psi-\angle A'_g.
\end{aligned}$$

The solution is acceptable only if δ and ω_n are real and positive.

Proof: The design specifications define the position of points $B_g=e^{j(\pi+\phi_m)}$ and $A_g=G(j\omega_g)$. According to Prop. 4, the compensators $C_g(s,\omega_n)$ which move point $A_g\in\mathscr{D}_{B_g}$ to point B_g are obtained using the parameters γ and δ given by (3.15). The free parameter ω_n can now be used to force the loop gain frequency response $L(j\omega,\omega_n)=C_g(j\omega,\omega_n)G(j\omega)$ to pass through point B_g with slope related to the angle ψ given by (3.56), see [26]. This problem can be solved under the following condition

$$\lim_{\Delta\omega\to 0}\angle(L(j(\omega_p+\Delta\omega),\omega_n)-B_g)=\psi. \tag{3.58}$$

Relation (3.58) can be approximated choosing a point $A'_g(\omega'_g)=G(j\omega'_g)$ at frequency $\omega'_g=\omega_g+\Delta\omega$, with $\Delta\omega$ small. The point $A'_g(\omega'_g)$ can be brought to $B'_g=L(j(\omega'_g,\omega_n)=A'_g(\omega'_g)C_g(j\omega'_g,\omega_n)$ using the

Inversion Formulae method. From (3.58) one obtains that

$$\begin{aligned}\angle\left(B'_g - B_g\right) &= \angle\left(A'_g(\omega'_g)C_g(j\omega'_g,\omega_n) - B_g\right)\\ &= \angle\left(A'_g(\omega'_g)\left(C_g(j\omega'_g,\omega_n) - \frac{B_g}{A'_g}\right)\right)\\ &= \angle\left(A'_g(\omega'_g)\left(X_C(\omega_n)+jY_C(\omega_n)-X_D-jY_D\right)\right)=\psi,\end{aligned} \tag{3.59}$$

where $X_C(\omega_n)$ and $Y_C(\omega_n)$ are the real and the imaginary part of $C_g(j\omega'_g,\omega_n)$, X_D and Y_D are the real and the imaginary part of $\frac{B_g}{A'_g}$. Equation (3.59) can be rewritten as follows

$$\frac{Y_C(\omega_n)-Y_D}{X_C(\omega_n)-X_D} = \tan\psi', \tag{3.60}$$

where $\psi' = \psi - \angle A'_g$. Equation (3.60) is a second order equation in the variable ω_n^2. The solution of this equation provides the value of ω_n given in (3.57). □

Numerical example. Consider the plant given in the previous example, and the set $C_g(j\omega,\omega_n)$ of controllers that meet the design specification on $\phi_m = 45^\circ$ at frequency $\omega_g = 2.75$. Calculate ω_n to adjust the loop slope of $L(j\omega) = C_{LL}(j\omega)G(j\omega)$ as described in Design Problem G.

Solution. Using (3.55) and (3.56), the complementary modulus margin is $M_c = 0.7654$ and from (3.56) it follows that $\psi = 67.5^\circ$. Choosing $\omega'_g = 3$ and using (3.57), one obtains $\delta = 3.3748$ and $\omega_n = 0.9143$. The corresponding loop gain frequency response is plotted in magenta in Fig. 3.32.

3.6 Comparison of the methods.

The Inversion Formulae method, useful to design Lead-Lag networks, allows to easily and exactly satisfy two dynamical requirements. The third parameter can be chosen in order to meet a further specification. The division of the design procedure in these two main parts can be used to simplify the classical methods. These are generally based on a simultaneous synthesis of the three parameters. The complexity of some of these procedures could be reduced with a hybrid method. Indeed two of the three parameters could be chosen by using the Inversion Formulae method, such to exactly satisfy two design specifications, the third parameter can be synthesized on the base of the classical methods. This idea leads to a renew interest on the study of classical design procedures.

In this chapter the Inversion Formulae method has been used to solve several design problems. The main advantages of the method are that it is exact, it can be obtained numerically or graphically on Nyquist diagrams, it can be used in written exercise test. Moreover the graphical solution, compared with other graphical approaches such as the one in [25], can be easily determined by ruler and compass in the complex plane by finding the intersections of the frequency response of the plant with particular design

circles. Moreover, the Inversion Formulae method provides *all* the solutions of the control problem and not only a subset of all the solutions, as it happens in [25]. The main disadvantage of the design procedure is that not always an acceptable solution exists.

The design procedure proposed to solve the Design Problem F employs the classical root-locus method to determine a good settling time of the step response. This is an important specification for the system performance, however the solution requires good knowledge on linear control theory and can be applied to plants without delays.

The procedure which solves the Design Problem G is important from an educational point of view, because it leads the students to connect some very important concepts of the control theory. Some of them are related to the M-constant locus, the sensitivity function, the complementary modulus margin and the resonance peak of the closed-loop system. The procedure guarantees good performance in almost all the closed-loop real systems. In the case of complex high-order systems, however, the tangent condition of the loop gain frequency response to the M-constant circle at the gain crossover frequency not always is sufficient to avoid that the loop gain frequency response enters into the constant M-circle at higher frequency. In these cases the procedure is not the optimal solution to guarantee a robust control. One of the main advantages of this method is that it requires the knowledge of the plant in only two points.

Chapter 4

Discrete-time Lead-Lag type regulators

Nowadays digital control of automatic systems is widely used for its benefits over analog control, including reduced parts count and greater flexibility. The discrete-time control design methods can be classified as indirect and direct. The first are widely used because require only limited knowledge of the discrete-time control theory and are based on the vast background of the continuous-time control. Conversely, direct design of classical discrete regulators receives far less attention than indirect design in control textbooks, i.e. [19], [28] and [29]. However, the discretization of a continuous-time control system creates new phenomena not present in the original continuous-time control system, such as considerable inaccuracies in the locations of poles and zeros [29]. In this chapter the Inversion Formulae method is employed to design the discrete time Lead-Lag type networks for robust control. The method has been introduced to the design of discrete time Lead and Lag regulators in [14]. This design procedure is reformulated in this thesis to use the same Inversion Formulae introduced in the Def. 1 for the continuous time case. Moreover the method has been extended to the design of discrete time Lead-Lag regulators [15]. In this way the same Inversion Formulae (2.21) can be used for all the types of Lead-Lag regulators, both in continuous and discrete time domains.

4.1 The structure of the considered discrete-time Lead-Lag type networks

Let us consider the following unified structure of Lead and Lag networks

$$C_{dL}(z) = \frac{(z+1)+\sigma_1(z-1)}{(z+1)+\sigma_2(z-1)}, \tag{4.1}$$

with unity steady-state gain $\gamma_0 = C_{dL}(1) = 1$. When $\sigma_1 > \sigma_2$, (4.1) is the transfer function of a Lead network, while when $\sigma_1 < \sigma_2$, (4.1) is the transfer function of a Leg network. The zero and the pole can be expressed as follows

$$z_0 = \frac{\sigma_1 - 1}{\sigma_1 + 1}, \qquad z_p = \frac{\sigma_2 - 1}{\sigma_2 + 1}.$$

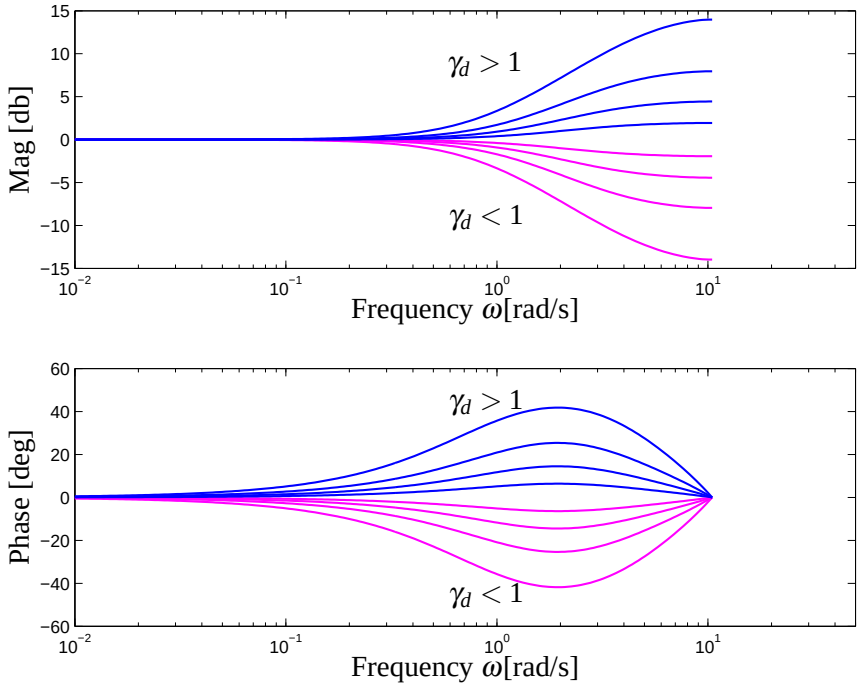

Figure 4.1: Bode magnitude and phase plots of $C_{dL}(\omega,T)$ on variation of γ_d.

The controller is a minimum-phase system when $|z_0| < 1$ and $|z_p| < 1$, that is when $\sigma_1 > 0$ and $\sigma_2 > 0$. The frequency response of $C_{dL}(z)$ is obtained when $z = e^{j\omega T}$ and $\omega \in [0, \frac{\pi}{T}]$, where T is the sampling period of the system. That is

$$C_{dL}(\omega,T) = C_{dL}(e^{j\omega T}) = \frac{1+jP(\omega,T)}{1+jQ(\omega,T)} = Me^{j\varphi}, \tag{4.2}$$

where

$$P(\omega,T) = \sigma_1\Omega(\omega), \qquad Q(\omega,T) = \sigma_2\Omega(\omega), \tag{4.3}$$

and

$$\Omega(\omega) = tan\frac{\omega T}{2}.$$

The high frequency gain γ_d of (4.1) can be written as

$$\gamma_d = C_{dL}(z)|_{z=-1} = \frac{\sigma_1}{\sigma_2} = \frac{P(\omega,T)}{Q(\omega,T)}.$$

It can be verify that $\gamma_d > 1$ in the case of Lead network, while $\gamma_d < 1$ in the case of Lag controller. The maximum (or the minimum) phase φ_{md} for $\omega \in [0, \frac{0}{\pi/T}]$ is

$$\varphi_{md} = \arcsin\left[\frac{\gamma_d - 1}{\gamma_d + 1}\right]$$

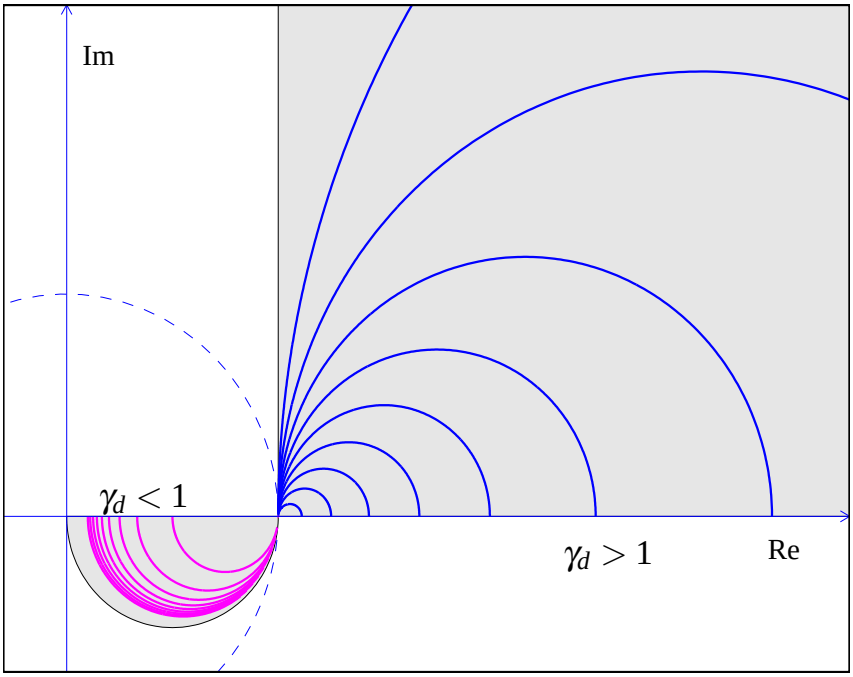

Figure 4.2: Nyquist plots of $C_{dL}(\omega,T)$ on variation of γ_d.

at frequency

$$\omega_{md} = \frac{1}{T}\arccos\left[\frac{z_0+z_p}{1+z_0z_p}\right].$$

The Bode and the Nyquist diagrams of $C_{dL}(\omega,T)$ for $\omega_{md}=1$ and $T=0.3$ on variation of $\gamma_d = [0.2 : 0.2 : 1, 1/(0.2 : 0.2 : 1)]$ are shown in Fig. 4.1 and 4.2. It can be easily shown that the Nyquist plots of $C_{dL}(\omega,T)$ are semicircles $C(\gamma_d)$ with center $C_0 = \frac{\gamma_d+1}{2}$ and radius $R_0 = \frac{|\gamma_d-1|}{2}$. The intersections of $C(\gamma_d)$ with the real axis occur at points 1 and γ_d.

Definition 2 *Given a point $B \in \mathbb{C}$, let us define* "admissible domain of discrete Lead and Lag compensators $C_{dL}(z)$ with respect to point B" *the set $\mathscr{D}_{dLB}$ defined as follows*

$$\mathscr{D}_{dLB} = \left\{A \in \mathbb{C} \,\middle|\, \exists\,\sigma_1,\sigma_2 > 0, \exists\,\omega \geq 0 : C_{dL}(\omega,T)\cdot A = B\right\}.$$

The shape of $\mathscr{D}_{dLB}$ for Lead and Lag compensators in the Nyquist plane are shown in gray in Fig. 4.2 and they are equal to the admissible domains of continuous time Lead and Lag networks (2.2) and (2.6) shown in Fig. 2.11 and 2.12.

The considered form of discrete-time Lead-Lag compensator can be expressed as follows

$$C_{LL}(z) = \frac{(z-1)^2 + 2\gamma_d\delta_d\Omega_n(z^2-1) + \Omega_n^2(z+1)^2}{(z-1)^2 + 2\delta_d\Omega_n(z^2-1) + \Omega_n^2(z+1)^2}, \tag{4.4}$$

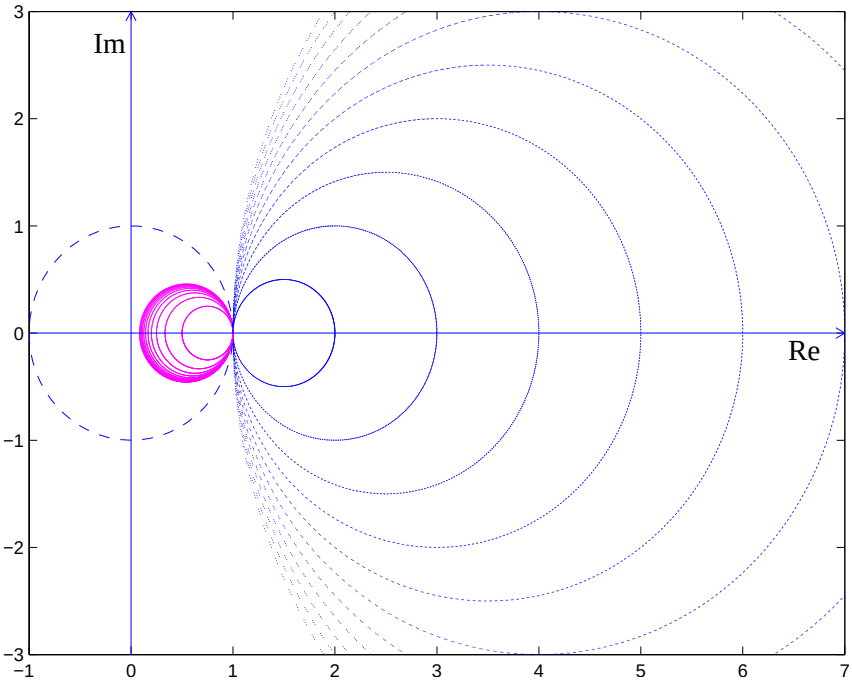

Figure 4.3: Nyquist diagrams of function $C_{LL}(\omega,T)$ when $\Omega_n = 1$, $\delta_d = 1.5$, $\gamma_d = [2:1:12]$ (blue lines) and $\delta_d = 1.5$, $\gamma_d = 1./[2:1:12]$ (magenta lines).

where γ_d, Ω_n and δ_d are assumed to be real and positive. The frequency response of (4.4) for $\omega \in [0, \frac{\pi}{T}]$ can be written as

$$C_{LL}(\omega,T) = C_{LL}(e^{j\omega T}) = \frac{1+jP(\omega,T)}{1+jQ(\omega,T)}, \tag{4.5}$$

where T is the sampling period,

$$P(\omega,T) = \frac{2\gamma_d\delta_d\Omega_n\Omega(\omega)}{\Omega_n^2-\Omega(\omega)^2}, \qquad Q(\omega,T) = \frac{2\delta_d\Omega_n\Omega(\omega)}{\Omega_n^2-\Omega(\omega)^2}, \tag{4.6}$$

and

$$\Omega(\omega) = \tan\frac{\omega T}{2}. \tag{4.7}$$

The proof hinges on the following equality

$$\frac{e^{j\omega T}-1}{e^{j\omega T}+1} = \tan\frac{\omega T}{2}.$$

The steady-state gain γ_{d0} of the discrete compensator (4.4) is unity, that is

$$\gamma_{d0} = \lim_{z\to 1} C_{LL}(z) = 1.$$

From (4.5) and (4.6) it follows that

$$\gamma_d = C_{LL}(e^{j\omega T})\Big|_{\omega=\frac{2}{T}\arctan\Omega_n} = \frac{P(\omega,T)}{Q(\omega,T)}. \tag{4.8}$$

As in the continuous time case, the shape of the frequency response (4.5) on the Nyquist plane is a circle $C(\gamma_d)$ with center C_0 and radius R_0:

$$C(\gamma_d) = C_0 + R_0\, e^{j\theta}, \qquad C_0 = \frac{\gamma_d+1}{2}, \qquad R_0 = \frac{|\gamma_d-1|}{2}, \tag{4.9}$$

where $\theta \in [0, 2\pi]$. The intersections of $C(\gamma_d)$ with the real axis occur at points 1 and γ_d. Notice that the shape does not depend on parameters $\delta_d > 0$ and $\Omega_n > 0$. From this property it follows that γ_d is the minimum (or maximum) amplitude of $C_{LL}(\omega,T)$ when $\gamma_d > 1$ (or $\gamma_d < 1$). When $\Omega_n = 1$, the frequency at the point $(\gamma_d, 0)$ is $\omega = \frac{\pi}{2T}$.

Definition 3 *Given a point $B \in \mathbb{C}$, let us define* "admissible domain of discrete Lead-Lag compensator $C_{LL}(z)$ to point B" *the set $\mathscr{D}_{dB}$ defined as follows*

$$\mathscr{D}_{dB} = \left\{ A \in \mathbb{C} \;\middle|\; \exists\, \gamma_d, \delta_d, \Omega_n > 0, \exists\, \omega \geq 0 : C_{LL}(\omega,T)\cdot A = B \right\}.$$

It can be easily shown that the domain $\mathscr{D}_{dB}$ on the Nyquist plane is equal to the Lead-Lag admissible domain $\mathscr{D}_B$ determined in the continuous time case.

Let $\mathscr{C}_{LL}(\gamma_d)$ denote the set of all the Lead-Lag compensators $C_{LL}(z)$ having the same parameter γ_d and the same shape on the Nyquist plane, that is

$$\mathscr{C}_{LL}(\gamma_d) = \left\{ C_{LL}(z) \text{ as in (4.4)} \;\middle|\; \delta_d > 0, \Omega_n > 0 \right\}. \tag{4.10}$$

Moreover, let $\mathscr{C}_{\gamma_d}(z) \in \mathscr{C}_{LL}(\gamma_d)$ denote one element of set $\mathscr{C}_{LL}(\gamma_d)$ chosen arbitrarily.

4.2 Synthesis of discrete-time Lead and Lag compensators

Let us refer to the block scheme of Fig. 6.1, where $HG(z)$ is the discrete system to be controlled, what cab be given directly in discrete time domain or it can be obtained by a continuous time plant $G(s)$ using a zero-order hold $H_0(s)$, that is

$$HG(z) = \mathscr{Z}[H_0(s)\,G(s)],$$
$$H_0(s) = \frac{1-e^{-Ts}}{s},$$

and T is the sampling period. Let $C(z)$ denote the discrete compensator (4.4) to be designed. The loop gain frequency response of the system is

$$L(\omega,T) = C(\omega,T)HG(\omega,T).$$

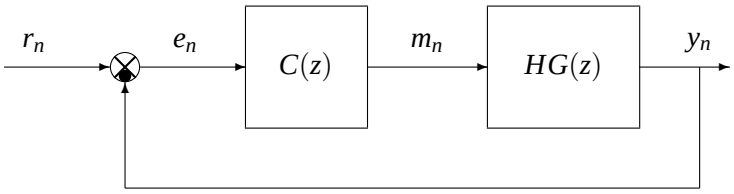

Figure 4.4: The considered block scheme for the discrete time case.

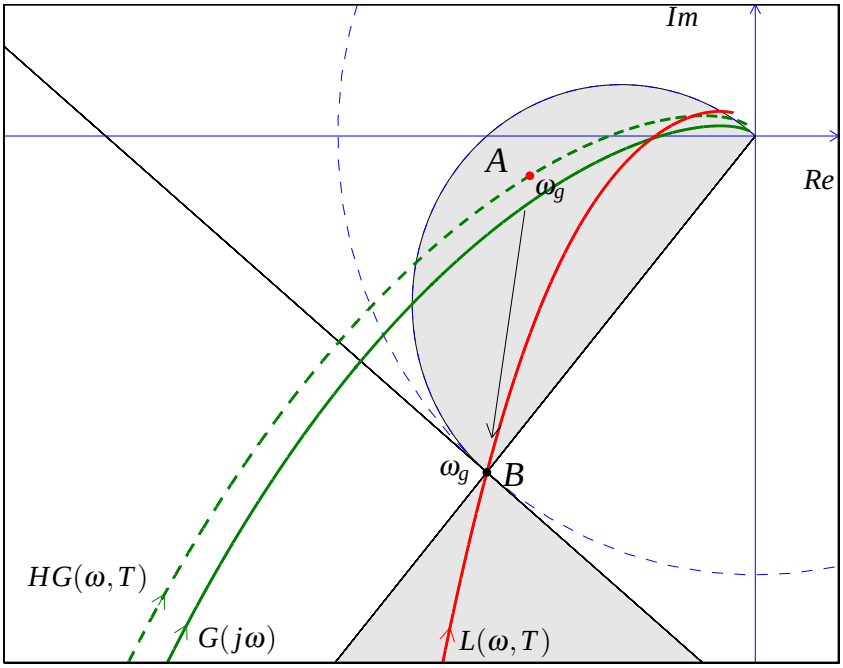

Figure 4.5: Solution of Design Problem *A* using discrete time Lead controller.

Let first consider the case of first order Lead and Lag networks. Due to the similarity of the considered structures in continuous and discrete time domains, the Inversion Formulae method, used to solve the Design Problems A and B, can be extended to a direct discrete design.

Design procedure. The numerical and graphical solutions of Design Problems A and B can be carried out as following described.

Step 1. *Determine the point* $B = M_B e^{j\varphi_B}$. This point is completely determined by the given design specifications, see (2.18).

Step 2. *Draw the admissible domain* $\mathscr{D}_{dLB}$. The admissible domains $\mathscr{D}_{dLB}$ of Lead and/or Lag compensators in the Nyquist or Nichols plane are shown in Fig. 2.11 and 2.12.

Step 3. *Plot the frequency response* $HG(\omega,T)$ *of the plant.* Let $A = HG(\omega_0,T) = M_A e^{j\varphi_A}$ denote a

point of $HG(\omega,T)$, which belongs to $\mathscr{D}_{dLB}$. This point is completely defined by the design requirements if the desired frequency of $L(\omega,T)$ at point B is given as design specification (i.e. the gain or the phase crossover frequency). The point A can be brought to B by a discrete time Lead or Lag controller if only if $A \in \mathscr{D}_{dLB}$. If there are no intersection points between $HG(\omega,T)$ and $\mathscr{D}_{dLB}$ the problem has no solutions.

Step 4. *Design the parameters of the compensator.* The values of σ_1 and σ_2 in (4.1) can be obtained by using the *Inversion Formulae* (2.21) with $P(A,B) = \sigma_1\Omega(\omega_0)$ and $Q(A,B) = \sigma_2\Omega(\omega_0)$, that is

$$\sigma_1 = \frac{M - \cos\varphi}{\Omega(\omega_0)\sin\varphi}, \qquad \sigma_2 = \frac{\cos\varphi - \frac{1}{M}}{\Omega(\omega_0)\sin\varphi}, \tag{4.11}$$

where $\Omega(\omega_0) = tan\frac{\omega T}{2}$.

The proof directly follows from (4.2), (4.3) and (2.21) as shown in the continuous time case.

Numerical examples

Let us consider the same numerical examples solved in Sec. 2.2 using the classical method.

Solution of Example 1: The discrete time plant $HG(z)$ to be controlled has been obtained by $G(s)$ employing a zero-order hold with $T = 0.1$s, that is

$$HG(z) = \frac{0.003218z^2 + 0.00996z + 0.00186}{z^3 - 2.273z^2 + 1.606z - 0.3329}.$$

The Nyquist plots of $G(j\omega)$ and $HG(\omega,T)$ are shown in continuous and dashed green curves in Fig. 4.5. The design requirement on the phase margin $\phi_m = 50^\circ$ specification defines the position of the point $B = M_B e^{j\varphi_B}$, i.e. $M_B = 1$ and $\varphi_B = 230^\circ$. The point $A = HG(\omega_g,T)$ is chosen in the admissible domain $\mathscr{D}_{dLB}$ at frequency $\omega_g = 2$, see Fig. 4.5. The values $M_A = 0.547$ and $\varphi_A = -170.5$, can be used to calculate the magnitude M, and the phase φ of the controller at frequency $\omega_g = 2$, see (4.11). The parameters of the controller that exactly solve the problem are $\sigma_1 = 16.3774$ and $\sigma_2 = 3.2772$. The corresponding loop gain frequency response $L(\omega,T)$ is shown in red in Fig. 4.5.

4.3 Synthesis of discrete-time Lead-Lag compensator

It is well known that also in discrete time domain the gain and the phase margins provide a two-points measure of how close the Nyquist plot is to the point -1 [30], thus they are indicators of the system robustness. An interesting problem to be solved is the Design Problem *C*, that is the three parameters of the compensator (4.4) have to be exploited such to satisfy both the gain and the phase margins specification and the given gain crossover frequency. The direct design of Lead-Lag regulators to solve the Design Problem *C* leads to a set of nonlinear and coupled equations difficult to be solved. However, an exact

solution can be obtained expressing the frequency response of the controller in polar form, as required by the Inversion Formulae method and using the following property.

Property 10 ***(From** A **to** B).* *Given a point $B \in \mathbb{C}$ and chosen a point A of the frequency response $HG(\omega,T)$ at frequency $\omega_A \in [0, \frac{\pi}{T}]$ belonging to the admissible domain $\mathscr{D}_{dB}$, the set $C_{LL}(z,\Omega_n)$ of all the discrete Lead-Lag compensators $C_{LL}(z)$ that move point A to point B is obtained from (4.4) using the parameters*

$$\gamma_d = \frac{P(A,B)}{Q(A,B)} > 0, \qquad \delta_d = Q(A,B)\frac{\Omega_n^2 - \Omega_A^2}{2\Omega_n\Omega_A} > 0 \tag{4.12}$$

for all $\Omega_n > 0$ such that $\delta_d > 0$, with $P(A,B)$ and $Q(A,B)$ obtained using (2.21) and $\Omega_A = \tan\frac{\omega_A T}{2}$.

Proof: The frequency response (4.5) at frequency ω_A can be written as follows:

$$C_{LL}(\omega_A,T) = \frac{1+jP(\omega_A,T)}{1+jQ(\omega_A,T)} = Me^{j\varphi}, \tag{4.13}$$

where M and φ can be expressed as in (2.21). Due to the similar structure of (3.3) and (4.5) the proof is similar to the one given for the continuous-time case.

□

In the case of discrete time systems, the Design Problem *C* can be reformulated as follows.

Design Problem C: Given the control scheme of Fig. 6.1, the transfer function $HG(z)$, the sampling period T and design specifications on the phase margin ϕ_m, gain margin G_m and gain crossover frequency ω_g, design a Lead-Lag compensator $C_{LL}(z)$ such that the loop gain transfer function $C_{LL}(\omega,T)HG(\omega,T)$ passes through point $B_g = e^{j(\pi+\phi_m)}$ for $\omega = \omega_g \in [0, \frac{\pi}{T}]$ and passes through point $B_p = -1/G_m$.

Solution: The solution can be obtained following a procedure very similar to the ones presented for the continuous time case.

Step 1. Draw the admissible domain $\mathscr{D}_{dB_g}$ of point $B_g = e^{j(\pi+\phi_m)}$ as shown in Fig. 4.6 and check whether point $A_g = HG(\omega_g,T)$ belongs to $\mathscr{D}_{dB_g}$.

Step 2. Determine the parameters $P_g = P(A_g,B_g)$ and $Q_g = Q(A_g,B_g)$ using the Inversion Formulae (2.21).

Step 3. Draw the circle $\mathscr{C}^-_{B_p\gamma_d}(j\omega)$ having its diameter on the segment defined by points B_p and $\frac{B_p}{\gamma_d}$, where $B_p = -1/G_m$ and $\gamma_d = \frac{P_g}{Q_g}$. If there are no intersections points of $\mathscr{C}^-_{B_p\gamma_d}(j\omega)$ with $HG(\omega,T)$, the Design Problem has no solutions. Otherwise let $A_{p_i} = \{A_{p_1}, A_{p_2}, ...\}$ denote the set of the intersections points of circle $\mathscr{C}^-_{B_p\gamma_d}(j\omega)$ with $HG(\omega,T)$ at frequencies $\omega_{p_i} = \{\omega_{p_1}, \omega_{p_2}, ...\}$. These points can also be

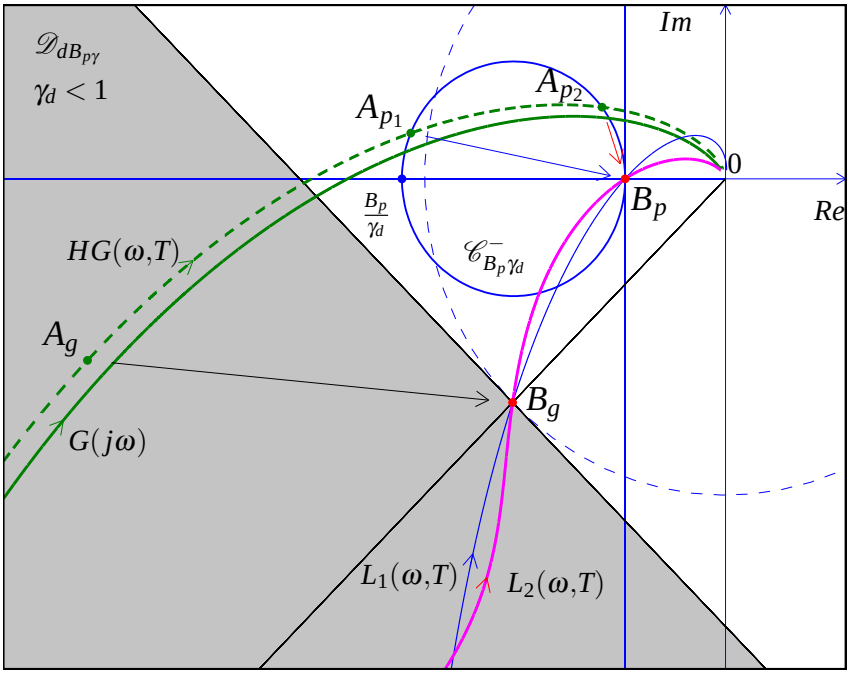

Figure 4.6: Graphical solution on the Nyquist plane of the Design Problem *C* for discrete time systems.

obtained solving the following relation (see Fig. 4.7)

$$\gamma_d = \gamma_{d\,p}(\omega_p) = \frac{\frac{M_{B_p}}{M_{A_p}(\omega_p)} - \cos(\varphi_{B_p} - \varphi_{A_p}(\omega_p))}{\cos(\varphi_{B_p} - \varphi_{A_p}(\omega_p)) - \frac{M_{A_p}(\omega_p)}{M_{B_p}}}. \tag{4.14}$$

Step 4. For each $\omega_p = \omega_{p_i}$ belonging to $[0, \frac{\pi}{T}]$ calculate δ_d and Ω_n as follows

$$\delta_d = Q_g \frac{\Omega_n^2 - \Omega_p^2}{2\Omega_n\Omega_p} > 0, \tag{4.15}$$

$$\Omega_n = \sqrt{\frac{Q_p\Omega_g - Q_g\Omega_p}{\frac{Q_p}{\Omega_g} - \frac{Q_g}{\Omega_p}}} > 0, \tag{4.16}$$

where $P_p = P(A_p, B_p)$ and $Q_p = Q(A_p, B_p)$ are obtained using (2.21) and $A_p = HG(\omega_p, T)$. The solutions are acceptable only if δ_d and Ω_n are real and positive.

The proof can be obtained in a similar way as in the continuous time case. Moreover, the design procedure can be easily modified in order to meet the design specifications on the phase margin ϕ_m, gain margin G_m and phase crossover frequency ω_p.

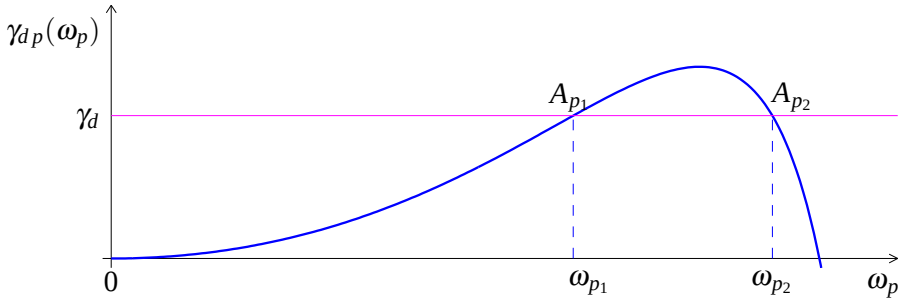

Figure 4.7: Plot of function $\gamma_{dp}(\omega_p)$ versus ω_p.

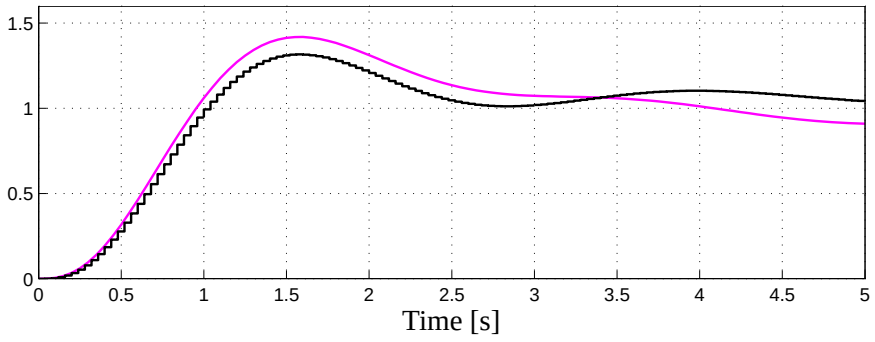

Figure 4.8: Step responses of the closed loop system in continuous time (magenta line) and discrete time (black line) cases.

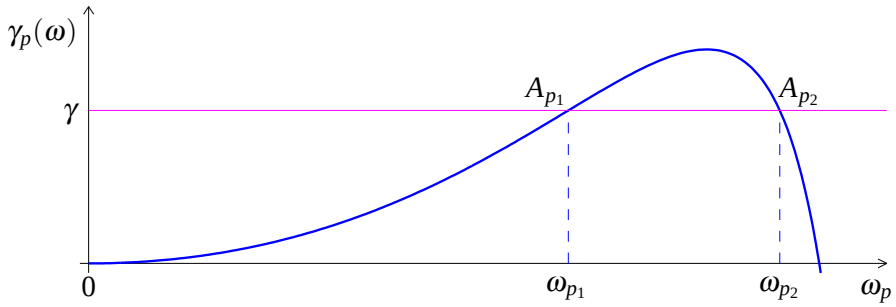

Figure 4.9: Plot of function $\gamma_p(\omega)$ versus ω_p.

4.4 Numerical examples

Example 2: Given the plant

$$G(s) = \frac{36(s+1.1)}{s(s+1.5)^2(s+3)}, \tag{4.17}$$

first design the continuous time Lead-Lag compensator (3.1) and then the discrete Lead-Lag compensator (4.4) in order to meet the phase margin $M_\varphi = 45^\circ$, the gain margin $G_m = 3$ and the gain crossover frequency $\omega_g = 1.8$. For the discrete time case a sampling period $T = 0.04$s can be considered.

Solution: The phase margin specification determines the point $B_g = e^{j225^\circ}$, that leads to the shape of the admissible domain $\mathscr{D}_{B_g}$ shown in Fig. 4.10. The point to be brought to B_g is $A_g = G(j\omega_g) = 2.2e^{-j162^\circ}$, that belongs to $\mathscr{D}_{B_g}$ as required by the method. Using (2.21) it follows that $P_g = -0.921$ and $Q_g = -0.921$. The parameter $\gamma = 0.327$ and point $B_p = 0.333e^{j180^\circ}$ define the blue circle $\mathscr{C}^-_{B_p\gamma}(j\omega)$ in Fig. 4.10. The intersections of $\mathscr{C}^-_{B_p\gamma}(j\omega)$ with $G(j\omega)$ are $A_{p_1} = 1.007e^{j174^\circ}$ and $A_{p_2} = 0.436e^{j154^\circ}$ at frequencies $\omega_{p_1} = 2.704$ and $\omega_{p_2} = 3.90$. These points can also be obtained solving relation $\gamma = \gamma_g(\omega_g)$, see Fig. 4.9. The solution for $\omega_p = \omega_{p_1}$ is not acceptable because $\delta < 0$. The corresponding loop transfer function $L_1(j\omega)$ is plotted in blue in Fig. 4.10. The second solution is obtained for $\omega_p = \omega_{p_2}$ and leads to $\delta = 1.63 > 0$ and $\omega_n = 1.04 > 0$. The obtained regulator is

$$C(s) = \frac{s^2 + 1.11s + 1.07}{s^2 + 3.39s + 1.07}. \tag{4.18}$$

The corresponding loop transfer function $L_2(j\omega) = G(j\omega)C(j\omega)$ is plotted in red in Fig. 4.10.

The discrete time system $HG(z)$ obtained by $G(s)$ using a sampling period T is the following

$$HG(z) = \frac{3.66\,10^{-4}z^3 + 1.04\,10^{-3}z^2 - 10^{-3}z - 3.1710^{-4}}{z^4 - 3.77z^3 + 5.33z^2 - 3.34z + 0.787}.$$

The points B_g and B_p are completely defined by the design specifications and are the same of the continuous time design. The point $A_g \in HG(e^{j\omega T})$ at frequency ω_g is $A_g = 2.2e^{-j165^\circ}$ and it belongs to the

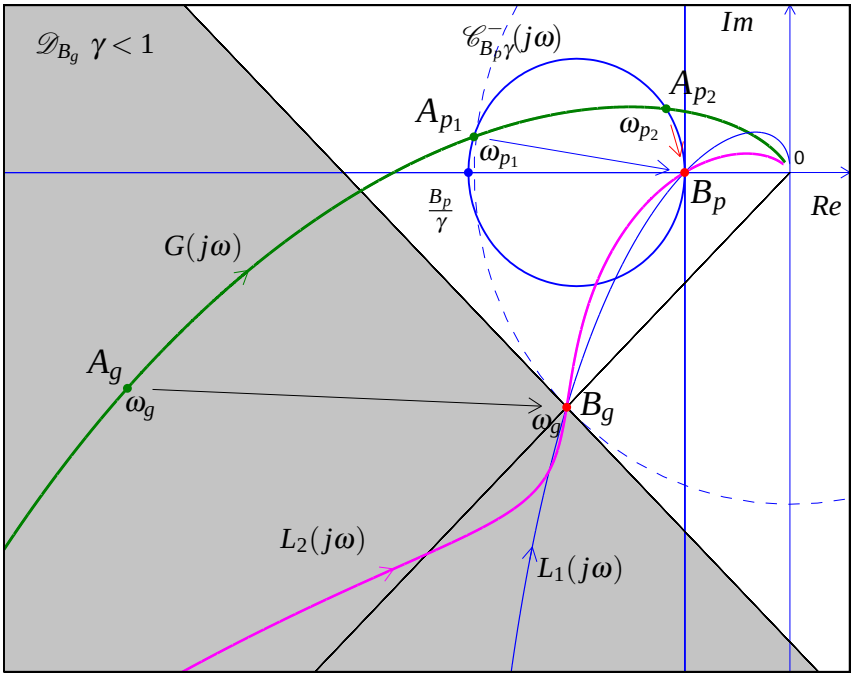

Figure 4.10: Graphical solution of Design Problem *C* on the Nyquist plane.

admissible domain $\mathscr{D}_{dB_g}$. Using the Inversion Formulae (2.21) $P_g = -0.828$ and $Q_g = -2.67$ can be obtained.

The parameter $\gamma_d = 0.310$ and point B_p define the circle $\mathscr{C}^-_{B_p\gamma_d}(j\omega)$ (see blue circle in Fig. 4.6). The intersections points with $HG(\omega,T)$ are $A_{p_1} = 1.06e^{j172^\circ}$ and $A_{p_2} = 0.469e^{j151^\circ}$ at frequencies $\omega_{p_1} = 2.64$ and $\omega_{p_2} = 3.78$. These points can be equivalently obtained solving relation (4.14), see Fig. 4.7.
The solution for $\omega_p = \omega_{p_1}$ is not acceptable because $\delta_d < 0$. The second solution is obtained for $\omega_p = \omega_{p_2}$, $\delta_d = 2.7163 > 0$ and $\gamma_d = 0.0147 > 0$. The following regulator is obtained

$$C_\gamma(z,\omega_{p_2}) = \frac{(z-1)^2 + 2.48\,10^{-2}(z^2-1) + 2.17\,10^{-4}(z+1)^2}{(z-1)^2 + 8.01\,10^{-2}(z^2-1) + 2.17\,10^{-4}(z+1)^2}.$$

The corresponding loop transfer function $L_2(\omega,T)$ is plotted in magenta in Fig. 4.6. The step responses of the closed loop system in continuous and discrete time cases are shown in Fig. 4.8.

4.5 Comparison with other methods

A graphical solution to exactly meet specifications on phase margin, gain margin and crossover frequency for the discrete and continuous design of all the compensators whose frequency response can be expressed as $C\frac{1+jB}{1+jA}$ is presented in [31]. From (4.5) it follows that this method can also be applied to the

discrete Lead-Lag regulator (4.4), however it is not directly described in [31]. One of the main advantages of the Inversion Formulae method is that the point A_p is directly determined in the complex plane by finding the intersections of the frequency response of the plant and particular design circles and not on an approssimate procedure. Moreover, the graphical solution for the direct design of discrete networks can be easily done on the Nyquist plane by ruler and compass, while the graphic construction given in [31] is based on the use of a special design chart. Another important aspect of the Inversion Formulae method is that it provides *all* the solutions of the control problem, whereas other graphical approaches, such as the one in [31], can only provide a subset of all the solutions.

Chapter 5

Continuous PID regulators

The proportional-integral-derivative (PID) compensators are widely used in the industrial processes to meet most of the control objectives, see [1], [32]-[35].

One of the main difference of PID controller compared to Lead-Lag network is the presence in its transfer function of a pole at the origin. It follows that this structure could be enough to meet the steady-state specification. For example, if the steady-state specification simply consists in achieving zero velocity error, the use alone of a compensator with a pole at the origin is sufficient to guarantee that this requirement is satisfied. In this case, the steady-state specification does not lead to constraints the static gain of the controller and this can be used to meet another requirement. However, there are steady-state requirements that lead to such constraints, for example a specification on the acceleration error. It follows that these two cases have to be considered separately in the design of PID controllers, see [9] and [13].

5.1 PID compensators: the general structure

The classical forms of PID networks are the following

- PID controller:
$$C_{\mathrm{PID}}(s) = K_p \left(1 + T_d\, s + \frac{1}{T_i\, s}\right) = K_P + K_D\, s + \frac{K_I}{s}, \tag{5.1}$$
- PI controller:
$$C_{\mathrm{PI}}(s) = K_p \left(1 + \frac{1}{T_i\, s}\right) = K_P + \frac{K_I}{s}, \tag{5.2}$$
- PD controller:
$$C_{\mathrm{PD}}(s) = K_p \left(1 + T_d\, s\right) = K_P + K_D\, s, \tag{5.3}$$

where the proportional, derivative and integrative terms K_P, K_D and K_I are assumed to be real and positive, or with $K_p = K_P, T_i = \frac{K_p}{K_I}, T_d = \frac{K_D}{K_p} > 0$. In addition to these controllers, sometimes the proper versions of the PID and PD controllers are also introduced. The second one is basically equivalent to a Lead network. These more complex structures will not be considered in this thesis. Their design using Inversion Formulae method is described in [9].

The frequency responses of the considered PID regulators can be expressed in a unified form as follows

$$C(j\omega) = P + jQ(\omega) = M_g e^{\varphi_g}, \tag{5.4}$$

where $P = K_P > 0$ and

$$\begin{aligned} Q(\omega) &= \omega K_D - \tfrac{K_I}{\omega}, \\ Q(\omega) &= -\tfrac{K_I}{\omega} < 0, \\ Q(\omega) &= \omega K_D > 0, \end{aligned}$$

in the case of PID, PI and PD respectively. In the case of PID controller $Q(\omega)$ is positive for $\omega > \sqrt{\frac{K_I}{K_D}}$ and negative for $0 < \omega < \sqrt{\frac{K_I}{K_D}}$.

The graphical representation of the frequency response of PID controller on the Nyquist plane is a vertical line passing through point $(K_P, 0)$, see Fig. 5.1. Variations on parameters determine the gray area of admissible values of M_g and φ_g useful in the synthesis procedure of the compensator.

Let $\mathscr{C}(K_P)$ and $\mathscr{C}^-(K_P)$ denote, respectively, the set of all the PID compensators $C_{\text{PID}}(s)$ having the same parameter K_P

$$\mathscr{C}(K_P) = \left\{ C(s) \text{ as in } (5.1) \;\middle|\; K_I > 0, K_D > 0 \right\}, \tag{5.5}$$

and the set of all the inverse functions $C(s)^{-1}$

$$\mathscr{C}^-(K_P) = \left\{ \frac{1}{C(s)} \;\middle|\; C(s) \in \mathscr{C}(K_P) \right\}. \tag{5.6}$$

It can be easily shown that the graphical representation of each element of $\mathscr{C}(K_P)$ on the Nyquist plane is a vertical straight line r which passes through point $(K_P, 0)$, see Fig. 5.2.

Property 11 *The shape of the frequency response of each element of set $\mathscr{C}^-(K_P)$ is a circle with center $C_0 = \frac{1}{2K_P}$ and radius $R_0 = \frac{1}{2K_P}$ which intersects the real axis in point 0 and point $\frac{1}{K_P}$.*

This graphical property hinges on the fact that the Nyquist diagram of $C^{-1}_{\text{PID}}(j\omega)$ is a circle

$$C^{-1}_{\text{PID}}(j\omega) = \frac{1}{C_{\text{PID}}(j\omega)} = C_0 + R_0 e^{j\theta(\omega)}, \tag{5.7}$$

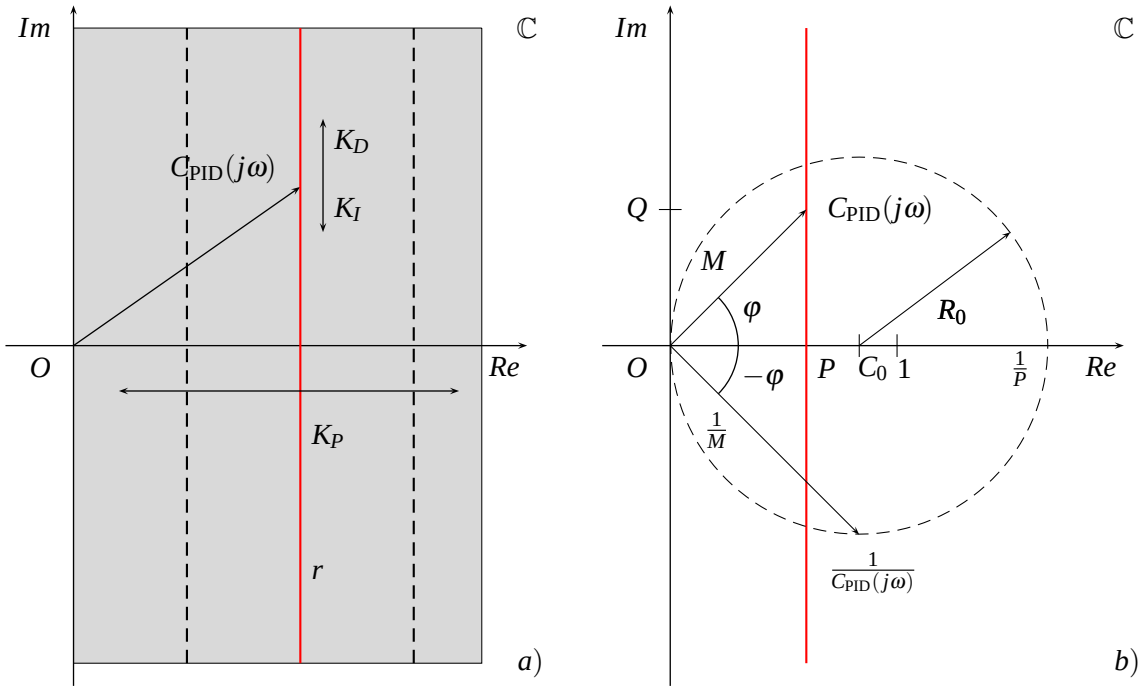

Figure 5.1: Nyquist plot of functions $C_{\mathrm{PID}}(j\omega)$ and $C_{\mathrm{PID}}{}^{-1}(j\omega)$.

where

$$C_0 = R_0 = \frac{1}{2P}, \qquad \theta(\omega) = -\arctan\frac{Q(\omega)}{P} \in [0, 2\pi], \qquad P = K_P.$$

Proof: The frequency response (5.4) can be written in polar form as follows

$$C_{\mathrm{PID}}(j\omega) = M(\omega)e^{j\varphi(\omega)},$$

where $M(\omega) = \frac{P}{\cos\varphi(\omega)}$ and $\varphi(\omega) = \arctan\frac{Q(\omega)}{P}$. It follows that $C^{-1}_{\mathrm{PID}}(j\omega)$ can be expressed in the form

$$\begin{aligned} C^{-1}_{\mathrm{PID}}(j\omega) &= \tfrac{1}{C_{\mathrm{PID}}(j\omega)} = \tfrac{\cos\varphi(\omega)}{P}e^{-j\varphi(\omega)} \\ &= \tfrac{1}{2P}[1+\cos(2\varphi(\omega))] - j\tfrac{1}{2P}\sin(2\varphi(\omega)) \\ &= \tfrac{1}{2P} + \tfrac{1}{2P}e^{-j2\varphi(\omega)}, \end{aligned}$$

for $Q(\omega) \in [-\infty, +\infty]$. The last relation clearly shows that the shape of $C^{-1}(j\omega)$ in the complex plane is a circle with center $C_0 = \frac{1}{2P}$ and radius $R_0 = \frac{1}{2P}$. □

The Nyquist diagrams of frequency responses of sets $\mathscr{C}(K_P)$ and $\mathscr{C}^-(K_P)$ for different values of parameter K_P are shown in Fig. 5.2.

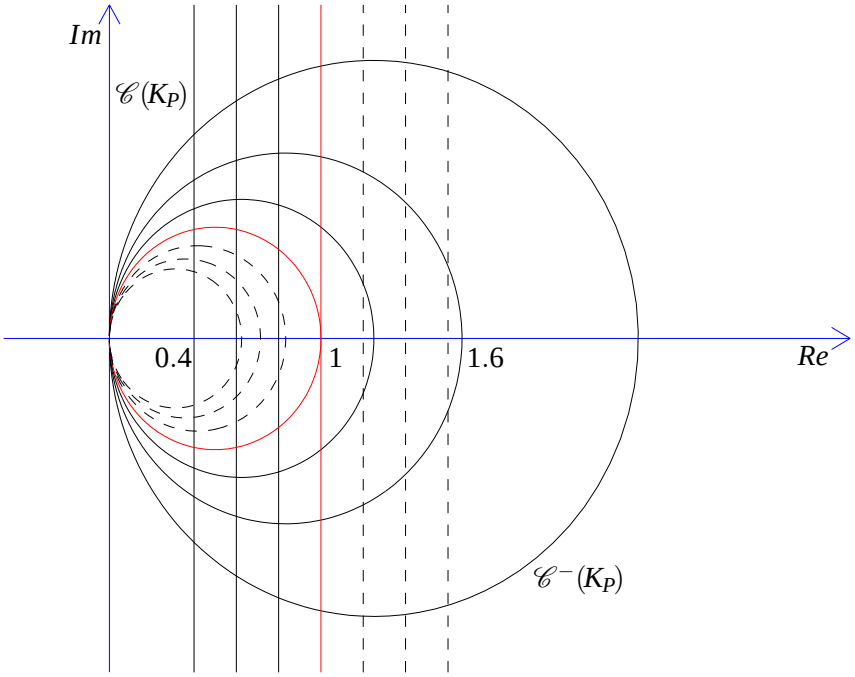

Figure 5.2: The Nyquist diagrams of frequency responses of set $\mathscr{C}(K_P)$ and $\mathscr{C}^-(K_P)$ for $K_P = 0.4 : 0.2 : 1.6$.

The graphical representations of the transfer functions of PI and PD regulators in the Nyquist plane on variation of their parameters are shown in Fig. 5.3-5.4. They are respectively positive and negative strict lines passing through point $(K_P, 0)$. It can be easily shown that their inverse are respectively negative and positive semicircles with center $C_0 = \frac{1}{2P}$ and radius $R_0 = \frac{1}{2P}$.

Definition 4 *Given a point $B \in \mathbb{C}$, let us define* "admissible domain of the PID compensator $C_{\text{PID}}(s)$ with respect to B" *the set $\mathscr{D}_B$ defined as follows:*

$$\mathscr{D}_B = \left\{ A \in \mathbb{C} \,\middle|\, \exists K_P, K_I, K_D > 0, \exists \omega \geq 0 : C_{\text{PID}}(j\omega) \cdot A = B \right\}.$$

It can be easily shown that the domain $\mathscr{D}_B$ on Nyquist plane is the half-plane which includes point B and is delimited by the straight line q passing through point O and perpendicular to segment $\overline{B0}$, see the gray region in Fig. 5.5.

Definition 5 *Given a point $B \in \mathbb{C}$, let $\mathscr{C}_B(K_P)$ and $\mathscr{C}_B^-(K_P)$ denote the sets of PID compensators defined as follows*

$$\mathscr{C}_B(K_P) = \left\{ B \cdot C_{\text{PID}}(s) \,\middle|\, C_{\text{PID}}(s) \in \mathscr{C}(K_P) \right\}, \tag{5.8}$$

$$\mathscr{C}_B^-(K_P) = \left\{ \frac{B}{C_{\text{PID}}(s)} \,\middle|\, C_{\text{PID}}(s) \in \mathscr{C}(K_P) \right\}, \tag{5.9}$$

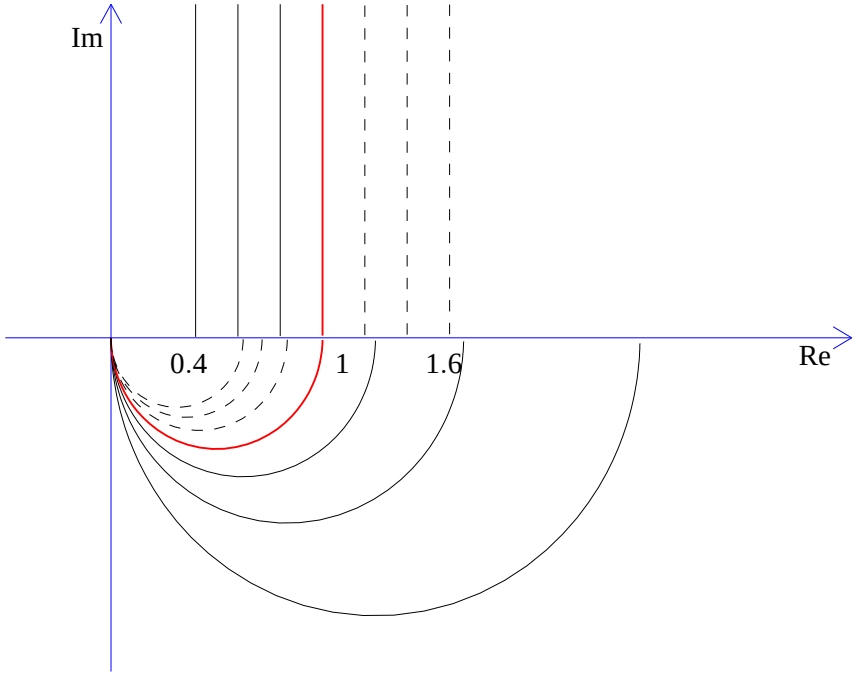

Figure 5.3: Graphical representation of on the Nyquist plane of $C_{\mathrm{PD}}(j\omega)$ for $K_P = 0.4 : 0.2 : 1.6$.

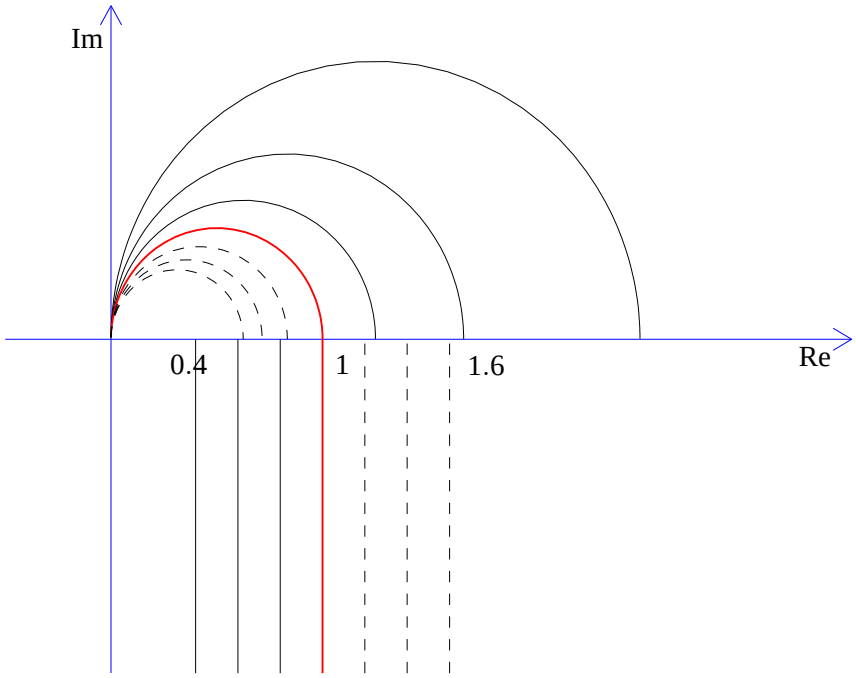

Figure 5.4: Graphical representation of on the Nyquist plane of $C_{\mathrm{PI}}(j\omega)$ for $K_P = 0.4 : 0.2 : 1.6$.

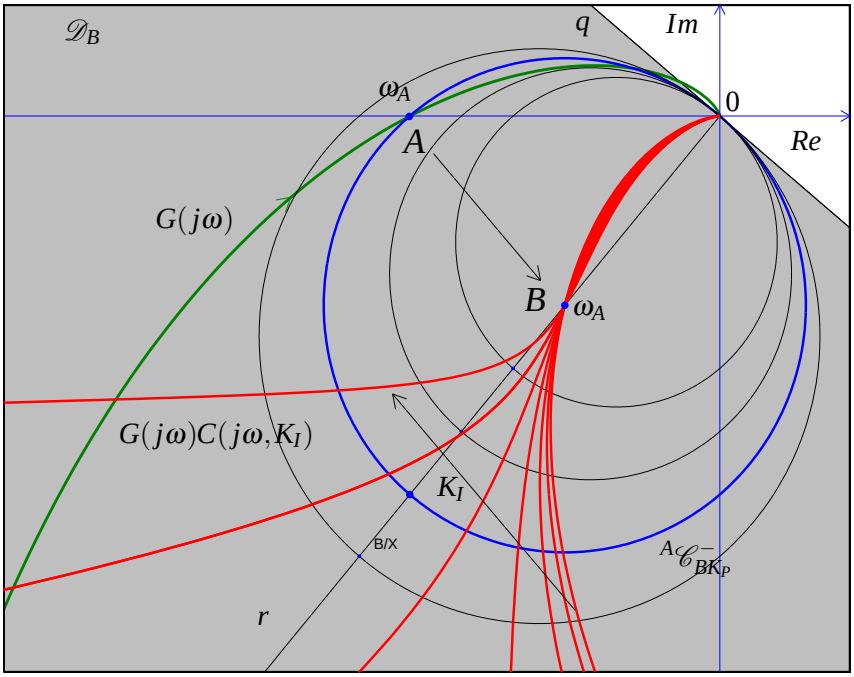

Figure 5.5: Controllable domain $\mathscr{D}_B$ and graphical design of compensators $C_{\text{PID}}(j\omega,K_I)$ moving point A to B.

with $\mathscr{C}(K_P)$ defined in (5.5). Moreover, let $\mathscr{C}_{BK_P}(s) \in \mathscr{C}_B(K_P)$ and $\mathscr{C}^-_{BK_P}(s) \in \mathscr{C}^-_B(K_P)$ denote particular elements of the two sets $\mathscr{C}_B(K_P)$ and $\mathscr{C}^-_B(K_P)$ chosen arbitrarily.

Definition 6 ***(PID Inversion Formulae)*** *Given two points $A = M_A e^{j\varphi_A}$ and $B = M_B e^{j\varphi_B}$ of the complex plane $\mathbb{C}$, the PID inversion formulae are defined as follows:*

$$\begin{cases} P(A,B) &= \dfrac{M_B}{M_A}\cos(\varphi_B - \varphi_A), \\ Q(A,B) &= \dfrac{M_B}{M_A}\sin(\varphi_B - \varphi_A). \end{cases} \tag{5.10}$$

Property 12 ***(From A to B)*** *Given a point $B \in \mathbb{C}$ and chosen a point $A = G(j\omega_A) \in \mathscr{D}_B$, the sets $C_{\text{PID}}(s,K_D)$ and $C_{\text{PID}}(s,K_I)$ of all the PID compensators $C_{\text{PID}}(s)$ that bring point A to point B is obtained from (5.1) using, respectively, the parameters*

$$K_P = P, \qquad K_I = K_D\omega_A^2 - Q\omega_A, \tag{5.11}$$

for all $K_D > \frac{Q}{\omega_A}$, or the parameters

$$K_P = P, \qquad K_D = \frac{Q}{\omega_A} + \frac{K_I}{\omega_A^2}, \tag{5.12}$$

for all $K_I > 0$, where coefficients $P = P(A,B)$ and $Q = Q(A,B)$ are obtained using (5.10).

Proof: For $\omega = \omega_A$, relation (5.4) can be rewritten as

$$C_{\text{PID}}(j\omega_A) = K_P + j\left(\omega_A K_D - \frac{K_I}{\omega_A}\right). \tag{5.13}$$

From relations $B = C_{\text{PID}}(j\omega_A)\cdot A$, it is evident that point $A = G(j\omega_A) = M_A e^{j\varphi_A}$ can be moved to point $B = M_B e^{j\varphi_B}$ if and only if

$$C_{\text{PID}}(j\omega_A) = \frac{M_B}{M_A} e^{j(\varphi_B - \varphi_A)} = P + jQ. \tag{5.14}$$

Solving equations (5.14) with respect to P and Q, one obtains the *PID Inversion Formulae* (5.10). Equations (5.11) and (5.12) follow directly from (5.13) and (5.14). □

Property 13 *The parameter K_P can be determined on the Nyquist plane as shown in Fig. 5.5:*

1. *draw the unique circle ${}^{A}\mathscr{C}_B^-$ passing through points A and O having its diameter on the straight line r which passes through points* 0 *and B;*
2. *the circle ${}^{A}\mathscr{C}_B^-$ intersects the straight line r in points O and $E = B/K_P$;*
3. *the parameter K_P is equal to the modulus of point B over the modulus of point E: $K_P = |B|/|E|$.*

Proof: It follows directly from Property 11 because the circle ${}^{A}\mathscr{C}_B^-$ on the Nyquist plane is the inverse of the frequency response $\mathscr{C}_{BK_P}(j\omega)$ of function $\mathscr{C}_{BK_P}(s) \in \mathscr{C}_B(K_P)$ and because the intersections of circle ${}^{A}\mathscr{C}_B^-$ with the straight line r occur in points O and $E = B/K_P$. □

5.2 Synthesis of PID compensators

Let us consider the case of given steady-state specifications that impose the value of the integrative term $K_I > 0$. This case occurs for example for type-0 systems and design specification on velocity error, or for type-1 systems and design specification on acceleration error. The fact that the integrative term K_I has been fixed do not reduce the admissible domain $\mathscr{D}_B$ with respect to B, that is still the gray region shown in Fig. 5.5. The other two degrees of freedom K_P and K_D of the regulator can be imposed to meet the phase margin ϕ_m and the gain crossover frequency ω_p. Let us extend the Inversion Formulae method to solve the Design Problem A using a PID regulator.

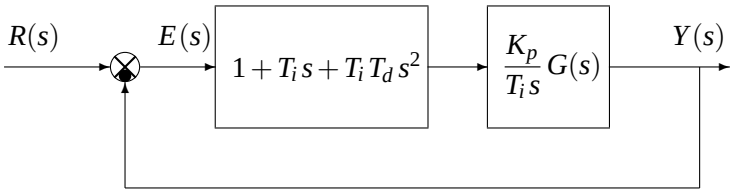

Figure 5.6: Modified feedback structure with unity DC gain controller.

Design Problem A: Given the transfer function $G(s)$, the steady-state specifications that impose the value of the integrative term $K_I > 0$ and design specifications on the phase margin ϕ_m, and gain crossover frequency ω_p, design a PID compensator $C_{\rm PID}(s)$ such that the loop gain transfer function $C_{\rm PID}(j\omega)G(j\omega)$ passes through point $B_p = e^{j(\pi+\phi_m)}$ for $\omega = \omega_g$.

Solution A: *If point $A = G(j\omega_A)$ belongs to the admissible domain $\mathscr{D}_B$ shown in Fig. 5.5, the solution follows directly from (5.12) of Property 12 with parameter K_I imposed by the steady-state specifications.*

Let us now consider an alternative and interesting way to solve numerically the Design Problem *A* employing the Inversion Formulae method. The factor K_I/s can be separated from $\bar{C}_{\rm PID}(s) = 1 + T_i s + T_i T_d s^2$, and viewed as part of the plant. In this way, the part of the controller to be designed is $\bar{C}_{\rm PID}(s)$, and the feedback scheme 1.1 reduces to that of Figure 5.6.

Let $\tilde{G}(s) \stackrel{\rm def}{=} \frac{K_p}{T_i s} G(s)$, so that the loop gain transfer function can be written as $L(s) = \bar{C}_{\rm PID}(s)\tilde{G}(s)$. The transfer functions $\tilde{G}(j\omega)$ and $\bar{C}_{\rm PID}(j\omega)$ can be written in polar form as

$$\tilde{G}(j\omega) = |\tilde{G}(j\omega)|\, e^{j \arg \tilde{G}(j\omega)},$$

$$\bar{C}_{\rm PID}(j\omega) = M(\omega)\, e^{j\,\varphi(\omega)},$$

so that the loop gain frequency response can be expressed as

$$L(j\omega) = |\tilde{G}(j\omega)|\, M(\omega)\, e^{j\left(\arg \tilde{G}(j\omega) + \varphi(\omega)\right)}.$$

If the crossover frequency ω_g and the phase margin ϕ_m of the loop gain transfer function $L(s)$ are assigned, the equations

$$|L(j\omega_g)| = 1, \qquad \phi_m = \pi + \arg L(j\omega_g)$$

must be satisfied, and as already observed these can be written as

$$M_g = 1/\ |\tilde{G}(j\omega_g)|\ , \qquad \varphi_g = {\rm PM} - \pi - \arg \tilde{G}(j\omega_g).$$

Alternatively, M_g and φ_g can be computed as functions of the frequency response of $G(s)$ at $\omega = \omega_g$:

$$M_g = \left| \frac{K_p}{T_i\, j\, \omega_g} G(j\omega_g) \right|^{-1} = \frac{\omega_g}{K_I\, |G(j\omega_g)|} \tag{5.15}$$

$$\begin{aligned} \varphi_g &= \mathrm{PM} - \pi - \arg\left[\frac{K_p}{T_i\, j\, \omega_g} G(j\omega_g) \right] \\ &= \mathrm{PM} - \frac{\pi}{2} - \arg G(j\omega_g), \end{aligned} \tag{5.16}$$

since $K_p, T_i > 0$. In order to find the parameters of the controller such that *i-a)* and *ii-a)* in Subsec. 2.3.2 are met, equation

$$M_g\, e^{j\,\varphi_g} = 1 + j\,\omega_g\, T_i - T_i\, T_d\, \omega_g^2 \tag{5.17}$$

must be solved in $T_i > 0$ and $T_d > 0$. The closed-form solution to this problem is given in the following theorem.

Theorem 1 *Equation (5.17) admits solutions in $T_i > 0$ and $T_d > 0$ if and only if*

$$0 < \varphi_g < \pi \qquad \textit{and} \qquad M_g \cos\varphi_g < 1. \tag{5.18}$$

If (5.18) are satisfied, the solution of (5.17) is given by

$$K_p = K_I \frac{1}{\omega_g} M_g \sin\varphi_g, \tag{5.19}$$

$$T_i = \frac{1}{\omega_g} M_g \sin\varphi_g, \tag{5.20}$$

$$T_d = \frac{1 - M_g \cos\varphi_g}{\omega_g M_g \sin\varphi_g}. \tag{5.21}$$

The two conditions (5.18) can be alternatively written as

$$\begin{aligned} \varphi_g \in \left(\arccos\frac{1}{M_g}, \pi \right) \quad &\text{if } M_g > 1, \\ \varphi_g \in (0, \pi) \quad &\text{if } M_g < 1. \end{aligned}$$

In fact, when $\varphi_g \in (0, \pi/2)$, condition $\cos\varphi_g < 1/M_g$ is always satisfied when $M_g < 1$, and is satisfied when $\varphi_g > \arccos(1/M_g)$ when $M_g > 1$. When $\varphi_g \in (\pi/2, \pi)$, the condition $\cos\varphi_g < 1/M_g$ is always satisfied since $\cos\varphi_g < 0$ and $(1/M_g) > 0$.

Let us now consider the case of steady-state specifications that do not constrain the value of K_I. The degree of freedom in the Property 12 can be utilized in order to satisfy another specification. In literature different methods can be found to impose the degree of freedom. In one of them the ratio $\sigma \stackrel{\text{def}}{=} T_d/T_i$ is

chosen to ensure that the zeros of the PID controller are real, [36]. The ratio σ is an important parameter. When $\sigma^{-1} \geq 4$, the zeros of the PID controller are real, and they are complex conjugate when $\sigma^{-1} < 4$. In the following Theorem, necessary and sufficient conditions are given for the solvability of $i-a)$ and $ii-a)$ in Subsec. 2.3.2 when specifications on the phase margin, gain crossover frequency and the ratio σ are given. In order to find the parameters of the controller such that *i-a)* and *ii-a)* are met, equation

$$\mathbf{C}_{\text{PID}}(j\omega_g) = M(\omega_g)e^{j\varphi(\omega_g)} = M_g e^{j\varphi_g}, \tag{5.22}$$

becomes

$$M_g\, e^{j\,\varphi_g} = K_p\, \frac{1 + j\,\omega_g\, T_i - \omega_g^2\, T_i\, T_d}{j\,\omega_g\, T_i}, \tag{5.23}$$

which must be solved in $K_p, T_i, T_d > 0$. By equating real and imaginary parts of both sides of (5.23) we get

$$\omega_g\, M_g\, T_i \cos\varphi_g = \omega_g\, K_p\, T_i, \tag{5.24}$$

$$-M_g\, \omega_g\, T_i \sin\varphi_g = K_p - K_p\, \omega_g^2\, T_i\, T_d, \tag{5.25}$$

in the three unknowns K_p, T_i and T_d.

Theorem 2 *([36, Ch. 4, pp. 140–141]). Let $\sigma = T_d/T_i$ be assigned. Equation (5.23) admits solutions in $K_p, T_i, T_d > 0$ if and only if $\varphi_g \in (-\pi/2, \pi/2)$. If this condition is satisfied, the solution of (5.23) is given by*

$$K_p = M_g \cos\varphi_g, \tag{5.26}$$

$$T_i = \frac{\tan\varphi_g + \sqrt{\tan^2\varphi_g + 4\,\sigma}}{2\,\omega_g\,\sigma}, \tag{5.27}$$

$$T_d = T_i\,\sigma. \tag{5.28}$$

Proof: **(Only if)**. As already observed, equating real part to real part and imaginary part to imaginary part in (5.23) results in (5.24) and (5.25). Since K_p must be positive, from (5.24) – which can be written as $K_p = M_g \cos\varphi_g$ – we get that φ_g must satisfy $-\pi/2 < \varphi_g < \pi/2$. If this inequality is satisfied, it is also easy to see that (5.25) always admits a positive solution. In fact, (5.25) can be written as

$$\omega_g^2\,\sigma\, T_i^2 - \omega_g\, T_i \tan\varphi_g - 1 = 0, \tag{5.29}$$

in T_i, that always admits two real solutions, one positive and one negative.
(If). From (5.26), it follows that (5.24) is satisfied. Moreover, since as aforementioned (5.25) can be written as (5.29) and $\sqrt{\tan^2\varphi + 4\,\sigma} > |\tan\varphi|$, the positive solution is given by (5.27). □

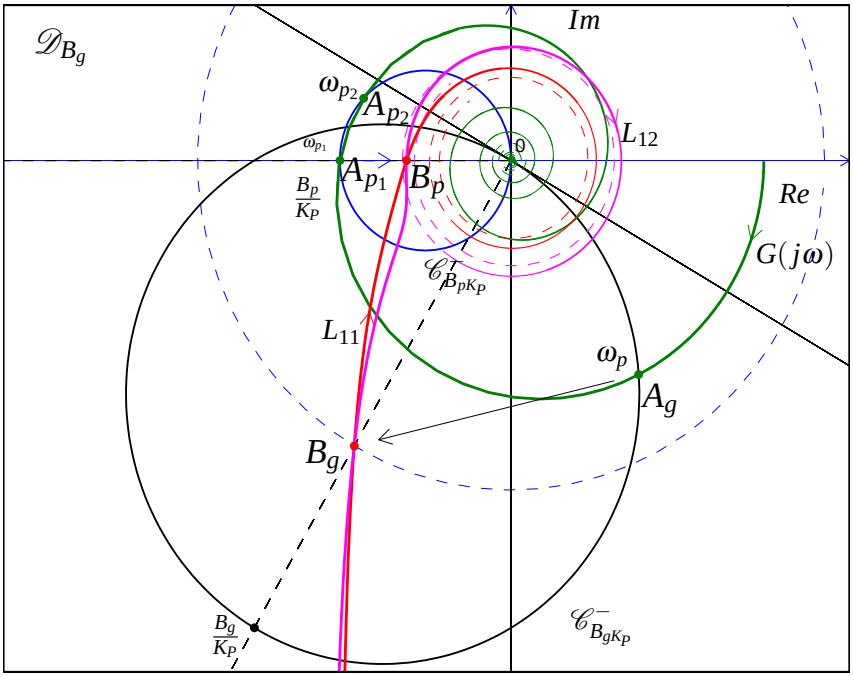

Figure 5.7: Graphical solution of Design Problem *C* on the Nyquist plane.

Another possibility to spend the degree of freedom K_I is to satisfy a gain margin constraint. Let us solve the Design Problem C employing a PID controller.

Design Problem C: Given the transfer function $G(s)$ and design specifications on the phase margin ϕ_m, gain margin G_m and gain crossover frequency ω_g, design a PID compensator $C_{\text{PID}}(s)$ such that the loop gain transfer function $C_{\text{PID}}(j\omega)G(j\omega)$ passes through point $B_g = e^{j(\pi+\phi_m)}$ for $\omega = \omega_g$ and passes through point $B_p = -1/G_m$.

Solution C: *Let $A_g = G(j\omega_g)$ denote the value of $G(j\omega)$ at the desired gain crossover frequency $\omega = \omega_g$, and let $B_g = e^{j(\pi+\phi_m)}$ and $B_p = -1/G_m = M_{B_p} e^{j\varphi_{B_p}}$ denote the points corresponding to the desired phase margin ϕ_m and gain margin G_m, respectively. The set $C_p(s,\omega_p)$ of all the PID compensators $C_{\text{PID}}(s)$ which solve Design Problem C is obtained from (5.1) using the parameters*

$$K_P = P_g > 0, \qquad K_D = \frac{Q_g\omega_g - Q_p\omega_p}{\omega_g^2 - \omega_p^2} > 0, \tag{5.30}$$

$$K_I = \frac{Q_g\omega_g\omega_p^2 - Q_p\omega_p\omega_g^2}{\omega_g^2 - \omega_p^2} > 0, \tag{5.31}$$

where the coefficients $P_g = P(A_g, B_g)$, $Q_g = Q(A_g, B_g)$, $P_p = P(A_p, B_p)$ and $Q_p = Q(A_p, B_p)$ are obtained using the inversion formulas (5.10) with $A_p = G(j\omega_p) = M_{A_p}(\omega_p)\, e^{j\varphi_{A_p}(\omega_p)}$, for all the frequencies ω_p

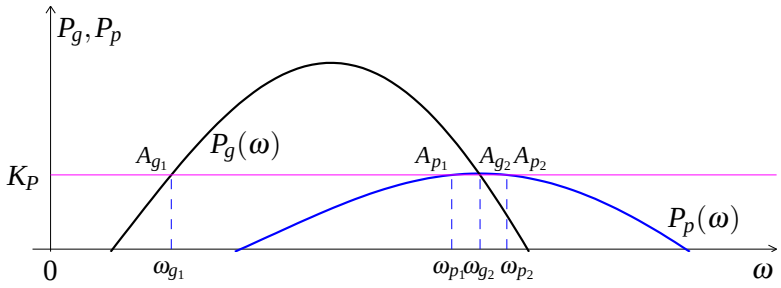

Figure 5.8: Functions $P_p(\omega)$ (blue) and $P_g(\omega)$ (black).

satisfying the relation

$$K_P = P_p(\omega_p) = \frac{M_{B_p}}{M_{A_p(\omega_p)}} \cos(\varphi_{B_p} - \varphi_{A_p}(\omega_p)). \tag{5.32}$$

A solution $C_p(s, \omega_p)$ of Design Problem C exists only if:
1) *the set S_{ω_p} of all the $\omega_p > \omega_g$ satisfying (5.32) is not empty;* 2) *$A_g \in \mathscr{D}_{B_g}$ and $A_p \in \mathscr{D}_{B_p}$;* 3) *the parameters K_I and K_D in (5.30) and (5.31) are real and positive.*

Proof: The design specifications define the position of points $B_g = e^{j(\pi+\phi_m)}$, $A_g = G(j\omega_g)$ and $B_p = -1/G_m$. According to Property 12, the compensators $C_p(s, K_D)$ which move point $A_g \in \mathscr{D}_{B_g}$ to point B_g are obtained using the parameters K_P and K_I in (5.11). The free parameter K_D can now be used to force the loop gain frequency response $C_p(j\omega, K_D)G(j\omega)$ to pass through point B_p. This condition can be satisfied only if a frequency ω_p exists such that compensator $C_p(s, K_D)$ moves point $A_p = G(j\omega_p) \in \mathscr{D}_{B_p}$ to point B_p, that is only if (5.32) holds. The frequencies $\omega_p \in S_{\omega_p}$ satisfying (5.32) are acceptable only if the compensator $C_g(s, K_D)$ which moves point A_p to point B_p, obtained using Property 12, is equal to the compensator $C_p(s, K_D)$. This condition is satisfied only if the two compensators share the same K_I and K_D, that is only if

$$K_I = \omega_g^2 K_D - Q_g \omega_g = \omega_p^2 K_D - Q_p \omega_p. \tag{5.33}$$

Solving (5.33) with respect to K_D one obtains the expression of K_D given in (5.30), that can be substituted in (5.33) obtaining (5.31). The solutions are acceptable only if $K_P, K_D, K_I > 0$. □

The solution of equation (5.32) can be obtained graphically, by plotting $P_p(\omega)$ and by finding all the frequencies $\omega_p \in S_{\omega_p}$ for which $P_p(\omega_p)$ intersects the horizontal line $P_g = K_P$, see Fig. 5.8. In the example of Fig. 5.8 it is $S_{\omega_p} = \{\omega_{p1}, \omega_{p2}\}$ and therefore there are two solutions: $C_p(s, \omega_{p1})$ and $C_p(s, \omega_{p2})$. The loop gain frequency responses $L_{11}(j\omega) = C_p(j\omega, \omega_{p1})G(j\omega)$ (red line) and $L_{12}(j\omega) = C_p(j\omega, \omega_{p2})G(j\omega)$ (magenta line) on the Nyquist plane are shown in Fig. 5.7. The two solutions satisfy the design specifications and are acceptable only if $K_D > 0$ and $K_I > 0$.

Property 14 *The frequencies $\omega_p \in S_{\omega_p}$ satisfying (5.32) can be graphically determined on the Nyquist plane as shown in Fig. 5.7:*

1. *Draw the circle $\mathscr{C}^-_{B_gK_P}(j\omega)$ on the Nyquist plane and determine the parameter K_P of compensator $C_p(s,K_D)$ as described in Property 13 when $A = A_g$ and $B = B_g$;*
2. *Draw the circle $\mathscr{C}^-_{B_pK_P}(j\omega)$ having its diameter on the segment defined by points O and $\frac{B_p}{K_P}$;*
3. *The intersections A_{p1}, A_{p2} of circle $\mathscr{C}^-_{B_pK_P}(j\omega)$ with $G(j\omega)$ correspond to the frequencies ω_{p1}, ω_{p2} belonging to set S_{ω_p}.*

Proof: The circles $\mathscr{C}^-_{B_gK_P}(j\omega)$ (black line) and $\mathscr{C}^-_{B_pK_P}(j\omega)$ (blue line) shown in Fig. 5.8 represent, respectively, the frequency responses of functions $\mathscr{C}^-_{B_gK_P}(s) \in \mathscr{C}^-_{B_g}(K_P)$ and $\mathscr{C}^-_{B_pK_P}(s) \in \mathscr{C}^-_{B_p}(K_P)$ with $K_P = P_p$ given in (5.32). These two circles can be easily determined on the Nyquist plane because the points A_g, B_g and B_p are known from the design specifications and K_P is given by the graphical construction described in Property 13. A frequency ω_p satisfying (5.32) exists only if

$$G(j\omega_p)C_{K_P}(j\omega_p) = B_p, \tag{5.34}$$

where $C_{K_P}(s)$ is the PID compensator (5.1) with the value of parameter K_P determined as described above. Relation (5.34) can also be rewritten as follows

$$G(j\omega) = \frac{B_p}{C_{K_P}(j\omega)} = \mathscr{C}^-_{B_{pK_P}}(j\omega), \tag{5.35}$$

with $\omega = \omega_p$, and therefore it can be solved graphically on the Nyquist plane by finding the intersections $\omega_p \in S_{\omega_p}$ of $G(j\omega)$ with $\mathscr{C}^-_{B_pK_P}(j\omega)$. □

The extension of the Inversion Formulae method to PID controller leads to solve the following design problems D and E with the same procedures introduced for the design of Lead-Leg controllers.

Design Problem D: Given the transfer function $G(s)$ and the design specifications on the phase margin ϕ_m, gain margin G_m and phase crossover frequency ω_p, design a PID compensator $C_{\rm PID}(s)$ such that the loop gain transfer function $C_{\rm PID}(j\omega)G(j\omega)$ passes through point $B_p = -1/G_m$ for $\omega = \omega_p$ and passes through point $B_g = e^{j(\pi+\phi_m)}$.

Solution D: *Let $A_p = G(j\omega_p)$ denote the value of $G(j\omega)$ at the desired phase crossover frequency ω_p, and let $B_g = e^{j(\pi+\phi_m)}$ and $B_p = -1/G_m = M_{B_p}e^{j\varphi_{B_p}}$ denote the points corresponding to the desired phase and gain margins. The set $C_g(s,\omega_g)$ of all the PID compensators $C_{\rm PID}(s)$ which solve Design Problem D is obtained from (5.1) using the parameters*

$$K_P = P_p > 0, \qquad K_D = \frac{Q_g\omega_g - Q_p\omega_p}{\omega_g^2 - \omega_p^2} > 0, \tag{5.36}$$

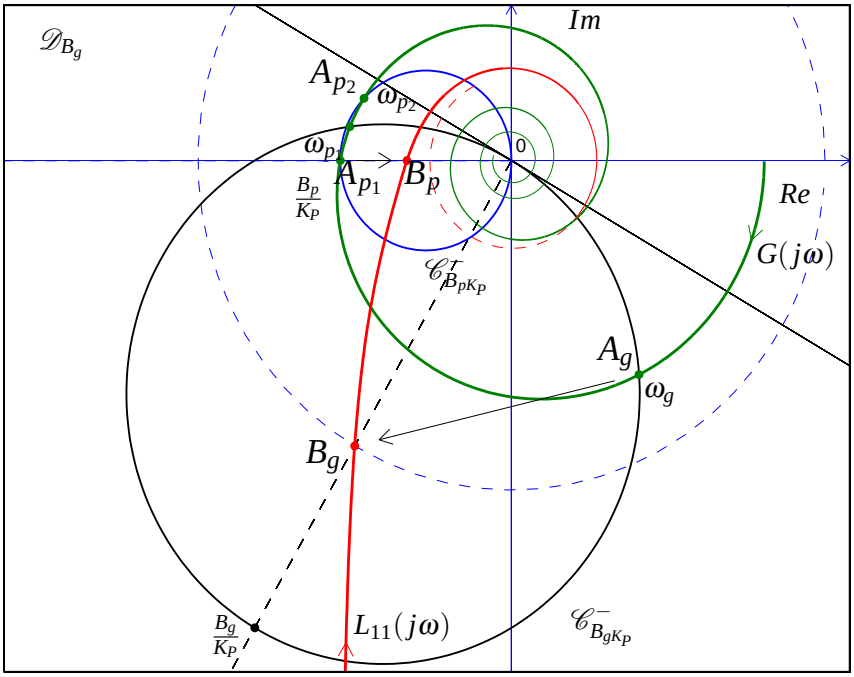

Figure 5.9: Graphical solution of Design Problem *D*.

$$K_I = \frac{Q_g\omega_g\omega_p^2 - Q_p\omega_p\omega_g^2}{\omega_g^2 - \omega_p^2} > 0, \tag{5.37}$$

where $P_g = P(A_g, B_g)$, $Q_g = Q(A_g, B_g)$, $P_p = P(A_p, B_p)$ *and* $Q_p = Q(A_p, B_p)$ *are obtained using the inversion formulas (5.10) with* $A_g = G(j\omega_g) = M_{A_g}(\omega_g)\, e^{j\varphi_{A_g}(\omega_g)}$, *for all the frequencies* ω_g *satisfying the relation*

$$K_P = P_g(\omega_g) = \frac{M_{B_g}}{M_{A_g(\omega_g)}} \cos(\varphi_{B_g} - \varphi_{A_g}(\omega_g)). \tag{5.38}$$

A solution $C_g(s, \omega_g)$ *exists only if:*
1) *the set* S_{ω_g} *of all the* $\omega_g > \omega_p$ *satisfying (5.38) is not empty;* 2) $A_g \in \mathscr{D}_{B_g}$ *and* $A_p \in \mathscr{D}_{B_p}$*;* 3) *the parameters* K_I *and* K_D *in (5.36) and (5.37) are real and positive.*

The proof is quite similar to the one given for Solution C.

Design Problem E: Given the transfer function $G(s)$ and the design specifications on the phase margin ϕ_m and gain margin G_m, design a PID compensator $C_{\text{PID}}(s)$ such that the loop gain transfer function $C_{\text{PID}}(j\omega)G(j\omega)$ passes through points $B_g = e^{j(\pi+\phi_m)}$ and $B_p = -1/G_m$.

Solution E: *Let* $B_g = e^{j(\pi+\phi_m)}$ *and* $B_p = -1/G_m = M_{B_p}\, e^{j\varphi_{B_p}}$ *denote the points corresponding to the desired phase margin* ϕ_m *and gain margin* G_m. *The set* $C_{K_P}(s, \omega_g, \omega_p)$ *of all the compensators* $C_{\text{PID}}(s)$ *which solve the Design Problem E is obtained as follows:*

a) *find all the pairs* $(\omega_g,\ \omega_p) \in S_{\gamma\omega}$ *of frequencies which solve the equation*

$$K_P = P_g(\omega_g) = P_p(\omega_p), \tag{5.39}$$

where the parameter $K_P > 0$ *is chosen arbitrarily,* $S_{K_P\omega}$ *is the set of all the pairs* $(\omega_g,\ \omega_p)$ *satisfying (5.39) with* $\omega_p > \omega_g$*, and functions* $P_g(\omega_g)$ *and* $P_p(\omega_p)$ *are defined in (5.38) and (5.32) with* $A_g = G(j\omega_g) = M_{A_g}(\omega_g)\, e^{j\varphi_{A_g}(\omega_g)}$ *and* $A_p = G(j\omega_p) = M_{A_p}(\omega_p)\, e^{j\varphi_{A_p}(\omega_p)}$.

b) *for each pair* $(\omega_g,\ \omega_p) \in S_{K_P\omega}$ *compute*

$$\begin{cases} K_D = \dfrac{Q_g\omega_g - Q_p\omega_p}{\omega_g^2 - \omega_p^2} > 0, \\ K_I = \dfrac{Q_g\omega_g\omega_p^2 - Q_p\omega_p\omega_g^2}{\omega_g^2 - \omega_p^2} > 0. \end{cases} \tag{5.40}$$

A solution exists only if:

1) K_P *satisfies*

$$0 < K_P < \min\left(\max(P_g(\omega_g)), \max(P_p(\omega_p))\right); \tag{5.41}$$

2) $S_{K_P\omega}$ *is not empty;*

3) $A_g(\omega_g) \in \mathscr{D}_{B_g}$ *and* $A_p(\omega_p) \in \mathscr{D}_{B_p}$*;*

4) K_D *and* K_I *in (5.40) are real and positive.*

Proof: The proof hinges on the fact that $C_{\text{PID}}(s)$ has to be design to move point $A_g = G(j\omega_g)$ to point B_g and point $A_p = G(j\omega_p)$ to point B_p. A solution $C_{K_P}(s, \omega_g, \omega_p)$ exists only if the frequencies ω_g and ω_p satisfy (5.38) and (5.32), that is only if they satisfy (5.39). For each value of K_P satisfying (5.41), one can find the set $S_{K_P\omega}$ of all the solutions (ω_g, ω_p) of (5.39).

The solutions of (5.39) can also be obtained graphically by plotting $P_g(\omega)$ and $P_p(\omega)$ and by finding, for each admissible value of K_P, all the pairs $(\omega_g, \omega_p) \in S_{\omega_g}$ where $P_g(\omega_g)$ and $P_p(\omega_p)$ intersect the horizontal line K_P, see Fig. 5.8. In the example of Fig. 5.8 there are three different solutions: $S_{K_P\omega} = \{(\omega_{g1}, \omega_{p1}), (\omega_{g1}, \omega_{p2}), (\omega_{g2}, \omega_{p2})\}$. The solution $(\omega_{g2}, \omega_{p1})$ is not admissible because $\omega_{g2} > \omega_{p1}$. The loop gain frequency responses $L_{11}(s)$, $L_{12}(s)$ and $L_{22}(s)$ of these three solutions on the Nyquist plane are shown in Fig. 5.10. These solutions are acceptable only if parameters K_D and K_I given in (5.40) are positive.

The solution of (5.39) can also be obtained on the Nyquist plane. Given points B_g and B_p and a desired value for $K_P > 0$, the circles $\mathscr{C}^-_{B_gK_P}(j\omega)$ and $\mathscr{C}^-_{B_pK_P}(j\omega)$ can be drawn on the Nyquist plane as the circles having their diameters on the segments defined by points $\{O, \frac{B_g}{K_P}\}$ and $\{O, \frac{B_p}{K_P}\}$, respectively, as described in Property (13). Each pair (ω_g, ω_p) corresponding to the intersections of $G(j\omega)$ with circles $\mathscr{C}^-_{B_gK_P}(j\omega)$ and $\mathscr{C}^-_{B_pK_P}(j\omega)$ is a possible solution for Design Problem E. If $G(j\omega)$ does not intersect both circles $\mathscr{C}^-_{B_gK_P}(j\omega)$ and $\mathscr{C}^-_{B_pK_P}(j\omega)$, the chosen value of K_P is not acceptable.

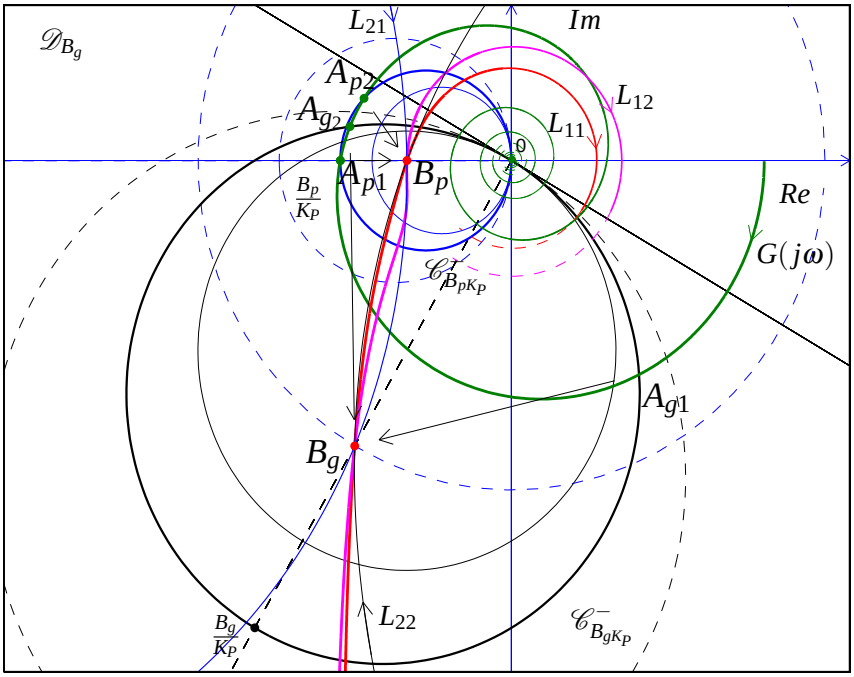

Figure 5.10: Graphical solution of Design Problem E.

□

5.3 Numerical examples

Example 1**.**

Design Problem A: Given the following type-1 plant

$$G(s) = \frac{40(s+1)}{s(s+1.5)^2(s+3)},$$

design a PID compensator $C_{\text{PID}}(s)$ in order to achieve the acceleration constant $K_a = 2$, the phase margin $\phi_m = 50^\circ$ and the gain crossover frequency $\omega_g = 2.5$.

Solution: The integral constant K_I is determined by steady-state requirement as

$$K_a = \lim_{s\to 0} s^2 C_{\text{PID}}(s)\, G(s) = \frac{40K_I}{1.5^2 \cdot 3} = 2,$$

that leads to $K_I = 0.337$. The point $A = G(j\omega_g) = 1.2e^{j178^\circ}$ belongs to the admissible domain $\mathscr{D}_B$ defined by $B = e^{-j230^\circ}$, see Fig. 5.11. From inversion formulae (5.10) it follows that $P = 0.514$ and $Q = 0.658$. Finally relations (5.12) lead to $K_P = 0.514$ and $K_D = 0.303$. The designed compensator (5.1) is

$$C_{\text{PID}}(s) = 0.514 + 0.303s + \frac{0.337}{s}.$$

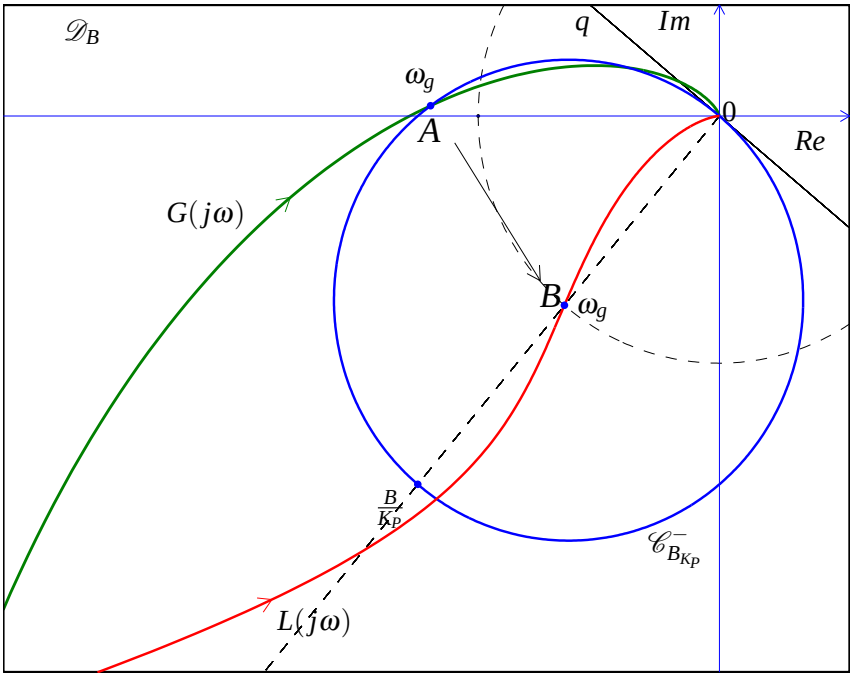

Figure 5.11: Example 1: graphical solution of Design problem A .

The corresponding loop gain transfer function $L(j\omega) = C_{\text{PID}}(j\omega)G(j\omega)$ is plotted in red in Fig. 5.11.

Example 2. All the graphical representations from Fig. 5.7 to Fig. 5.10 used in the solutions of the presented Design Problems C, D and E refer to the system proposed in [35]:

$$G(s) = \frac{1}{0.12s^2 + 1.33s + 1.24} e^{-2s},$$

with the following design specifications: $\phi_m = 60^\circ$, $G_m = 3$, gain crossover frequency $\omega_g = 0.3325$, and phase crossover frequency $\omega_p = 1.1052$. The modulus and the phase of points B_g and B_p are: $M_{B_g} = 1$, $\varphi_{B_g} = -120^\circ$, $M_{B_p} = 0.333$ and $\varphi_{B_p} = 180^\circ$. The value of K_P obtained in (5.30), (5.36) and used in Design Problem E is $K_P = P_g = P_p = 0.6107$. The frequencies obtained solving equations (5.32), (5.38) and (5.39) are $\omega_{g1} = \omega_g = 0.332$, $\omega_{g2} = 1.18$, $\omega_{p1} = \omega_p = 1.1052$ and $\omega_{p2} = 1.257$ (see Fig. 5.8). The corresponding points on $G(j\omega)$ are $A_{g1} = 0.767\, e^{-j57.9^\circ}$, $A_{g2} = A_g = 0.525\, e^{j168.7^\circ}$, $A_{p1} = A_p = 0.546\, e^{j180^\circ}$ and $A_{p2} = 0.506\, e^{j158.1^\circ}$.

Design Problem C: The set of regulators satisfying the Design Problems C are:

$$C_p(s, \omega_{p1}) = \frac{0.3449s^2 + 0.6107s + 0.4212}{s}, \tag{5.42}$$

$$C_p(s, \omega_{p2}) = \frac{0.4706s^2 + 0.6107s + 0.4351}{s}. \tag{5.43}$$

The corresponding loop gain transfer functions $L_{11}(j\omega)$ (red line) and $L_{12}(j\omega)$ (magenta line) are plotted in Fig. 5.7.

Design Problem D: Given ω_p as phase crossover specification, the two solutions of equation (5.38) are $\omega_{g1}, \omega_{g2} = \{0.332, 1.18\}$. The second is not admissible because $\omega_{g2} > \omega_p$. The unique admissible solution is the PID (5.42). The corresponding loop gain transfer functions $L_{11}(j\omega)$ (red line) is plotted in Fig. 5.9.

Design Problem E: Given B_g, B_p and K_P, the four solutions $(\omega_{gi}, \omega_{pj})$ of equation (5.39) can be graphically determined as shown in Fig. 5.8. The two acceptable regulators (5.42), (5.43) are obtained for $(\omega_{g1}, \omega_{p1})$ and $(\omega_{g1}, \omega_{p2})$. The solution determined by $(\omega_{g2}, \omega_{p1})$ is not acceptable because $\omega_{g2} > \omega_{p1}$. The solution determined by $(\omega_{g2}, \omega_{p2})$ is not acceptable because the PID parameters K_D and K_I are negative and the controlled system is unstable.

Example 3. Let us consider the following plant

$$G(s) = \frac{s+10}{s(s^2+2s+10)},$$

design a compensator that meets the following specifications:

- zero velocity error;
- phase margin equal to 45°;
- gain crossover frequency equal to 3 rad/sec.

The steady-state specification is automatically satisfied by using a PID controller or a PI controller. Let us consider the case of a PID controller. The extra freedom in this case can be used to select the ratio T_i/T_d. Let us choose for example $T_i/T_d = 8$, so that $\sigma = 1/8$ guarantees that the zeros of the PID controller are real. Then, we compute M_g and φ_g:

$$\begin{aligned} M_g &= \frac{1}{|G(3\,j)|} = 3\sqrt{\frac{37}{109}} \simeq 1.7479, \\ \varphi_g &= \mathrm{PM} - (\pi + \arg\bar{G}(3\,j)) \\ &= \frac{7}{4}\pi - \arctan\frac{3}{10} + \arctan 6 \simeq 18.84^\circ. \end{aligned}$$

Since $\varphi_g \in (-\pi/2, \pi/2)$, the problem admits a solution with a PID controller. Using (5.26-5.28) we find $K_p = 1.6542$, $T_i = 1.5017$ sec and $T_d = 0.1877$ sec. This choice guarantees that the controller has real zeros, which in this case are -4.5471 and -0.7802.

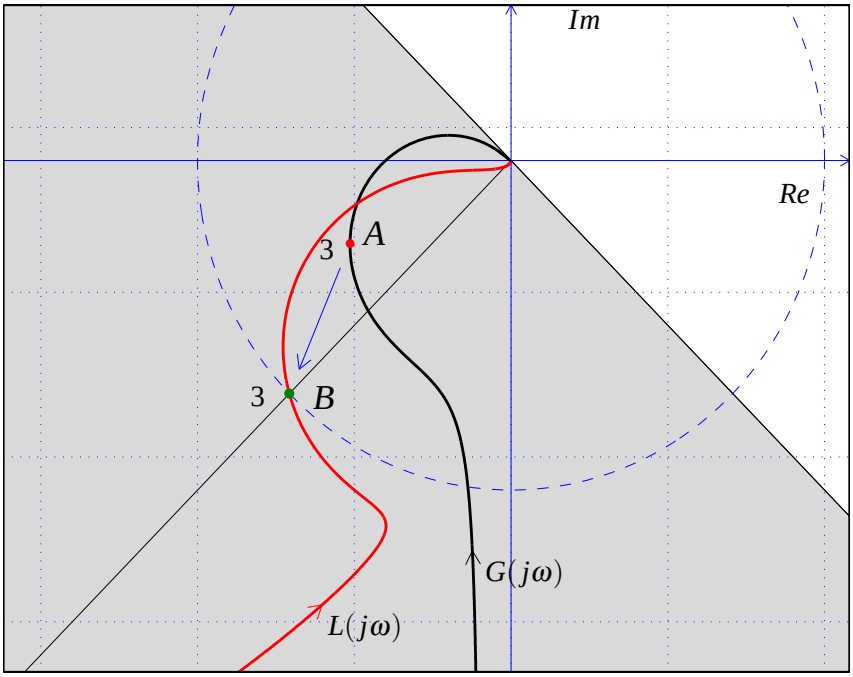

Figure 5.12: Design of PID compensator on the Nyquist plane to meet the specifications of Example 3.

Let us attempt to solve the same problem with a PI controller. To this end, we compute

$$\varphi_g = \phi_m - \frac{\pi}{2} - \arg G(j\omega_g) \simeq 108.8384^\circ,$$

so that a PI controller solving the problem does not exist.

The graphical representation of the problem solution with PID regulator is shown in Fig. 5.12. The designed PID brings the point $A = G(j\omega_g)$ to $B = e^{j(\phi_m+\pi)}$. The gray area corresponds to the set of admissible points that can be brought to B by a PID controller.

Example 4. Given the plant of the previous example, design a compensator that meets the following specifications:

- zero velocity error and acceleration error not greater than 0.2;
- phase margin equal to 45°;
- gain crossover frequency equal to 3 rad/sec.

The correct compensator structure to be employed in this case is the PID controller. As already observed, the steady-state requirement in this case imposes the ratio $K_I = K_p/T_i$. In particular, in this

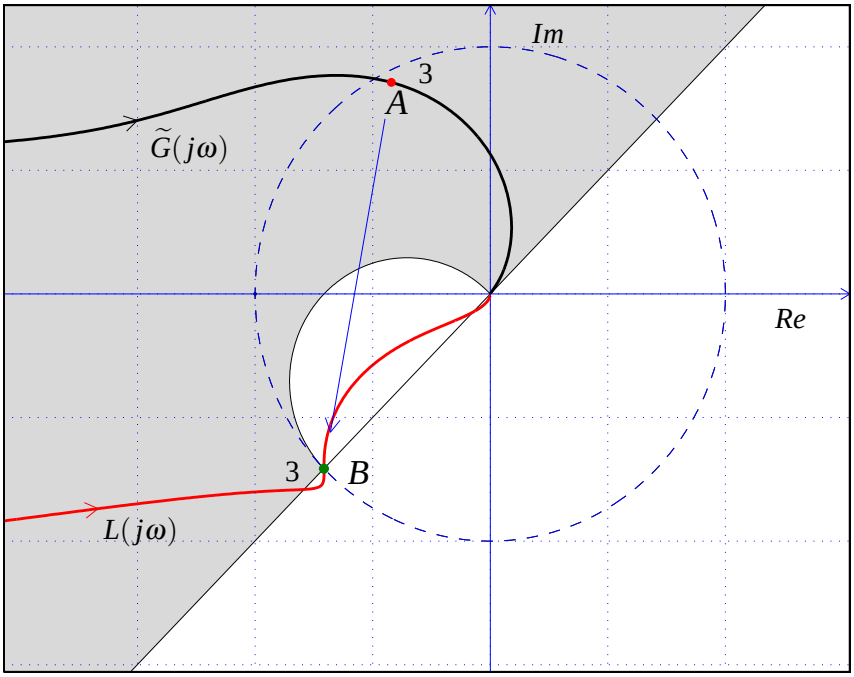

Figure 5.13: Design of PID controller on the Nyquist plane to meet the specifications of Example 4.

case we need $K_I \geq 5$. Let us choose $K_I = 5$. Hence,

$$\begin{aligned} M_g &= \frac{\omega_g}{K_I\,|G(j\omega_g)|} \simeq 1.0487, \\ \varphi_g &= \phi_m - \frac{\pi}{2} - \arg G(j\omega_g) \simeq 108.8384^\circ. \end{aligned}$$

The conditions $0 < \varphi_g < \pi$ and $M_g \cos\varphi_g < 1$ are both satisfied, so that the problem admits solutions. The parameters of the controller in this case are

$$T_i = \frac{M_g \sin\varphi_g}{\omega_g} \simeq 0.3308\,\text{sec}$$

$$T_d = \frac{1 - M_g\cos\varphi_g}{\omega_g M_g \sin\varphi_g} \simeq 0.4496\,\text{sec}$$

$$K_p = K_i T_i \simeq 1.6542.$$

As such, the PID controller

$$C_{\text{PID}} = 1.6542\left(1 + \frac{1}{0.3308\,s} + 0.4496\,s\right)$$

solves the control problem. However, since in this case $T_i < 4T_d$, the zeros of the compensator are complex conjugate and equal to $-1.1122 \pm 2.3423\,j$. The Nyquist plot of $\tilde{G}(j\omega)$ is shown in Fig. 5.13.

It can be shown that $\tilde{G}(j\omega)$ is a rotation and an amplification of $G(j\omega)$ and the area of points that can be brought to B by the controller is shown in gray.

Chapter 6

Discrete time PID regulators

In this chapter the Inversion Formulae method is extended to a direct approach for the design of the discrete proportional-integral-derivative (PID) regulators for robust control. The tuning of regulator parameters leads to achieve steady-state requirements, phase margin, gain margin and gain or phase crossover frequency specifications. The similarity of the continuous and discrete design methods and the simplicity of the graphical solutions allow an easy use of the discrete direct procedure.

6.1 Discrete PID compensator: the general structure

Referring to the block scheme of Fig. 6.1, $HG(z)$ is the discrete system to be controlled,

$$HG(z) = \mathscr{Z}[H_0(s)\,G(s)],$$

where $H_0(s) = \frac{1-e^{-Ts}}{s}$ is the zero-order hold, while $C_d(z)$ is the discrete-time PID compensator having the following structure:

$$C_d(z) = \overline{K}_P + \overline{K}_D \frac{z-1}{z+1} + \overline{K}_I \frac{z+1}{z-1}. \tag{6.1}$$

Let us now design the regulator $C_d(z)$ in order to meet design specifications on the phase and gain margins and on the gain crossover frequency.

The frequency response of (6.1) for $\omega \in [0, \frac{\pi}{T}]$ and sampling period T is

$$C_d(e^{j\omega T}) = P + jQ(\omega, T), \tag{6.2}$$

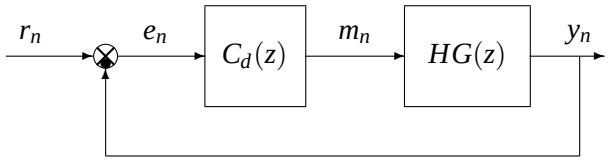

Figure 6.1: The considered block scheme for the discrete-time case.

where

$$\begin{aligned} P &= \overline{K}_P, \\ Q(\omega,T) &= \overline{K}_D\Omega(\omega) - \tfrac{\overline{K}_I}{\Omega(\omega)}, \\ \Omega(\omega) &= \tan\tfrac{\omega T}{2}. \end{aligned}$$

Let us define $\mathscr{C}_d(\overline{K}_P)$ as the set of all the PID compensators $C_d(z)$ having the same parameter $\overline{K}_P$, that is

$$\mathscr{C}_d(\overline{K}_P) = \left\{ C_d(z) \text{ as in (6.1)} \;\middle|\; \overline{K}_I > 0, \overline{K}_D > 0 \right\}, \tag{6.3}$$

and let $\mathscr{C}_d^-(\overline{K}_P)$ denote the set of all the inverse functions $C_d(z)^{-1}$ having the same parameter $\overline{K}_P$:

$$\mathscr{C}_d^-(\overline{K}_P) = \left\{ \frac{1}{C_d(z)} \;\middle|\; C_d(z) \in \mathscr{C}_d(\overline{K}_P) \right\}. \tag{6.4}$$

As for the continuous-time case, the graphical representation of each element of $\mathscr{C}_d(\overline{K}_P)$ on the Nyquist plane is a vertical straight line which passes through point $(\overline{K}_P, 0)$, see Fig. 6.2. Moreover the Nyquist plot of each element of $\mathscr{C}_d^-(\overline{K}_P)$ is a circle with center C_0 and radius R_0, where

$$C_0 = \frac{1}{2\overline{K}_P}, \qquad\qquad R_0 = \frac{1}{2\overline{K}_P}.$$

It can be easily shown that the graphical representation of the admissible domain $\mathscr{D}_B$ for reaching point B on the Nyquist plane is equal to the domain considered for continuous-time case, see Fig. 5.5.

The property *From A to B* for discrete time PID compensators can be expressed as follows.

Property 15 ***(From** A **to** B**).*** *Given a point $B \in \mathbb{C}$ and chosen a point $A = HG(\omega_A, T) \in \mathscr{D}_B$ on the frequency response of the plant at frequency $\omega_A \in [0, \frac{\pi}{T}]$, the sets $C_d(z, \overline{K}_D)$ and $C_d(z, \overline{K}_I)$ of all the PID compensators $C_d(z)$ that bring point A to point B are obtained from (6.1) using, respectively, the parameters*

$$\overline{K}_P = P(A,B), \qquad\qquad \overline{K}_I = \overline{K}_D\Omega_A^2 - Q(A,B)\Omega_A, \tag{6.5}$$

for all $\overline{K}_D > \frac{Q}{\Omega_A}$, or the parameters

$$\overline{K}_P = P(A,B), \qquad\qquad \overline{K}_D = \frac{Q(A,B)}{\Omega_A} + \frac{\overline{K}_I}{\Omega_A^2}, \tag{6.6}$$

for all $\overline{K}_I > 0$, where $P(A,B)$ and $Q(A,B)$ are obtained using the same Inversion Formulae defined for the continuous-time case (5.10) and $\Omega_A = \tan\frac{\omega_A T}{2}$.

The proof can be obtained similarly to the proof of Prop. 12.

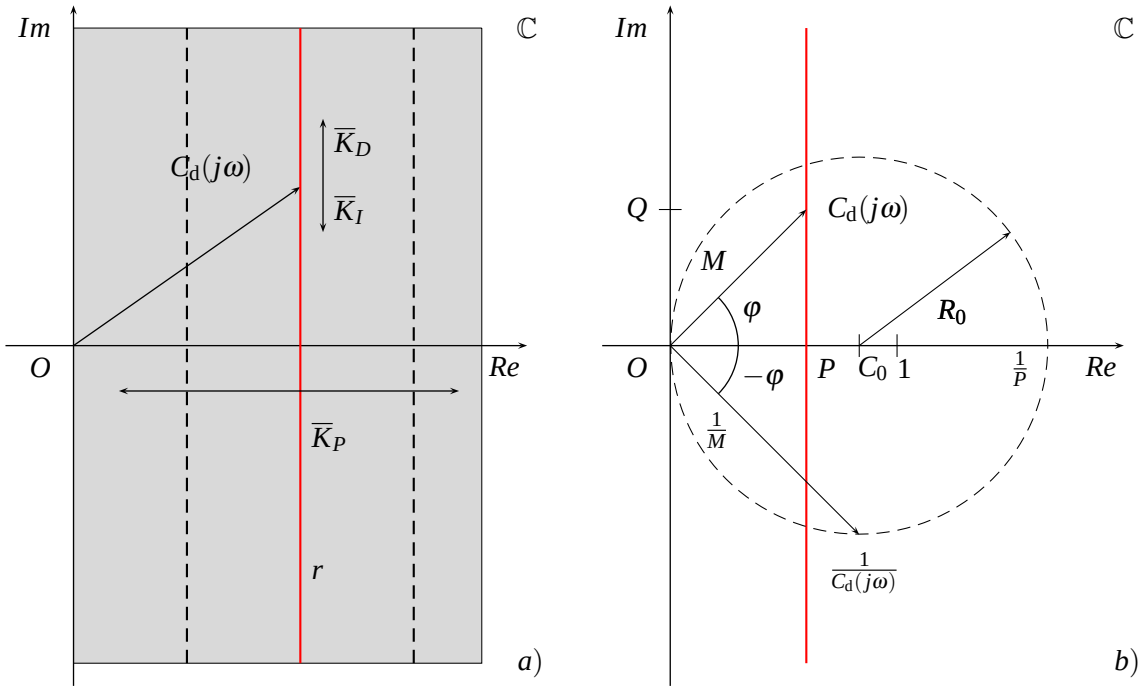

Figure 6.2: Nyquist plot of functions $C_d(j\omega)$ and $C_d^{-1}(j\omega)$.

6.2 Synthesis of discrete PID compensator

The Prop. 15 and the Inversion Formulae (5.10) can be used to solve all the design problems considered in the continuous time case.

Design Problem A: Given the control scheme of Fig. 6.1, the transfer function $HG(z)$, the steady-state specifications that impose the value of $\overline{K}_I$ and the design specifications on the phase margin ϕ_m and gain crossover frequency $\omega_g \in [0, \frac{\pi}{T}]$, design a discrete-time compensator $C_d(z)$ such that the loop gain transfer function $C_d(\omega,T)HG(\omega,T)$ passes through point $B = e^{j(\pi+\phi_m)}$ at $\omega = \omega_g$.

Solution A: *If the point $A_g = HG(\omega_g,T)$ belongs to the admissible domain $\mathscr{D}_B$ shown in Fig 6.3, the solution can be obtained using the parameters $\overline{K}_P$ and $\overline{K}_D$ given by (6.6) and $\overline{K}_I > 0$ is determined by the steady-state specifications.*

Let us now consider the case of steady-state specifications that do not constrain the value of $\overline{K}_I$.

Design Problem C: Given the transfer function $HG(z)$ and the design specifications on the phase margin ϕ_m, gain margin G_m and gain crossover frequency $\omega_g \in [0, \frac{\pi}{T}]$, design a discrete compensator $C_d(z)$ such that the loop gain transfer function $C_d(\omega,T)HG(\omega,T)$ passes through point $B_g = e^{j(\pi+\phi_m)}$

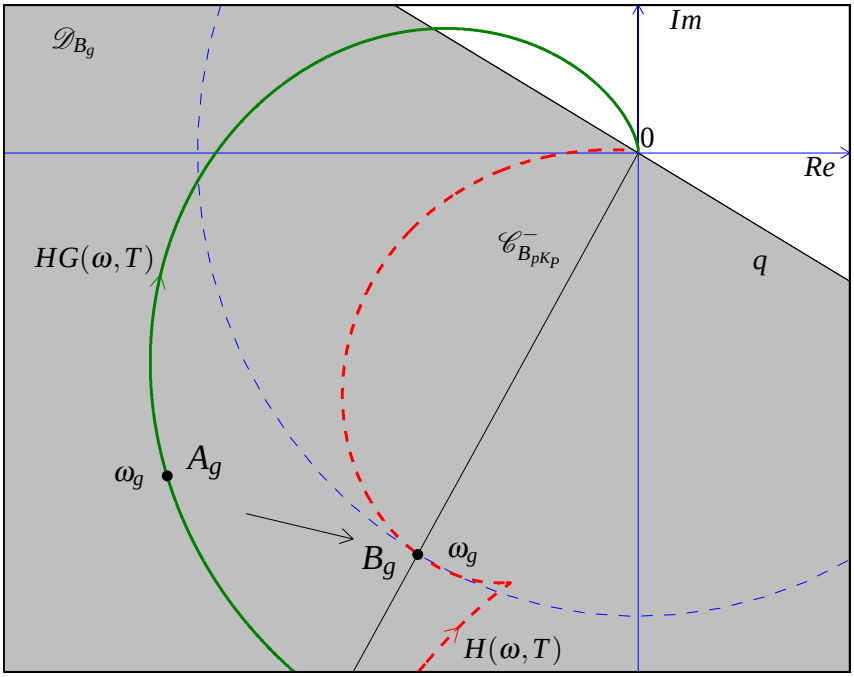

Figure 6.3: Graphical solution of Design Problem A (solution b) of Example 1).

for $\omega = \omega_g$ and passes through point $B_p = -1/G_m$.

Solution C: *The numerical and graphical solutions can be obtained following this direct procedure.*

Step 1. *Draw the admissible domain $\mathscr{D}_{B_g}$ of point $B_g = e^{j(\pi+\phi_m)}$ defined by the straight line q passing through point O and perpendicular to segment $\overline{B_g O}$, see Fig. 6.4.*

Step 2. *Check whether the point $A_g = HG(\omega_g, T)$ belongs to $\mathscr{D}_{B_g}$. If not the problem has not acceptable solutions.*

Step 3. *Determine the parameters $P_g = P(A_g, B_g)$, $Q_g = Q(A_g, B_g)$ using the Inversion Formulae (5.10).*

Step 4. *Draw the circle $\mathscr{C}^-_{B_p\overline{K}_P}$ having its diameter on the segment defined by points O and $\frac{B_p}{\overline{K}_P}$, where it is $B_p = -1/G_m$ and $\overline{K}_P = P_g$. If there are not intersections points of $\mathscr{C}^-_{B_p\overline{K}_P}$ with $HG(\omega,T)$, the problem has no acceptable solutions. Otherwise let A_{pi} denote the intersections points of circle $\mathscr{C}^-_{B_p\overline{K}_P}$ with $HG(\omega,T)$ at frequencies ω_{pi}. These points can also be obtained solving the following equation*

$$\overline{K}_P = P_p(\omega_p) = \frac{M_{B_p}}{M_{A_p(\omega_p)}} \cos(\varphi_{B_p} - \varphi_{A_p}(\omega_p)). \tag{6.7}$$

Step 5. *For $\omega_p = \omega_{pi} \in [0, \frac{\pi}{T}]$, the set of all the compensators $C_d(z)$ which solve Design Problem C is*

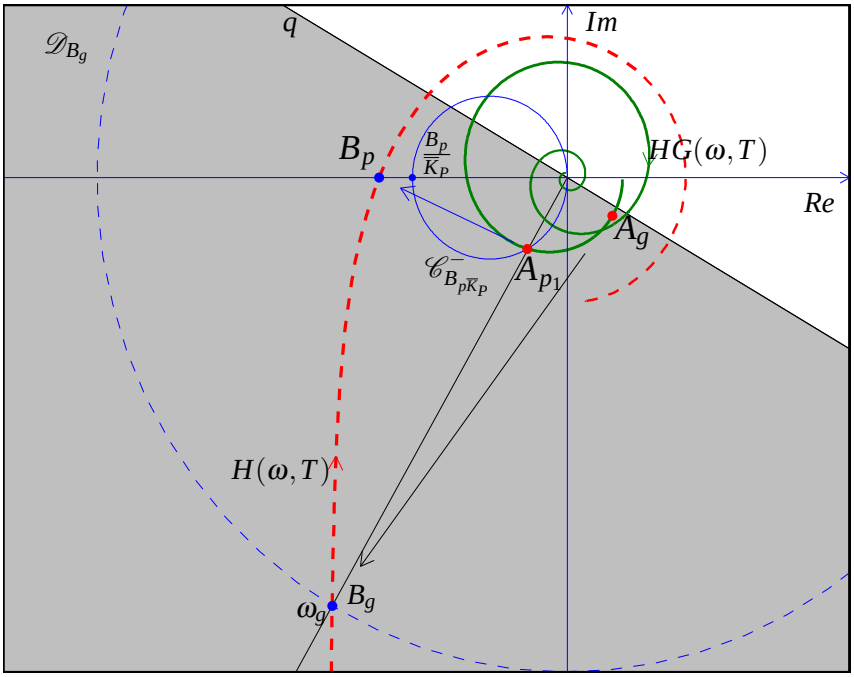

Figure 6.4: Graphical solution of Design Problem *C* on the Nyquist plane (solution of Example 2).

obtained from (6.1) using the parameters

$$\overline{K}_P = P_g > 0, \qquad \overline{K}_D = \frac{Q_g\Omega_g - Q_p\Omega_p}{\Omega_g^2 - \Omega_p^2} > 0, \tag{6.8}$$

$$\overline{K}_I = \frac{Q_g\Omega_g\Omega_p^2 - Q_p\Omega_p\Omega_g^2}{\Omega_g^2 - \Omega_p^2} > 0, \tag{6.9}$$

where $\Omega_g = \tan\frac{\omega_g T}{2}$, $\Omega_p = \tan\frac{\omega_p T}{2}$ *and parameters* $P_g = P(A_g, B_g)$, $Q_g = Q(A_g, B_g)$, $P_p = P(A_p, B_p)$ *and* $Q_p = Q(A_p, B_p)$ *are obtained using the Inversion Formulae (5.10), with* $A_p = HG(\omega_p, T) = M_{A_p}(\omega_p)\, e^{j\varphi_{A_p}(\omega_p)}$. *The solution is admissible only if the parameters* $\overline{K}_I$ *and* $\overline{K}_D$ *in (6.8) and (6.9) are real and positive.*

The proof is quite similar to the one given for the Solution C using continuous time PID regulator.

Design Problem D: Given the transfer function $HG(z)$ and the design specifications on the phase margin ϕ_m, gain margin G_m and the phase crossover frequency ω_p, design a PID compensator $C_d(z)$ such that the loop gain transfer function $C(\omega,T)HG(\omega,T)$ passes through point $B_p = -1/G_m$ for $\omega = \omega_p$ and passes through point $B_g = e^{j(\pi+\phi_m)}$.

Solution D: *Let* $A_p = HG(\omega_p, T)$ *denote the value of* $HG(\omega,T)$ *at the desired phase crossover frequency* ω_p, *and let* $B_g = e^{j(\pi+\phi_m)}$ *and* $B_p = -1/G_m = M_{B_p}\, e^{j\varphi_{B_p}}$ *denote the points corresponding to*

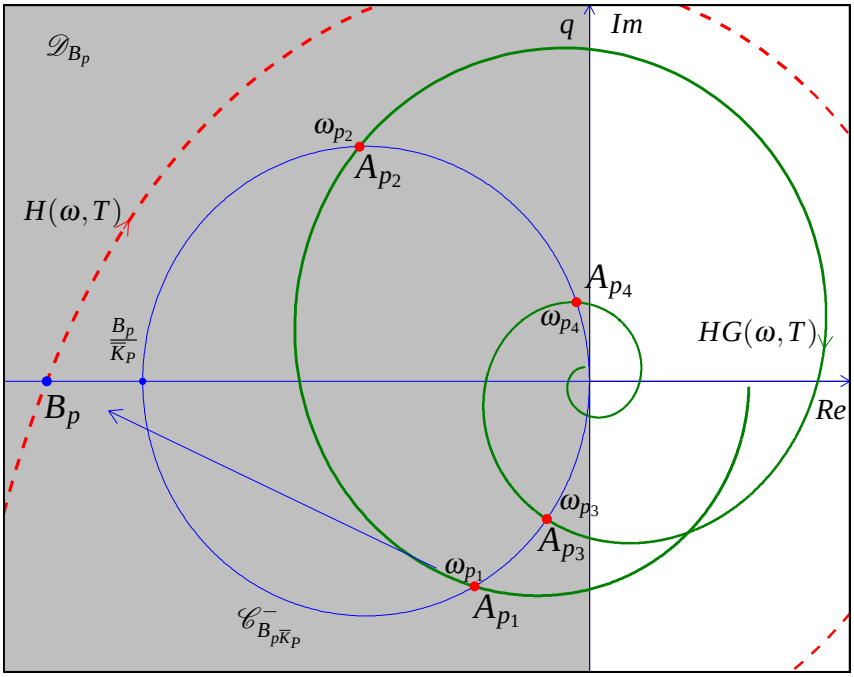

Figure 6.5: Zoom of the graphical solution of Design Problem *C*: set of points $A_{pi} = (A_{p1}, A_{p2}, A_{p3}, A_{p4}...)$ that can be moved to point B_p by the controller.

the desired phase and gain margins. The set $C_{gd}(z,\omega_g)$ of all the PID compensators $C_d(z)$ which solve Design Problem D is obtained from (6.1) using the parameters

$$\overline{K}_P = P_p > 0, \qquad \overline{K}_D = \frac{Q_g\Omega_g - Q_p\Omega_p}{\Omega_g^2 - \Omega_p^2} > 0, \tag{6.10}$$

$$\overline{K}_I = \frac{Q_g\Omega_g\Omega_p^2 - Q_p\Omega_p\Omega_g^2}{\Omega_g^2 - \Omega_p^2} > 0, \tag{6.11}$$

where $P_g = P(A_g, B_g)$, $Q_g = Q(A_g, B_g)$, $P_p = P(A_p, B_p)$ and $Q_p = Q(A_p, B_p)$ are obtained using the inversion formulas (5.10) with $A_g = HG(\omega_g, T) = M_{A_g}(\omega_g)\, e^{j\varphi_{A_g}(\omega_g)}$, for all the frequencies ω_g satisfying the relation

$$\overline{K}_P = P_g(\omega_g) = \frac{M_{B_g}}{M_{A_g(\omega_g)}} \cos(\varphi_{B_g} - \varphi_{A_g}(\omega_g)). \tag{6.12}$$

A solution $C_{gd}(z,\omega_g)$ exists only if: 1) the set S_{ω_g} of all the $\omega_g > \omega_p$ satisfying (5.38) is not empty; 2) $A_g \in \mathscr{D}_{B_g}$ and $A_p \in \mathscr{D}_{B_p}$; 3) the parameters $\overline{K}_P$, $\overline{K}_D$ and $\overline{K}_I$ in (6.10) and (6.11) are real and positive.

The proof is quite similar to the one given for the solution of Design Problem D using continuous time PID regulator.

6.3 Numerical examples

Example 1. Let us consider the following plant

$$G(s) = \frac{0.7}{(s+0.3)(s^2+0.6s+1)}. \tag{6.13}$$

a) Design the continuous-time PID compensator (5.1) satisfying the following design specifications: phase margin $\phi_m = 60^\circ$, gain margin $G_m = 4.5$ and gain crossover frequency $\omega_g = 0.91$. **b)** Design the discrete-time PID compensator $C_d(z)$ for the discrete system $HG(z)$ with $T = 0.1$s to meet the following design specifications: velocity constant $K_v = 3$, phase margin $\phi_m = 60^\circ$ and gain crossover frequency $\omega_g = 0.91$.

Solution: a) Referring to Fig. 6.6, the point $A_g = G(j\omega_g) = 1.28e^{-j144^\circ}$ belongs to the admissible domain $\mathscr{D}_{B_g}$ for reaching point $B_g = e^{j240^\circ}$. From (5.10) it is $P_g = 0.714$ and $Q_g = 0.322$. The circle $\mathscr{C}^-_{B_pK_P}(j\omega)$ with the diameter $\left(O, \frac{B_p}{K_P}\right)$, $B_p = -1/G_m$ and $K_P = P_g$ intersects $G(j\omega)$ in point $A_{p1} = 0.196e^{j129^\circ}$ at frequency $\omega_{p1} = 1.68$. From (5.30) and (5.31) it is $K_D = 0.5953$ and $K_I = 0.1998$. The loop gain frequency response $H_1(j\omega)$ is the dashed red line shown in Fig. 6.6.
b) The discrete-time system to be controlled is

$$HG(z) = 10^{-4}\frac{1.14z^2 + 4.457z + 1.09}{z^3 - 2.903z^2 + 2.817z - 0.9139}. \tag{6.14}$$

The integral constant K_I is determined by the velocity constant requirement

$$K_v = \lim_{z\to 1}\frac{1-z^{-1}}{T}C_d(z)HG(z) = \frac{2\cdot 6.687\cdot \overline{K}_I}{0.1} = 3,$$

which leads to $\overline{K}_I = 0.0224$. The point $A_g = HG(e^{j\omega_g T}) = 1.28e^{-j147^\circ}$ belongs to the domain $\mathscr{D}_{B_g}$, see Fig. 6.3. From (5.10) it follows that $P(A,B) = 0.699$ and $Q(A,B) = 0.354$. Finally from (6.6) it is $\overline{K}_P = 0.699$ and $\overline{K}_D = 18.6$. The designed compensator is

$$C_d(z) = 0.699 + 18.6\frac{z-1}{z+1} + 0.0224\frac{z+1}{z-1}.$$

The correspondent loop gain frequency response $H(\omega,T) = HG(\omega,T)C_d(\omega,T)$ is the dashed red line in shown in Fig. 6.3.

Example 2. Given the following nonminimum phase plant proposed in [37]

$$G(s) = \frac{s^3 - 4s^2 + s + 2}{s^5 + 8s^4 + 32s^3 + 46s^2 + 46s + 17}e^{-s}, \tag{6.15}$$

synthesize a discrete-time PID compensator $C_d(z)$ for system $HG(z)$ with $T = 0.3$s to meet the following design specifications: phase margin $\phi_m = 60^\circ$, gain margin $G_m = 2.5$ and gain crossover frequency

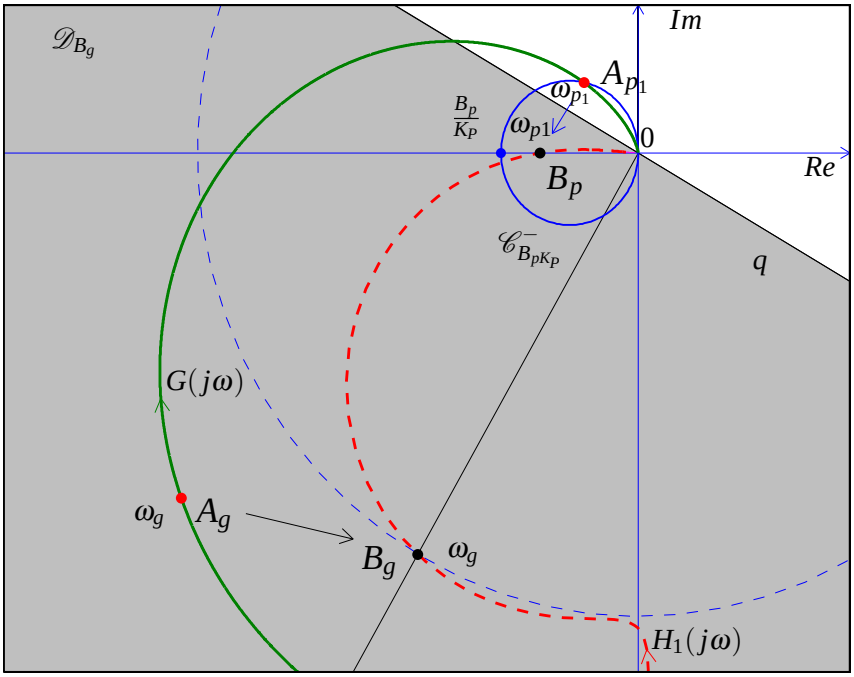

Figure 6.6: Graphical solution a) of Example 1.

$\omega_g = 0.2$.

Solution The point $A_g = HG(e^{j\omega_g T}) = 0.123e^{-j38.6^\circ}$ belongs to the domain $\mathscr{D}_{B_g}$, see Fig. 6.4. From (5.10) it follows that $P(A,B) = 1.21$ and $Q(A,B) = -8.03$. The intersections points of $\mathscr{C}^-_{B_p\overline{K}_P}$ with $HG(\omega,T)$ occur at frequencies $\omega_{pi} = (0.6\ ,\ 1.06\ ,\ 2.49\ ,\ 3.88, ...)$. One possible solution is obtained moving the point A_{p_1} at frequency (ω_{p1}) to point B_g using relations (6.8) and (6.9). The obtained designed parameters are $\overline{K}_P = 1.21$, $\overline{K}_D = 7.10$ and $\overline{K}_I = 0.247$. The corresponding loop gain frequency response $H(\omega,T)$ is plotted in dashed red line in Fig. 6.4 and 6.5.

6.4 Comparison with other methods

One of the main advantages of the graphical solution presented in this chapter over other graphical approaches, such as the one in [31], is that it can be easily determined in the complex plane by finding the intersections of the frequency response of the plant with particular design circles. This graphical solution can be easily obtained by students in valuation test without the use of computer. Moreover, the method based on Inversion Formulae provides *all* the solutions of the control problem and not only a subset of all the solutions, as it happens in [31]. The proposed method has the advantage to avoid the double transformation as required by the classical indirect method and it is not based on trial-and-error

procedure, such as the classical methods based on the use of Bode plot, see [17].

Conclusions

This thesis presents a design method for all types of standard compensators that are ubiquitously addressed in control subjects, and which represent the very vast majority of compensators used in industry. The method, based on the so-called Inversion Formulae, enables the synthesis to be carried out precisely and just with the aid of a pen and a piece of paper. This represents the most remarkable value and potential of this method in control education and in industrial applications. In fact, these techniques do not rely on iterative procedures to be performed on Bode or Nyquist plots.

In Chap. 1 the formulation of the considered Design Problems and the importance of their design specifications have been presented. In Chap. 2 the comparison of the classical method based on the Bode diagrams and the Inversion Formulae method for the design of first order Lead and Lag regulators have been described. It can be easily shown the effectiveness of the Inversion Formulae method both for numerical and graphical solutions. The method leads to an exact solution using simple closed form formulae and can satisfy both the phase margin and the gain crossover specifications, while the classical method can satisfy only one of them. The Inversion Formulae method appears therefore to be very suitable for numerical exercises that can test students' skills in every single aspect of the compensator design process. In Chap. 3 it is described how this method can be used to exactly solve the Design Problems addressed in Chap. 1 using second order Lead-Lag controllers. A general form of Lead-Lag compensators which include real or complex zeros and poles has been considered. Necessary and sufficient conditions to exactly satisfy specifications on the gain and phase margins have been proposed together with a simple graphical solution on the Nyquist plane. Moreover the use of the Inversion Formulae enables two parameters of the compensator to be computed in closed form to exactly satisfy the phase margins and the gain crossover frequency specifications. An open research problem is to determine the design procedures to select the third parameter such to satisfy another specification. The root locus and the contour locus methods have been used to synthesize this third parameter to maximize the distance of the poles of the system closed-loop characteristic equation from the imaginary axis. In this way the settling time of the system step response can be optimized. Another tuning procedure has been proposed, this aims to maximize the complementary modulus margin in order to optimize the system resonance peak. In Chap. 4 a numerical and graphical direct method, useful to solve the Design Problems formulated in Chap. 1

using discrete time Lead-Lag type regulators, has been described, see [14], [15]. This method has the advantage to avoid the double transformation in continuous and in discrete time domains as required by the classical indirect method. It is relevant to notice that all the proposed design procedures, based on the synthesis of continuous and discrete Lead-Lag type regulators, are based on the same Inversion Formulae.

In the second part of the thesis the Inversion Formulae method has been addressed to the synthesis of PID regulators, both in continuous and discrete time domains. Exactly the same design procedures introduced for the synthesis of Lead-Lag regulators have been applied to PID regulators. Also in this case, unique Inversion Formulae for all types of PID controllers have been found.

The simplicity of the method and its graphical interpretation seem to be useful both for educational and industrial purposes. It is well known that in the process of learning the graphical representation of a numerical solution makes it easier to understand and easier to recall. The drawing and the comparison of the same function plotted in different diagrams, i.e. the loop gain frequency response on the Bode, the Nyquist and the Nichols diagrams, have a great educational value. They emphasize some properties hidden in a single representation and lead to a deeper knowledge of the concepts. The relevance of these methods for written exercises has been demonstrated in this thesis with many Question examples, that are extremely difficult to tackle with the standard approaches, and that shed some light on some aspects of the control design that would otherwise remain neglected.

Appendix A

Appendix A: Lead-Lag compensators with real poles and real zeros

The classical form $C_r(s)$ of the Lead-Lag compensator with real poles is

$$C_r(s) = \frac{(1+\tau_1 s)(1+\tau_2 s)}{(1+\alpha\tau_1 s)(1+\frac{\tau_2}{\alpha}s)} \tag{A.1}$$

with $0 < \tau_1 < \tau_2$ and $0 < \alpha < 1$. The asymptotic amplitude Bode diagram of $C_r(j\omega)$ is shown in Fig. A.1. The relations that link the parameters τ_1, τ_2 and α of compensator $C_r(s)$ to parameters γ, δ and ω_n of compensator $C(s)$ are

$$\tau_1 = \frac{\gamma\delta - \sqrt{\gamma^2\delta^2 - 1}}{\omega_n}, \qquad \tau_2 = \frac{\gamma\delta + \sqrt{\gamma^2\delta^2 - 1}}{\omega_n},$$

$$\alpha = \frac{\delta - \sqrt{\delta^2 - 1}}{\gamma\delta - \sqrt{\gamma^2\delta^2 - 1}}; \qquad \gamma = \frac{\tau_1 + \tau_2}{\alpha\tau_1 + \frac{\tau_2}{\alpha}},$$

$$\omega_n = \frac{1}{\sqrt{\tau_1\tau_2}}, \qquad \delta = \frac{\omega_n}{2}\left(\alpha\tau_1 + \frac{\tau_2}{\alpha}\right).$$

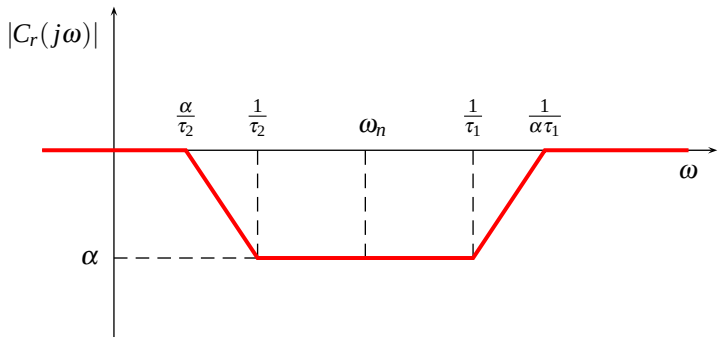

Figure A.1: Asymptotic amplitude Bode diagram of compensator $C_r(s)$.

For compensator $C_r(s)$ the admissible domain coincides with the admissible domain $\mathscr{D}_1$ of compensator $C(s)$, see Fig. 3.3.

Bibliography

[1] C.H. Lee. *A survey of PID controller design based on gain and phase margins,* International Journal of Computational Cognition, vol.2, no.3,pp 63-100, Sept 2004.

[2] C.L. Phillips. *Analytical Bode Design of Controllers,* IEEE Transactions on Education, vol. E-28, no. 1, pp. 43-44, 1985.

[3] G. Marro. *Controlli Automatici,* Zanichelli Ed., Bologna (Italy), 2004.

[4] G. Marro and R. Zanasi. *New Formulae and Graphics for Compensator Design,* IEEE International Conference On Control Applications, Trieste, Italy, September 1-4, 1998.

[5] R. Zanasi. *Esercizi di Controlli Automatici,* Progetto Leonardo Ed., Bologna (Italy), 1999.

[6] A. Ferrante, A. Lepschy, and U. Viaro. *Introduzione ai Controlli Automatici,* UTET Universit, 2000.

[7] R. Zanasi. *Esercizi di Controlli Automatici,* Progetto Leonardo Ed., Bologna (Italy), 2nd edition, 2011.

[8] R. Zanasi, S. Cuoghi, and L. Ntogramatzidis. *Analytical and Graphical Design of Lead-Lag Compensators, International Journal of Control,* 84(11): 1830–1846, 2011.

[9] L. Ntogramatzidis, and A. Ferrante. *Exact Tuning of PID Controllers in Control Feedback Design,* IET Control Theory & Applications, 5(4): 565–578, 2011.

[10] R. Zanasi, S. Cuoghi, L. Ntogramatzidis. *Analytical design of Lead-Lag Compensators on Nyquist and Nichols planes,* IEEE IFAC World Congress, International Federation of Automatic Control, Milan, Italy, 28/08-2/09/2011.

[11] R. Zanasi, S. Cuoghi, L. Ntogramatzidis. *Lead-Lag compensators: analytical and graphical design on Nyquist plane,* IEEE CDC-ECC, Conference on Decision and Control and European Control Conference, Orlando, FL, USA, 12-15/12/2011.

[12] R. Zanasi and S. Cuoghi. *Design of Lead-Lag compensators for robust control*, IEEE ICCA11, International Conference on Control and Automation, Santiago, Chile 19-21/12/2011.

[13] R. Zanasi and S. Cuoghi. *Analytical and Graphical Design of PID Compensators on the Nyquist plane*, IEEE IFAC Conference on Advances in PID Control PID'12, International Federation of Automatic Control, Brescia, Italy, 28-30 March 2012 (accepted).

[14] R. Zanasi and R. Morselli. *Discrete Inversion Formulas for the Design of Lead and Lag Discrete Compensators*, European Control Conference, 23-26 August 2009, Budapest, Hungary.

[15] R. Zanasi and S. Cuoghi. *Direct method for digital Lead-Lag design: analytical and graphical solutions*, IEEE CASE, Conference on Automation Science and Engineering, Trieste, Italy, 24-27/08/2011.

[16] R. Zanasi and S. Cuoghi. *Direct methods for the synthesis of PID compensators: analytical and graphical design*, IEEE IECON, Industrial Electronics Conference, Melbourne, Australia, 7-10/11/2011.

[17] G. Franklin, J.D. Powell, and A. Emami-Naeini. *Feedback Control of Dynamic Systems*, Prentice Hall, 2006.

[18] J.J. DAzzo and C.H. Houpis. *Linear Control System Analysis and Design*, McGraw-Hill, New York, 4th edition, 1995.

[19] R.C. Dorf and R.H. Bishop. *Modern Control Systems*, Prentice Hall, Upper Saddle River, NJ, 2008.

[20] K. Ogata. *Modern Control Engineering*, 4th Edition, Prentice-Hall, Prentice Hall, Upper Saddle River, NJ, 2009.

[21] Y. Chen. *Replacing a PID controller by a lag-lead compensator for a robot-a frequency-response approach*, IEEE Transactions on Robotics and Automation, vol.5, no.2, pp.174-182, Apr 1989.

[22] W.C. Messner, M.D. Bedillion, L. Xia, and D.C. Karns. *Lead and Lag Compensators with Complex Poles and Zeros: design formulas for modeling and loop shaping*, IEEE Control System Magazine, vol. 27, no. 1, pp. 44–54, 2007.

[23] S.S. Flores, A.M. Valle and B.A. Castillejos. *Geometric Design of Lead/Lag Compensators Meeting a Hinf Specification*, 4rd ICEEE International Conference On Elettrical and Electronics Engineering, Mexico City, Mexico, September 5-7, 2007.

[24] W. Messner. *Formulas for Asymmetric Lead and Lag Compensators*, American Control Conference, Hyatt Regency Riverfront, St. Louis, MO, USA, 10–12 June 2009.

[25] K.S. Yeung, K.W. Wong and K.L. Chen. *A Non Traial-and-Error Method for Lag-Lead Compensator Design*, IEEE Transactions on Education, E-41, no. 1, Feb. 1998.

[26] D. Garcia, A. Karimi, R. Longchamp and S. Dormido. *PID Controller Design with Constraints on Sensitivity Functions Using Loop Slope Adjustment*, American Control Conference Minneapolis, Minnesota, USA, June 14-16, 2006.

[27] D. Garcia, A. Karimi, R. Longchamp. *PID controller design with specifications on the infinity-norm of sensitivity functions*, 16th IFAC World Congress, July, 2005.

[28] N.S. Nise. *Control Systems Engineering*, 5rd Edition, Wiley, Hoboken, NJ, 2008.

[29] K. Ogata. *Discrete-Time Control Systems*, 2nd edn. Prentice-Hall, Upper Saddle River, NJ, 1995.

[30] G.F. Franklin, J.D. Powell, A. Emami-Naeini. *Feedback Control of Dynamic Systems*, 6th edn., Pearson Prentice Hall, Upper Saddle River, NJ, 2009.

[31] K.S. Yeung and K.H. Lee. *A universal design chart for linear time-invariant continuous-time and discrete-time compensators*, IEEE Transactions on Education, vol.43, no.3, pp.309-315, Aug 2000.

[32] K.J. Aström, and T. Hagglund. *Automatic Tuning of Simple Regulators with Specifications on Phase and Amplitude Margins*, Automatica: Vol. 20, no. 5, pp. 645-651, 1984.

[33] W.K. Ho, O.P. Gan, E.B. Tay and E.L. Ang. *Performance and gain and phase margins of well-known PID tuning formulas*, IEEE Transactions on Control Systems Technology: vol 4, pp. 473-7, 1996.

[34] H.W. Fung, Q.G. Wang and T.H. Lee. *PI tuning in terms of gain and phase margins*, Automatica: 34(9):1145-9,1998.

[35] Q.G. Wang, H.W. Fung, and Y. Zhang. *PID tuning with exact gain and phase margins*, ISA Transactions, 38, 243–249, 1999.

[36] K.J. **r**Aström, and T. Hagglund. *Advanced PID Control*, Instrument Society of America, Research Triangle Park, NC, 2006.

[37] K. Keunsik and C.K. Young. *The Complete Set of PID Controllers with Guaranteed Gain and Phase Margins*, Decision and Control and European Control Conference, CDC-ECC, Dec. 2005